DESIGN AND ANALYSIS OF SLIDING MODE CONTROL AND SLIDING SURFACE FOR MIMO SYSTEMS

Thesis submitted to

UNIVERSITY OF CALICUT

in partial fulfillment for the award of the degree of

DOCTOR OF PHILOSOPHY

By

LISY E. R.

Under the Guidance of

Dr. M.NANDAKUMAR AND Dr. ANASRAJ R.

Department of Electrical Engineering

Government Engineering College, Thrissur

University of Calicut

JULY 2019

Department of Electrical Engineering

GOVERNMENT ENGINEERING COLLEGE

THRISSUR – 680009

Certificate

This is to certify that the thesis entitled "**Design and Analysis of Sliding mode control and Sliding surface for MIMO systems**" is the record of bonafide research work done by **Ms. LISY E. R.** under our supervision and guidance at Department of Electrical Engineering, Govt. Engineering College, Thrissur in partial fulfillment of the requirements for the Degree of Doctor of Philosophy under the Faculty of Engineering, University of Calicut.

Dr. ANASRAJ R.   **Dr. M. NANDAKUMAR**

Thrissur-9

30-07-2019

Certified that the suggestions/corrections from the adjudicators as per Ref. No. 160115/RESEARCH-C-ASST-1/2019/Admn dated 10-02-2020 from the Director of Research, University of Calicut has been incorporated in the Thesis

Dr. ANASRAJ R.   **Dr. M. NANDAKUMAR**

Thrissur-9

13.03.2020

DECLARATION

I, **LISY E. R** hereby declare that the thesis entitled "**Design and Analysis of Sliding mode control and Sliding surface for MIMO systems**" is based on the original work done by me under the guidance of **Dr. M.NANDAKUMAR**, Professor, Department of Electrical Engineering, Govt. Engineering College, Thrissur and **Dr. ANASRAJ R.**, Professor, Department of Electrical Engineering, Govt. Engineering College, Thrissur for the award of Ph.D under University of Calicut. I further declare that this work has not been included in any other thesis submitted previously for the award of any degree, diploma, associateship or fellowship or any other title for recognition.

Thrissur

30.07.2019

Lisy E. R.

Certified that the suggestions/corrections from the adjudicators as per Ref. No. 160115/RESEARCH-C-ASST-1/2019/Admn dated 10-02-2020 from the Director of Research, University of Calicut has been incorporated in the Thesis

Thrissur

13.03.2020

Lisy E. R.

ACKNOWLEDGEMENT

Thrissur-9   **LISY E. R.**
30.07.2019

Abstract

The nature is embedded with non-linear systems. The non-linear systems are generally multiple input multiple output ones. All the control Engineers expect the system to deliver the expected performance. The expected performance depends on the nature of the control strategy adopted.

This thesis proposes the design of sliding surfaces and sliding mode controllers for multiple input multiple output (MIMO) systems. Two types of MIMO systems are taken in to consideration. The first one is 2-degree of freedom (2-dof) TRMS system which is a highly coupled non-linear Electromechanical MIMO system and second is dual input buck boost converter (DIBB) which is a non-linear electrical Multiple input system. In both systems, the control action employed is sliding mode control since it is insensitive to parametric variation and external disturbance.

The work includes design of both linear and non-linear sliding surface for 2-dof TRMS using optimal design procedure and principle of variable damping ratio concept respectively. It is found that there is a presence of chattering in the control signal. Hence the work incorporate the design of super-twisting controller which is a continuous controller to eliminate the chattering in the output signal. The super-twisting control employed in non-linear sliding mode control with non-linear sliding surface design fetches good

results. It is found that the scheme can reduce settling time of 2-dof TRMS. The applicability of the designed non-linear sliding surface has been tested both in simulation and in real time experiments. The performance of non-linear sliding mode controller with super-twisting controller is also compared with the third order super-twisting controller, Linear surface design and PID controller design.

The work has been extended to dual input buck boost converter to know the effect of control of different type system. In this the design of conventional sliding mode controller, the design of super-twisting controller and the design of modified integral sliding mode Control (ISMC) have been done for the output voltage regulation of DIBB converter. The design method is clearly illustrated for dual input buck boost converter with the above control strategies.

The first stage of the research work is concerned with the modeling of 2-dof TRMS multiple input multiple output (MIMO) System and design of the decoupler to eliminate the coupling effect between the main and tail rotors of 2-dof TRMS. The second stage of the work involves the design of PID controller and design of linear sliding surface and non-linear sliding mode controller for 2-dof TRMS. The third stage of the work involves
1) The design of non-linear sliding surface using variable damping ratio concept and non-linear sliding mode controller with the application of super-twisting STC for 2-dof TRMS.
2) The real time implementation of non-linear sliding surface for 2-dof TRMS.
3) The design of third order super-twisting controller for 2-dof TRMS.
4)The comparison between all these controllers for 2-dof TRMS.

In the Fourth stage, the above mentioned controllers are employed in purely electrical DIBB system. It is found that the super-twisting control works well in dual input buck boost converter as it reduces chattering while keeping the robustness of the system. The results have been analysed in terms

of robustness and found that the performance of DIBB system with super-twisting algorithm combined with integral sliding mode controller fetches good results.

Keywords: Two Degree of Freedom Twin Rotor MIMO System,Linear sliding surface, Optimal sliding surface, State feed back controller, Non-linear sliding surface, Non-linear sliding mode controller, Super-twisting controller, Third order super-twisting controller, Integral sliding mode controller.

Contents

List of Figures

xiii

List of Tables

List of Symbols and Abbreviation

1 τ_1 : Torque developed in main Rotor of 2-dof TRMS

2 τ_2 : Torque developed in tail Rotor of 2-dof TRMS

3 u_1 : Control signal given to pitch of 2-dof TRMS

4 u_2 : Control signal given to yaw of 2-dof TRMS

5 LSS : Linear sliding surface

6 NLSS : Non-linear sliding surface

7 SMC : Sliding mode control

8 NSMC : Non-linear sliding mode control

9 STC : Super-twisting control

10 ISMC : Integral sliding mode control

11 S : Sliding surface

12 ψ : Pitch angle of 2-dof TRMS

13 ϕ : Yaw angle of 2-dof TRMS

14 L : Inductance value

15 C : Capacitance value

16 f : Switching frequency

17 TRMS : Twin Rotor MIMO system

18 DIBB : Dual Input Buck Boost Converter

Chapter 1

Introduction

All systems are non-linear in nature. Systems with multiple input multiple output (MIMO) are generally dealt in all engineering disciplines. They are referred to as multi variable systems. When multiple inputs are manipulated simultaneously to control multiple outputs the performance will be achieved in a more optimal manner. For reasons of economics, the control systems design is done in an off line mode which will be later tuned to make a smooth operating condition in reliable manner. The expected performance of the system mainly depends on the modeling and control strategy that are adopted. In the literature, there are many methods available. Pole placement, Block back stepping control, Model reference adaptive control, Model predictive control, Multi variable PID control etc. are some of the general control strategies adopted for MIMO systems. The control design becomes challenging when there is strong interactions in the input-output channels and there are non-linearity in the dynamical behaviour. Parameter uncertainties and the time delay also make the situation complex. Depending on these dynamical properties, each type of system shall exhibit different performance for the same type of control strategy.

In this work, two cases are considered. First one is electromechanical system known as Twin Rotor MIMO system and second one is pure electri-

cal system namely Dual input Buck Boost converter have been considered to the investigation of the effect of control strategy on the system's inherent dynamical properties or changes occurring due to some structural modification.

A design engineer expects all systems to be robust in nature and also insensitive to the parametric variation. Among the control strategies listed above the sliding mode control (SMC) brings out the expected performance in terms of robustness and insensitivity to parametric variation. Hence, in this thesis it is proposed the design of a sliding surfaces and sliding mode controllers for multiple input multiple output systems.

The two types of MIMO systems considered are 1) A 2-degree of freedom (2-dof) TRMS system which is a highly coupled non-linear electro mechanical system and 2) A dual input buck boost converter (DIBB) which is purely electrical MIMO system. The controlling of closed loop system is done by sliding mode control as it is insensitive towards parametric variation and external disturbances. There are two steps in designing sliding mode control. They are design of sliding surface and design of sliding mode control.

The sliding surfaces considered for 2- dof TRMS system are 1) The linear sliding surface design using optimal design procedure and 2) non-linear sliding surface design using the principle of variable damping ratio. The controllers designed for 2-dof MIMO systems are non-linear controller using state feedback control structure, non-linear sliding mode with super-twisting control applied and third order super-twisting controller. The linear sliding surface enables the system trajectory to be robust by designing a suitable non-linear sliding mode control (SMC). This scheme is able to reduce the settling time and peak overshoot of the response for 2-dof TRMS. But, the existence of non-linear sliding surface improves the robustness of the system. Then the performance of 2-dof TRMS using the non-linear sliding surface is compared with the conventional linear sliding surface, PID control design and third order super-twisting control design. It is observed that not only

the settling time but the peak overshoot of the system also are found reduced with the use of non-linear sliding surface design. The system becomes more robust with the application of non-linear sliding surface. The applicability of the designed surface has been tested both in simulation and in real time.

In the case of the dual input buck boost converter (DIBB), the error between the actual value of the output voltage and the reference value is taken as the error surface. The controllers designed for dual input buck boost converters are 1) conventional sliding mode controller 2) super-twisting controller and 3)super-twisting controller applied in integral sliding mode controller (ISMC). The comparison between these controllers has also been done. It is found that the chattering in control as well as in output can be reduced with the use of continuous controller like super-twisting controller. Moreover the reaching time and chattering in control signal can be reduced with the use integral sliding mode controller applied with super-twisting controller.

1.1 Objectives

The main objectives of the thesis can be enumerated as:

- Modeling of 2-dof TRMS by including all non-linearities

- Design of decoupler for 2-dof Twin Rotor MIMO System to eliminate the coupling effects between the main and tail rotor of 2-dof TRMS.

- Design and validation through simulation of PID Controller for 2-dof TRMS.

- Design and validation through simulation of linear sliding surface using optimal design procedure and non-linear controller using state feedback controller for 2-dof TRMS.

- Design and validation through both simulation and real time imple-
  mentation of non-linear sliding surface and non-linear sliding mode
  controller with super-twisting algorithm for 2-dof TRMS.

- Design of third order super-twisting controller for 2-dof TRMS and the
  validation of the controller using simulation.

- Design of PI controller for DIBB and the validation of the controller.

- Design of conventional sliding mode controller for DIBB and the vali-
  dation of the controller.

- Design and validation through simulation of super-twisting controller
  for DIBB.

- Design and validation through simulation of Integral sliding mode with
  discontinuous and continuous controller to reduce chattering as well as
  reaching time for DIBB.

1.2 Organization of the thesis

The chapters of this thesis are organized as follows:

For stating the problem and developing solution approach, a thorough review
has been conducted. This is to analyse the various types of control strategies
applied in MIMO systems. These are described in chapter 2.

The modeling of 2-dof TRMS including all system related non-linearities
and effects of coupling are carried out. Also the design of decoupler for 2-dof
TRMS is designed to eliminate the coupling effects between the main and
tail rotors. These are discussed in chapter 3.

Design and validation through simulation of linear sliding surface using optimal design procedure and non-linear controller design using state feedback controller for 2-dof TRMS are discussed in chapter 4.

In chapter 5, the design and validation of non-linear sliding surface and non-linear controller with super-twisting control applied for 2-dof TRMS through simulation and real time are dealt with. Also the design of third order super-twisting controller for 2-dof TRMS and the validation of the controller using simulation are explained in this chapter.

Chapter 6 begins with the design and validation PI controller for Dual input Buck Boost Converter (DIBB) followed by design of conventional sliding mode controller. The presence of chattering is mitigated using super-twisting controller which is clearly dealt in this chapter. Integral sliding mode with discontinuous and continuous controller to reduce reaching time as well as chattering for dual input buck boost converter are also discussed in this chapter. Finally conclusion and scope for future work are given in chapter 7.

Chapter 2

Literature Review and Problem Definition

2.1 Introduction

Even though multi variable control theory is a subject of recent origin, a lot of research is going across the world. A stable time invariant controller for an open loop unstable system has been designed for multi variable system [1]. The advantages of such system are minimum control action, robustness etc. But this controller cannot be used for tracking purpose since the sensors may make wrong measurement. The researchers are in search of other types of controllers . The output feedback controller for a class of non-linear systems is designed in [2]. The advantage of such controllers is that the knowledge of upper bounds of perturbation is not necessary. A novel controller is designed for a class of non-affine MIMO systems to achieve a uniform semi-global asymptotic stability by combining the h-infinity and back stepping control [3]. The Robust stabilization of MIMO non-linear systems by back stepping is designed by Liu et.al. [4]. They utilized a smooth feedback law for a class of minimum phase systems. All the above mentioned controllers are employed to achieve asymptotic stability. A method for block back stepping

controller is proposed to solve tracking problem based on Lyapunov stability theorem [5].

Some authors have designed the adaptive control strategy, which will provide superior tracking capability in comparison with fixed gain controllers [6]. The limitations of this methods are 1) The time needed for parametric tuning is high. 2) It is difficult to find Lyapunov function for the control of each system. Some authors have also designed the model reference adaptive controller which is a popular technique and efficient approach in improving tracking capability, in comparison with fixed gain controllers [7]. This controller also suffers from the problem of tuning of parameters with Lyapunov function. A novel approach was designed by using robust fixed point transformation by J.K. Tar et.al. [8]. This controller avoids the use of sophisticated tuning process.

Some authors designed model predictive control to control MIMO systems for getting good tracking performance. But the model restrictions have to be taken in to account [9]-[11]. The implementation of field programmable gate array in combination with model predictive control for improving the response speed is designed by K.V. Ling and others in [12]. But it is conventionally used for controlling single input single output systems. The algorithm which is implemented by Sajin and et.al. can solve the problem of loop interaction hence can be applied in MIMO systems[13].

The well-known Nasubuam control is applied in MIMO system by decomposing the MIMO systems in to several separate SISO systems [14]. In [15], a classical Nusubuam gain is employed to identify control direction of each SISO systems. C. Chen and et.al investigated a fuzzy asymptotic control for MIMO systems with unknown identical control directions [16]. In this paper, using newly constructed nusubuam technique, the authors have found a feasible solutions for the problems such as input non-linearities , external

disturbances, unknown identical control directions etc.

The other control strategies are Vibration control [17], Non-linear disturbance observer [18], Sliding mode control[19]. In sliding mode control (SMC), the authors have considered the system non-linearity as uncertainty. In a neural composite learning control using on-line recorded data, the neural networks are used for uncertainty approximation [20]. The authors have updated neural weights using tracking error and a composite learning algorithm is designed by them. Among the control strategies available the sliding mode control is best suited for the control of MIMO systems as it is insensitive to parametric variation and external disturbances.

2.2   Motivation to the Problem

Applying sliding mode control in multiple input multiple output systems is the problem area. Two different type of systems are considered for analysis. Generally electromechanical systems will be having high time constant and will show slow response. The pure electrical system will be having low time constant and will show fast response. The problem is to analyse various types of sliding mode controllers and sliding surfaces for these two types of systems and to check which type of sliding mode controller and sliding surface will give a better result. The two systems considered in this thesis are 2-dof TRMS(electro mechanical MIMO system) and dual input buck boost system (DIBB) as a pure electrical MIMO system. When multiple input multiple output (MIMO) systems are considered, the coupling effect between the input-output pairs may come in to action. Controlling of such system become a difficult task. The 2-degree of freedom Twin Rotor Multiple input Multiple output system (2-dof TRMS) is one such non-linear electro-mechanical system. The 2-dof TRMS is a setup that resembles to the helicopter [21]. The setup is shown in figure 2.1. In the proposed work the TRMS of 2-degree freedom TRMS with model number 33-949 has been considered.

Figure 2.1: TRMS SYSTEM

2.2.1   Dynamics of 2-dof TRMS

The figure 2.2 shows the TRMS system with the vertical movement and horizontal movement forces marked. The moment due to vertical movement of 2-dof TRMS consists of moment due to pitch angle acceleration $\ddot{\psi}$, moment due to non-linear characteristics M_1, moment due to gravity M_{FG}, frictional force moment $M_{B\psi}$ and gyroscopic moment M_G. The following equation shows the relation between these terms are given in [1].

$$\ddot{\psi}I_1 = M_1 - M_{FG} - M_{B\psi} - M_G \tag{2.1}$$

10
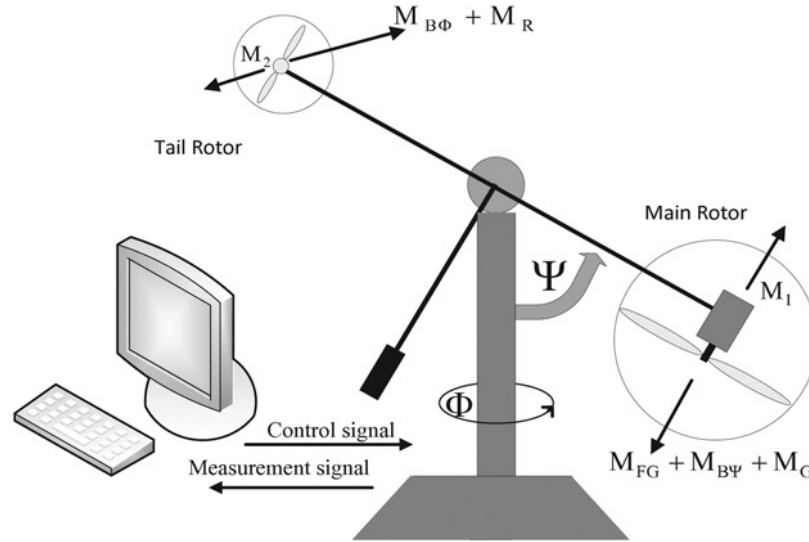
Figure 2.2: TRMS SYSTEM with the vertical movement and horizontal movement forces marked

The moment due to non-linear static characteristic M_1 is related with the torque τ_1 developed in the main rotor as:

$$M_1 = a_1 \tau_1{}^2 + b_1 \tau_1 \tag{2.2}$$

where a_1 and b_1 are constants. Now the relation between gravity moment M_{FG} and pitch angle ψ is given by

$$M_{FG} = M_g \sin(\psi) \tag{2.3}$$

where M_g is the gravity constant. The relation between frictional force moment $M_{B\psi}$, pitch angle velocity $\dot{\psi}$ and yaw angle velocity $\dot{\phi}$ is given by:

$$M_{B\psi} = B_{1\psi}\dot{\psi} - \frac{0.0326}{2}\sin(2\psi)\dot{\phi}^2 \tag{2.4}$$

11

The relation between gyroscopic moment M_G and yaw angle velocity $\dot{\phi}$ is given by:

$$M_G = K_{gy} M_1 \dot{\phi} \cos(\psi) \tag{2.5}$$

Similarly, the moment due to horizontal movement is given as:

$$\ddot{\phi} I_2 = M_2 - M_{B\phi} - M_R \tag{2.6}$$

Here $\ddot{\phi}$ represents the yaw angle acceleration, M_2 represents the moment due to non-linear static characteristic of tail rotor, $M_{B\phi}$ represents frictional force moment and M_R represents cross reaction moment. The moment due to non-linear static characteristic of tail rotor M_2 is related with torque τ_2 developed in the tail rotor as:

$$M_2 = a_2 {\tau_2}^2 + b_2 \tau_2 \tag{2.7}$$

where a_2 and b_2 are constants. The relation between frictional force moment $M_{B\phi}$ and yaw angle velocity is given by:

$$M_{B\phi} = \dot{\phi} B_{1\phi} \tag{2.8}$$

The following equation approximates the cross reaction moment;

$$M_R = K_c \frac{T_o s + 1}{T_p s + 1} M_1 \tag{2.9}$$

where T_P and T_o represent the cross reaction moments parameters for pitch and yaw respectively.

By observing these moment equations we can see that the system is highly non-linear and heavily cross coupled. Hence identification of a decoupler through which the coupling effects can be made to zero for 2-dof TRMS becomes the first motivation. the controlling of 2-dof TRMS becomes a challenging task. The controlling of 2-dof TRMS with a suitable controller which give excellent transient performance while retaining the robustness
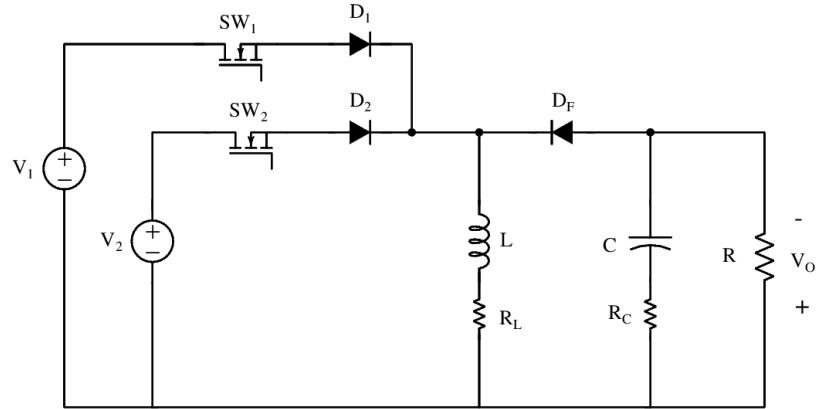
Figure 2.3: Dual input Buck boost converter.

becomes the second motivation. A detailed account on the recent works on TRMS is given in Section 2.3.

Since, TRMS works on electro mechanical actuators, it is slow compared to the electronic systems like power converters. So, there is a natural curiosity to know how the control algorithms will work in fast acting system. Hence, the work was extended to the case of double input buck boost converter (DIBB).

2.2.2 Dual input buck boost converter

The dual input buck boost converter is a pure electrical non-linear MIMO system where it is difficult to control the system due to non-linearity and coupling effects. Figure 2.3 shows the dual input buck boost converter (DIBB)[22]. There are two input voltages are V_1 and V_2. The diodes D_1 and D_2 are connected in such way so as to prevent the current flow from V_1 to V_2. Here the input V_1 is considered to be renewable energy source and V_2 is a stiff source. The diode D_F is the free wheeling diode. R_L the small resistance of the inductor, R_C is the small resistance of the capacitor. The output voltage V_o is taken across the load resistance R. There are three modes of
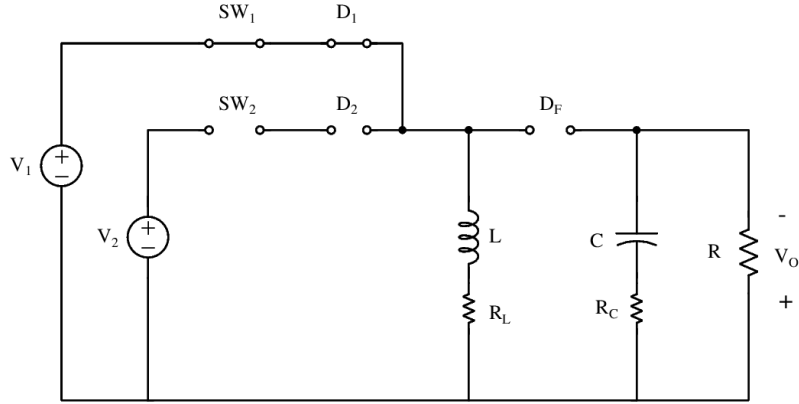
Figure 2.4: Mode 1 operation of DIBB.

operation and these modes of operation are explained in [22]. The mode 1 operation of DIBB is given in figure 2.4. During this mode of operation, the inductor L is connected to the input voltage 1 (V_1) through SW_1 and D_1. The voltage across the capacitor discharges through the load and the current through the inductor L builds up.

The mode 2 operation of DIBB is given in Fig.2.5. During this mode of operation, inductor L is connected to the input voltage2 (V_2) through SW_2 and D_2. The current through inductor L builds up and capacitor discharges through the load. The mode 3 operation of DIBB is given in Fig.2.6. During this mode of operation, the capacitor gets charged through inductor L.

The three modes of operation can be modelled in state space as follows: The voltage across the capacitor is taken as the state variable x_1 and current through the inductor is taken as the state variable x_2. The state model for the first mode of operation of DIBB is given by:

$$
\begin{bmatrix} \dot{x}_1 \\ \dot{x}_2 \end{bmatrix} = \begin{bmatrix} \dfrac{R_L}{L} & 0 \\ 0 & \dfrac{-1}{C(R+R_c)} \end{bmatrix} \begin{bmatrix} x_1 \\ x_2 \end{bmatrix} + \begin{bmatrix} \dfrac{1}{L} \\ 0 \end{bmatrix} V_1 \qquad (2.10)
$$

14
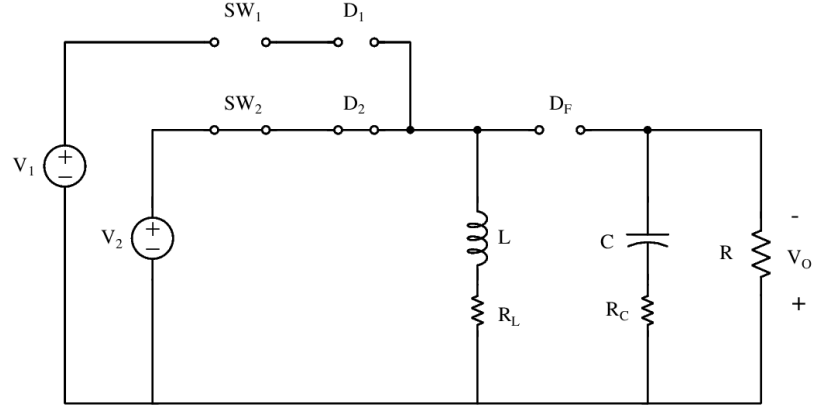
Figure 2.5: Mode 2 operation of DIBB.
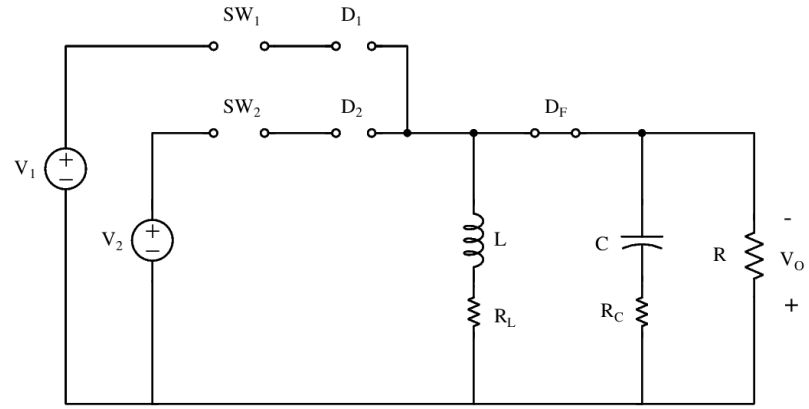
Figure 2.6: Mode 3 operation of DIBB.

The output voltage equation for the first mode of operation is given by:

$$v_o = \begin{bmatrix} 0 & \dfrac{R}{(R + R_c)} \end{bmatrix} \begin{bmatrix} x_1 \\ x_2 \end{bmatrix} \tag{2.11}$$

The state model for the second mode of operation of DIBB is given by:

$$\begin{bmatrix} \dot{x}_1 \\ \dot{x}_2 \end{bmatrix} = \begin{bmatrix} \dfrac{R_L}{L} & 0 \\ 0 & \dfrac{-1}{C(R+R_c)} \end{bmatrix} \begin{bmatrix} x_1 \\ x_2 \end{bmatrix} + \begin{bmatrix} \dfrac{1}{L} \\ 0 \end{bmatrix} V_2 \qquad (2.12)$$

The output voltage equation for the second mode of operation is given by:

$$v_o = \begin{bmatrix} 0 & \dfrac{R}{(R+R_c)} \end{bmatrix} \begin{bmatrix} x_1 \\ x_2 \end{bmatrix} \qquad (2.13)$$

Although the state equations given in equations (2.10) and (2.12) looks same the input voltages are different. The state model for the third mode of operation is given by:

$$\begin{bmatrix} \dot{x}_1 \\ \dot{x}_2 \end{bmatrix} = \begin{bmatrix} R_L + RR_c & \dfrac{-R}{L(R+R_c)} \\ \dfrac{R}{C(R+R_c)} & \dfrac{-1}{C(R+R_c)} \end{bmatrix} \begin{bmatrix} x_1 \\ x_2 \end{bmatrix} \qquad (2.14)$$

The output voltage equation for third mode of operation is given by:

$$v_o = \begin{bmatrix} R_c R & \dfrac{R}{(R+R_c)} \end{bmatrix} \begin{bmatrix} x_1 \\ x_2 \end{bmatrix} \qquad (2.15)$$

The authors have derived an average transfer function. Also they have designed a proportional integral (PI) controller using pole placement techniques. But the determination of the average transfer function model for the closed loop system is very complex which is one of the draw back of the above mentioned control strategy. Thus the aim is to get a robust chattering free controller for dual input buck boost converters. So this become the third motivation. A detailed account on the recent works on DIBB is given in Section 2.4.

2.3 Review of control strategies available for TRMS

2.3.1 PID control

PID is one of the control algorithms mostly used in 2-dof TRMS [23]-[24]. The control scheme for PID is proportional to the actuating signal in addition to integral and derivative of actuating signal. The PID control strategy is very simple in structure and the well-known ziegler method is available for tuning of k_P, k_D and k_I. The main drawbacks of PID control method is the existence of high overshoot and high settling time. The use of binary genetic algorithm on controller tuning for improving system performance has been designed by authors [25]-[26]. The gains tuned by the binary genetic algorithm gave better result than the previous algorithms. The disadvantage of genetic algorithm is that the searching process is time consuming. To overcome this problem, a non-linear control design which provide narrow initial search has been designed by Jih Gao and et.al [27]. Although it can track the desired path more efficiently, it loses its tracking property when the external disturbance or disturbance through input channel is applied. Meta and et.al.proposed a fuzzy logic based methods for on-line selection of proportional, integral and derivative gains [28]. Keya Li developed a PID tuning method based on non-linear optimization. But while solving using non-linear optimization, the feasible regions will have multiple peaks and valleys and there is no general way to determine which peak is tallest or which value is smallest [29]. There will be some some uncertainty in the status of the problem . Based on the multi variable frequency response criterion, Campestrini L and et.al.presented a method to tune PID parameters. However an adequate stability can be obtained only if the frequency response of the process satisfies certain constraints, and design can fail if a bad ultimate point is identified [30]. Fuzzy PID [31] can be used for non-linear system has

ability to perform better against the linear PID. But it has a disadvantage of increased number of membership functions. The above draw backs are eliminated by sliding mode control.

2.3.2 Advanced controllers

The advantage of using sliding mode control are mainly two fold. a) There is order reduction for the system and b) The sliding motion is completely insensitive to parametric variation and external disturbance [32]. The invariance towards matched disturbance makes the sliding mode control an attractive one. There are two steps in designing the sliding mode control. The first step is to design the sliding surface and the second step is to design the sliding mode control. The first step itself is having two phases. In the initial phase, states are being driven towards the surface and this phase is referred to as reaching phase. The second phase is the sliding phase. The system become insensitive to the matched disturbance only when the system reaches the sliding phase.

The draw backs mentioned with PID control in the previous section can be eliminated by sliding mode control as presented by su and et.al in [33]-[34]. Although they could attain a good tracking performance with less overshoot, they failed to reduce settling time because of the selection of linear switching surface for a non-linear system. In this context fuzzy controllers were designed for tracking pitch and yaw position [35]. The fuzzy rules vary for different applications and there are many such rules. Moreover, it loses its tracking performance when a disturbance is applied. On the other hand the sliding mode control is applied with fuzzy control to improve the tracking performance at the time of matched disturbance [36]-[37]. It can be seen that the fuzzy sliding mode control reduces the chattering problem which is found in pure sliding mode controller. Based on previous discussion, a new fuzzy integral sliding mode controller is designed to produce control action

for pitch and yaw in [38]. The reaching conditions and stability of 2-dof TRMS are guaranteed in the fuzzy integral sliding mode control. Moreover, there is reduction in chattering and the system remains insensitive to external disturbances. Some authors have proposed a method using evolving neuro-fuzzy network with fast learning adaptive procedure [39]. Although the control using robust H-Infinity algorithm gives good result, the authors could not give attention in improving the transient performance [40]. A good control for 2-dof TRMS is obtained with the use of linear quadratic regulator (LQR) [41]. But there is a need of full state feedback which may not always be possible because of cost factor or availability of sensors or due to other reasons [42]. The draw back of linear quadratic gaussian [43] is that a precise model is required to realize better tracking performance. Particle swam optimiser has been chosen by Roshini and et.al. as the stochastic optimization algorithm for the the design of optimal state feed back controller for twin rotor MIMO system [44]. The disadvantage of particle swam optimization is that it is easy to fall in local optimum in high dimensional space and it has low convergence rate in the iterative process. S.Mandal and et.al proposed an adaptive second order sliding mode controller [45]. The major advantage of adaptive tuning method is that the advance knowledge of upper bound of system uncertainty is not a necessary requirement. This is because adaptive second order sliding mode controller uses a proportional plus integral sliding surface. Here the system stability and robustness are proved by using Lyapunov criterion. The disadvantage of above control strategy is that the coupling effect between pitch and yaw is taken as uncertainty. Also in papers[46]-[48], the design engineers have taken coupling effect as uncertainty. But coupling effect is made to zero using decoupler, without considering the coupling effects as an uncertainty. The authors reduced the coupling effect to zero in [49]. They could not give due attention to the improvement in transient performance of 2-dof TRMS. Considering the above mentioned aspects of TRMS viz the accuracy in the improvement of the system performance

depends on the way how the the surface is defined, the control engineers have taken alternative methods. They have employed decoupler where the coupling effects is made to zero along with excellent transient performance of less settling time and no overshoot.

2.3.3   Review of decoupling of TRMS

The limitation of the controllers mentioned in previous Section is that they haven't used the decouplers to eliminate the coupling between pitch and yaw. However, a robust dead beat controller has been designed to reduce the cross coupling effect [50]. But here, the cross coupling effect has been taken as disturbance and also from the simulation result it is observed that the control effort is large. Jatin kumar and etal. designed decoupling methods for MIMO system using minimal-di method (that is decoupler is designed including minimum number of unstable poles and zeros) in [51]. They have used SISO controllers for 2-dof TRMS along with loop robustness and disturbance rejection properties. Although they tried to introduce decoupling, loop robustness and disturbance rejection etc., the authors did not give much importance to the transient responses. Hence the present work includes the minimal-di method to reduce the coupling effects between pitch and yaw in an efficient way. The next Section deals with the control strategies for dual input buck boost converter.

2.4   Control strategies available for Dual input buck boost converter

The renewable source of energy such as solar, wind, tidal power etc. are used in many tropical regions. Integration of the above energy sources is inevitable to tap the maximum energy from these sources [22]. In dual input converter two voltage sources are combined.

The output voltage regulation is well illustrated in various topologies [52]-[55]. The use of multi-winding transformers is avoided in [56]-[57]. But none of these topologies consider power budgeting issue. Generally, the control loop used for output voltage regulation as well as power budgeting issues are very complex in [58]-[59]. The authors have combined all state space models during each state mode of operation and derived an average transfer function. Also they have designed a proportional integral (PI) controller using pole placement techniques In [60]. Duty ratio of one of the power switch is fixed while other one is varied to get output voltage regulation. But the determination of transfer function model is very complex which is one of the draw back of the above mentioned control strategies. Also through literature survey it is noticed that the multi variable control was not used extensively in DIBB. In [61] the small signal modelling of double input converters based on H-bridge cells is done. In this thesis also the determination of small signal model is complex.

2.5 Problem definition

The identification of the problem is the difficulty in applying sliding mode control in MIMO systems. In all MIMO systems the system will have non-linearities and coupling effect. When there are non-linearities and coupling effects it will be difficult to model and control the system.

Two different type of systems are considered for analysis. Generally electromechanical systems will be having high time constant and will show slow response. The pure electrical system will be having low time constant and will show fast response. The problem is to analyse various types of sliding mode controllers and sliding surfaces for these two type of systems and to check which type of sliding mode controller and sliding surface will give a better result. The two systems considered in this thesis are 2-dof TRMS(electro mechanical MIMO system) and dual input buck boost converter (DIBB) as

a pure electrical MIMO system.

Considering an electromechanical system 2-dof TRMS, the behaviour of 2-dof TRMS resembles to that of a helicopter whose performance is described as highly unstable non-linear dynamics with heavy cross-coupling effects. Hence the thesis addresses modeling of 2-dof TRMS by taking all non-linearities and coupling effects into consideration and design of a decoupler to eliminate the cross coupling effect.

PID controller is one of the control algorithms mostly used in 2-dof TRMS. But there exists high overshoot and settling time. These drawbacks are claimed to have been eliminated by some researchers using sliding mode control (SMC). Although they could attain a good tracking performance with less overshoot, they failed to reduce settling time because of the selection of linear switching surface for a non-linear system. Even if 2-dof TRMS with fuzzy sliding mode controller alleviates chattering effects and remain robust to external disturbance, it has inherent drawback of increased number of membership functions. Some authors proposed an adaptive second order sliding mode controller where the coupling effect between pitch and yaw is taken as uncertainty. They claims that the control action can reduce the coupling effect. But coupling effect is to be made zero using decoupler, without considering the coupling effects as an uncertainty. In literature, although some of the authors reduced the coupling effort to zero, they could not give due attention to the improvement in transient performance of 2-dof TRMS. Considering the above mentioned aspects of 2-dof TRMS, in the present work, the aim is to identify a non-linear sliding surface with high robustness property and validate through both simulation and real time implementation for 2-dof TRMS.

Considering a pure electrical MIMO system dual input buck boost converters (DIBB), the authors have combined all state space models during each state mode of operation and derived an average transfer function. Also the authors have designed a proportional integral (PI) controller using pole

placement techniques. Duty ratio of one of the power switches is fixed while other one is varied to get output voltage regulation. But the determination of average transfer function model is very complex which is one of the draw back of the above mentioned control strategy. Hence the aim is to design a robust chattering free controller for the expected performance of dual input buck boost converter (DIBB).

2.6   Methodology

The Methodology followed involves both simulation and laboratory experimentation. In the case of part 1 of the work that was pertaining to 2-dof TRMS, investigations were carried out using the dynamical model of the TRMS that was available. For DIBB, the simulations were carried out using Matlab and the models obtained were subsequently used in formulating advanced control strategy to incorporate sliding mode control. The details can be seen in subsequent chapters. The work is divided in two parts: Part 1 deals with TRMS and part 2 is pertaining to DIBB. An analysis of the result and the view on the effectiveness in the control strategies in the different time frames of system dynamics is given to throw light on findings.

Chapter 3

Modeling and Decoupler design of 2-dof Twin Rotor MIMO system

3.1 Introduction

The system modelling plays an crucial role in the study analysis of any system. The accuracy in system modelling guarantees the accuracy in system performance. For any system the modelling has to be done before the application of control signal. There are two types of modelling namely transfer function modelling and state space modelling. The transfer function model is simple and powerful, but it is having following draw backs. 1) It is applicable only to linear time invariant system. 2) It is restricted to single input single output system. 3) It Provides no information regarding the internal state of the system. Also 4) The separate transforms are needed for time domain and discrete domain.

The advantages of using state variable approaches are as follows 1) This approach can be applied to both time varying and time in-varying system. 2) The same mathematical formulation can be used for continuous and discon-

tinuous system. Since the system considered in this thesis is highly non-linear multiple input multiple output system, the state space modelling approach is done. The transfer function model is derived from state space modelling. The information about the coupling effect between the signals can be visualized more easily in transfer function model. Hence in this chapter, the state space modelling of 2-dof TRMS has been done from the dynamics of the 2-dof TRMS which is given in [21]. Since the system is found to be heavily coupled, a decoupler is designed using minimal-di method.

3.2 State space Modeling of 2-dof TRMS

It is evident that the system is non-linear from the above set of equations (2.1) to (2.9). These set of equations can be converted in to state space model as follows: The state space model given below consists of state equation and output equation.

The state equation is given by:

$$\dot{X} = EX + KU + N \tag{3.1}$$

The output equation is:

$$Y = HX + IU \tag{3.2}$$

where $EX + KU$ represents the linear part of the system and N represents non-linear part. The matrix E represents the system matrix, K accounts for the input distribution matrix, X is the state vector, Y is the output vector and U is the control input. U is given by: $U = \begin{bmatrix} u_1 \\ u_2 \end{bmatrix}$, where u_1 is the input (control) voltage applied to main rotor and u_2 is the input (control) voltage applied to tail rotor. The maximum and minimum input(control) voltages for both main rotor and tail rotors are between $+2.5V$ and $-2.5V$ [21].

The state vector X of 2-dof TRMS is given by

$$X = \begin{bmatrix} \psi & \dot{\psi} & \phi & \dot{\phi} & \tau_1 & \tau_2 \end{bmatrix}^T \tag{3.3}$$

where

ψ : Pitch angle of 2-dof TRMS

ϕ : Yaw angle of 2-dof TRMS

$\dot{\psi}$: Pitch angle velocity

$\dot{\phi}$: Yaw angle velocity

τ_1 : Torque developed in main rotor

τ_2 : Torque developed in the tail rotor

Hence the derivative of X is

$$\dot{X} = \begin{bmatrix} \dot{\psi} & \ddot{\psi} & \dot{\phi} & \ddot{\phi} & \dot{\tau}_1 & \ddot{\tau}_1 \end{bmatrix}^T \tag{3.4}$$

The output vector Y is given by

$$Y = \begin{bmatrix} \psi & \phi \end{bmatrix}^T \tag{3.5}$$

Generally, all the researchers and academicians neglected the coupling that exists between pitch and yaw and they modelled the system accordingly. But the coupling effect also has to be taken in to consideration. It can be written as

$$\dot{\psi} = d(\psi)/dt \tag{3.6}$$

Linear part of the pitch is represented by:

$$\ddot{\psi} = -\frac{B_{1\psi}}{I_1}\dot{\psi} + \frac{b_1}{I_1}\tau_1 - \frac{k_{gy}}{I_1}b_1 \cos(\psi)\dot{\phi}\tau_1 \tag{3.7}$$

Here the term $\dfrac{k_{gy}}{I_1}b_1$ represents the coupling term. By substituting the values for k_{gy}, I_1 and $B_{1\psi}$ from the table (8.1) in appendix the equation (3.7)

27

becomes:

$$\ddot{\psi} = -0.0882\dot{\psi} + 1.358\tau_1 \tag{3.8}$$

similarly

$$\dot{\phi} = d(\phi)/dt \tag{3.9}$$

and

$$\ddot{\phi} = -\frac{B_{1\phi}}{I_2}\dot{\phi} + \frac{b_2}{I_2}\tau_2 - \frac{k_c}{I_2}b_1\tau_1 \tag{3.10}$$

substituting the values , $I_2, B_{1\phi}, b_2 and k_c$ from the table (8.1) equation (3.10) becomes:

$$\ddot{\phi} = -5\dot{\phi} + 1.675\tau_1 + 4.5\tau_2 \tag{3.11}$$

The time derivative of the torque developed in the main rotor is represented by:

$$\dot{\tau}_1 = -\frac{T_{10}}{T_{11}}\tau_1 + \frac{k_1}{T_{11}}u_1 \tag{3.12}$$

Substituting the values of T_{11}, k_1, T_{10} from Table (8.1) in appendix:

$$\dot{\tau}_1 = -0.909\tau_1 + u_1 \tag{3.13}$$

The time derivative of torque developed in the tail rotor is represented by:

$$\dot{\tau}_2 = -\frac{T_{20}}{T_{21}}\tau_2 + \frac{k_2}{T_{22}}u_2 \tag{3.14}$$

Substituting the values of T_{21}, k_2, T_{22} from Table (8.1) in appendix:

$$\dot{\tau}_2 = -\tau_2 + 0.8u_2 \tag{3.15}$$

From equations (3.6),(3.8),(3.9),(3.11),(3.13) and (3.15) the state matrix

E, input matrix K, output matrix H and I are calculated as:

$$E = \begin{bmatrix} 0 & 1 & 0 & 0 & 0 & 0 \\ 0 & -0.0882 & 0 & 0 & 1.358 & 0 \\ 0 & 0 & 0 & 1 & 0 & 0 \\ 0 & 0 & 0 & -5 & 1.675 & 4.5 \\ 0 & 1 & 0 & 0 & -0.909 & 0 \\ 0 & 1 & 0 & 0 & 0 & -1 \end{bmatrix} \quad (3.16)$$

Input vector K is given by

$$K = \begin{bmatrix} 0 & 0 \\ 0 & 0 \\ 0 & 0 \\ 0 & 0 \\ 1 & 0 \\ 0 & 0.8 \end{bmatrix} \quad (3.17)$$

The output matrix H is obtained as:

$$H = \begin{bmatrix} 1 & 0 & 0 & 0 & 0 & 0 \\ 0 & 0 & 1 & 0 & 0 & 0 \end{bmatrix} \quad (3.18)$$

and

$$I = \begin{bmatrix} 0 & 0 \\ 0 & 0 \end{bmatrix} \quad (3.19)$$

The non-linearities associated with the 2-dof TRMS are parabolic non-linearity and trigonometric non-linearity. The non-linear term $0.1985\tau_1^2 - 0.047\sin(\psi) + 0.239 sin(2\psi)\dot{\phi}^2 - 6.75 * 10^{-4}\cos(\psi)\dot{\phi}\tau_1^2$ corresponds to $\ddot{\psi}$ and $\tau_2^2 + 0.135\tau_1^2$ corresponds to $\ddot{\phi}$. Now the non-linear part in the equation(3.1) N is written as;

$$N = \begin{bmatrix} n_1 \\ n_2 \\ n_3 \\ n_4 \\ n_5 \\ n_6 \end{bmatrix} \tag{3.20}$$

The non-linear part related with pitch angle position and yaw angle position are given by n_2, n_5 respectively. These are expressed as:

$$n_2 = \frac{a_1}{I_1}\tau_1^2 - \frac{M_g}{I_1}\sin\psi + \frac{0.0326}{2I_1}sin(2\psi)\dot{\phi}^2 \\ -k_{gy}a_1\cos(\psi)\dot{\phi}\tau_1^2 \tag{3.21}$$

$$n_5 = \frac{a_2}{I_2}\tau_2^2 - \frac{1.75}{I_2}k_ca_1\tau_1^2 \tag{3.22}$$

The non-linear part can also be written in matrix form by substituting the parameter values from the Table(8.1) in appendix. The non-linearity Matrix N is given by:

$$N = \begin{bmatrix} 0 \\ [0.1985\tau_1^2 - 0.047\sin(\psi) + 0.239sin(2\psi)\dot{\phi}^2 - \\ 6.75*10^{-4}\cos(\psi)\dot{\phi}\tau_1^2] \\ 0 \\ \tau_2^2 + 0.135\tau_1^2 \\ 0 \\ 0 \end{bmatrix} \tag{3.23}$$

Referring to the Table (8.1)in appendix, the various parameter values are substituted for $n_2$and n_5, the maximum value for n_2 is calculated as $n_{2max} = 0.875$ and maximum value for n_5 is calculated as $n_{5max} = 1.68$
From the values obtained E, K, H and I, the transfer function can be derived

using the equation:

$$G(s) = H(SI - A)^{-1}B + I \tag{3.24}$$

Thus the transfer function obtained is:

$$G(s) = \begin{bmatrix} \dfrac{1.358}{s(s + 0.08819)(s + 0.9090)} & 0 \\ \dfrac{1.675}{s(s + 0.9090)(s + 5)} & \dfrac{3.6}{s(s + 1)(s + 5)} \end{bmatrix} \tag{3.25}$$

This Section has dealt with the state space modeling and transfer function modeling of 2-dof TRMS system. It is quite clear from the transfer function G(s) given in equation (3.25) that coupling exists between pitch and yaw of 2-dof TRMS. The existing coupling term as revealed in G(s)has to be nullified. The decoupler to be designed is given in the next Section.

3.3   Design of Decoupler for 2-dof TRMS

The transfer function of 2-dof TRMS equation (3.25) reveals that there exists coupling between the yaw (ϕ) and input signal (u_1) given to pitch. Also it is obvious that there is no coupling between pitch (ψ) and input signal given to yaw (u_2). The above coupling effects can be nullified by designing a suitable decoupler which is also known as pre-compensator. This is dealt in this Section.

For a given MIMO plant G, a method to design pre-compensator (decoupler) Z is available in [43]. Figure 3.1 represents the system with decoupler. Hence ψ_r and ϕ_r represent the reference pitch and yaw angle respectively and these are given as controller inputs to two 2-dof SISO controllers. The controller outputs v_1 and v_2 are the inputs to the pre-compensator (decoupler). The decoupler outputs are u_1 and u_2 respectively and these are given as the inputs to the system. While designing the decoupler Z, it is to be ensured that the unstable poles and zeros are not cancelled against each other to
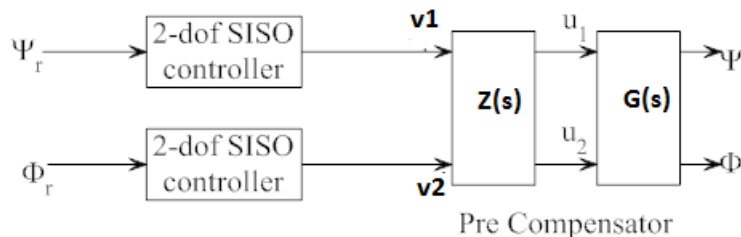
Figure 3.1: 2-dof TRMS with decoupler.

ensure the controllability of the system. To avoid the cancellation of unstable poles and zeros the $minimal - d_i$ (minimum number of unstable poles and zeros including those at infinity) is calculated first and then decoupler is designed accordingly. The method of calculation of decoupler Z in [43] is applied here. The decoupler for 2-dof TRMS is conceived as below:

The decoupler is given by

$$Z = G^{-1}D. \tag{3.26}$$

where $D = minimal - d_i = GZ = \text{diag}\ (d_i)$ where G is the system transfer function. From the transfer function obtained in equation 3.24, it is obvious that G has unstable poles at $s = 0$. The pole at $s = -0.0881$ which is very near to zero is also taken as unstable pole. The zeros are at $s = \text{inf}$. Then using G and G^{-1}, the terms necessary for the design of $minimal - d_i$ in this model is calculated using the procedure explained below [43]:

The $minimal - d_i$ consists of two terms d_1 and d_2. $l_1^{\text{inf}}(G^{-1}) = l_2^{\text{inf}}(G^{-1}) = 3$. $l_1^{\text{inf}}(G^{-1})$ represents the number of poles present in the d_1 of minimal-$d_i and l_2^{\text{inf}}(G^{-1})$ represents the number of poles present in the d_2 of $minimal - d_i$. From the above design procedure for $minimal - d_i$, it is noted that d_1 consists of three poles. The d_2 consists of three poles. Also $k_1^0(G) = 1$, $k_2^0(G) = 1, k_1^{-0.08819}(G) = 1$ and $k_2^{-0.08819}(G) = 0$

These terms are used for calculating the the factors that must be present in

32

$minimal - d_i$s as:

$\beta^0(d_1) = k_1^0(G) = 1$, using this equation it is calculated that there is a pole at origin in the term d_1 of minimal-d_i.

$\beta^0(d_2) = k_2^0(G) = 1$ using this equation it is calculated that there is a pole at origin in the term d_2 of minimal-d_i.

$\beta^{-0.08819}(d_1) = k_1^{-0.08819}(G) = 1$, using this equation it is calculated that the $s = -0.08819$ is present in the term d_1 of $minimal - d_i$.

$\beta^{-0.08819}(d_2) = k_2^{-0.08819}(G) = 0$. using this equation it is calculated that the pole at $s = -0.08819$ is not present in d_2 of $minimal - d_i$.

Thus the poles that are present in the d_1 are one at origin, second one at $s = -0.0889$. The third one is assumed to be at $s = \alpha_1$. The zeros of d_1 are at infinity. The poles in the term d_2 are one at origin. The other two poles are assumed to be at $s = \alpha_2$ and $s = \alpha_3$ and three zeros at infinity.

Now $minimal - d_i$s become:

$$d_1 = \frac{1}{s(s + 0.0881)(s + \alpha_1)} \tag{3.27}$$

and

$$d_2 = \frac{1}{s(s + \alpha_2)(s + \alpha_3)} \tag{3.28}$$

For simplicity and to match with system taken, it is assumed that $\alpha_1 = \alpha_2 = 0.9090$ and $\alpha_3 = 5$. The diagonal matrix D is given by $D = $ diag $minimal - (d_i)$

$$D = \begin{bmatrix} \dfrac{1}{s(s + 0.0881)(s + 0.9090)} & 0 \\ 0 & \dfrac{1}{s(s + 0.9090)(s + 5)} \end{bmatrix} \tag{3.29}$$

The inverse of transfer function function G is calculated using Matlab as:

$$G^{-1} = \begin{bmatrix} \dfrac{s^3 + 0.9972s^2 + 0.08017s}{1.358} & 0 \\ -0.3426(s + 0.08819)s(s + 1) & \dfrac{s^3 + 6s^2 + 5s}{3.6} \end{bmatrix} \tag{3.30}$$

Now the pre-compensator (decoupler) $Z(s)$ is calculated from the equation (3.26) as:

$$Z(s) = \begin{bmatrix} \dfrac{0.736}{1} & 0 \\ \dfrac{-0.34(s + 1)}{s + 0.9090} & \dfrac{0.277(s + 1)}{s + 0.9090} \end{bmatrix} \tag{3.31}$$

With the introduction of decoupler, the coupling term of 2-dof TRMS system $G(s)$ is made to zero. Now the net transfer function of the 2-dof TRMS system is obtained as:

$$G_1(s) = \begin{bmatrix} \dfrac{0.99994}{s^3 + 0.9972s^2 + 0.08017s} & 0 \\ 0 & \dfrac{0.9999}{s^3 + 6s^2 + 5s} \end{bmatrix} \tag{3.32}$$

To match with our system $G(s)$ given in equation (3.32), the first row is multiplied with 1.358 and the second row with 3.6. Then the modified transfer function of the decoupled system becomes:

$$G_2(s) = \begin{bmatrix} \dfrac{1.358}{s^3 + 0.9972s^2 + 0.08017s} & 0 \\ 0 & \dfrac{3.6}{s^3 + 6s^2 + 5s} \end{bmatrix} \tag{3.33}$$

From equation (3.33), The pitch transfer function is given by:

$$\psi(s) = \frac{1.358}{s^3 + 0.9972s^2 + 0.08017s} u_1(s) \tag{3.34}$$

The yaw angle transfer function is given by:

$$\phi(s) = \frac{3.6}{s^3 + 6s^2 + 5s} \tag{3.35}$$

Thus, the transfer function of the decoupled system for pitch and yaw are obtained.

3.4 Conclusion

The state space modeling of 2-dof TRMS using the dynamics which is dealt in this chapter. It is to be noted that the system is highly non-linear. Therefore, the modelling has been done by including all non-linearities. Also from the transfer function obtained, it is concluded that the system is heavily coupled. In order to eliminate the coupling effect a decoupler is designed using minimal-di method. The decoupler thus obtained nullifies the cross-coupling effect between pitch and yaw of the TRMS system. Hence the next step is the design controller suitable for the 2-dof TRMS. The sliding mode control is suitable for controlling the TRMS system as it is invariant to parametric variation and external disturbance. This design needs the sliding mode control design and sliding surface design. Hence the next chapter is dealt with the sliding mode controller design and linear sliding surface design for 2-dof TRMS.

Chapter 4

Design of Linear Sliding Surface for 2-dof Twin Rotor MIMO system

4.1 Introduction

The PID controller is a commonly used controller for Multiple Input Multiple Output systems. If the precise model of the system is available in hand, the PID controller will perform well. But it has some drawbacks of high settling time and overshoot. Also the PID controller is not resilient to the external disturbances. Hence the aim of this chapter is to design a sliding mode controller for 2-dof TRMS. Design of linear sliding surface is the first and foremost one prior to the design of sliding mode controller. For any system under consideration sliding surface can be linear or non-linear. The linear sliding surface (LSS) is designed using optimal sliding surface design procedure in variable structure system. This system involves the design of sliding surfaces for both pitch and yaw angles. The design of sliding surfaces in both above mentioned cases are synthesized using quadratic minimization approach [63].

This chapter is organised as follows: The design of PID controller for 2-dof TRMS is explained in Section 4.2 followed by the simulation analysis in Section 4.3. The design of linear sliding surfaces for pitch and yaw angles of 2-dof TRMS are discussed in Sections 4.4 and 4.5, respectively. Section 4.6 describes the design of feedback controller for pitch and yaw. The simulation results with linear surface design are presented in Section 4.7. The performance comparison of the linear sliding surface design (LSS) with PID controller is given in Section 4.8. The analysis of the results is carried out in Section 4.9. Finally conclusion is given in Section 4.10.

4.2   PID controller design

From the decoupled transfer function for pitch angle obtained in equation (3.34), it is noted that the system does not have delay time, hence the PID controller is designed using Ziegler- Nichols ultimate gain method [62]. By setting the values of $K_I = 0$, $K_D = 0$, the value K_u is increased till the sustained oscillation is obtained as explained in [62]. The proportional constant K_p is given by:

$$K_p = 1.2K_u \tag{4.1}$$

The values of K_I and K_D are calculated from the following relation

$$K_I = \frac{1.2K_u}{T_u} \tag{4.2}$$

$$K_D = \frac{3K_u * T_u}{40} \tag{4.3}$$

4.2.1   Calculation of K_P, K_I and K_D for Pitch

The equation (3.34) shows the pitch angle transfer function and equation (3.35) shows the yaw angle transfer function. The PID controller is designed

for both pitch angle and yaw angle as per [62]. In this method K_u is adjusted till the sustained oscillation is obtained.

The figure 4.1 shows the sustained oscillation obtained for the pitch angle transfer function when zeiglers method is used. The time period between two consecutive positive or negative peaks is taken as T_u. The value of T_u pitch angle is obtained as 22.3 (34.3-12). proportional constant K_P, Integral constant K_I and derivative constant K_D are calculated using the equations (4.1),(4.2) and (4.3) respectively as: $K_P =.0356$ $K_I = 0.0991$. $K_D = 0.0032$ for pitch angle PID controller design.
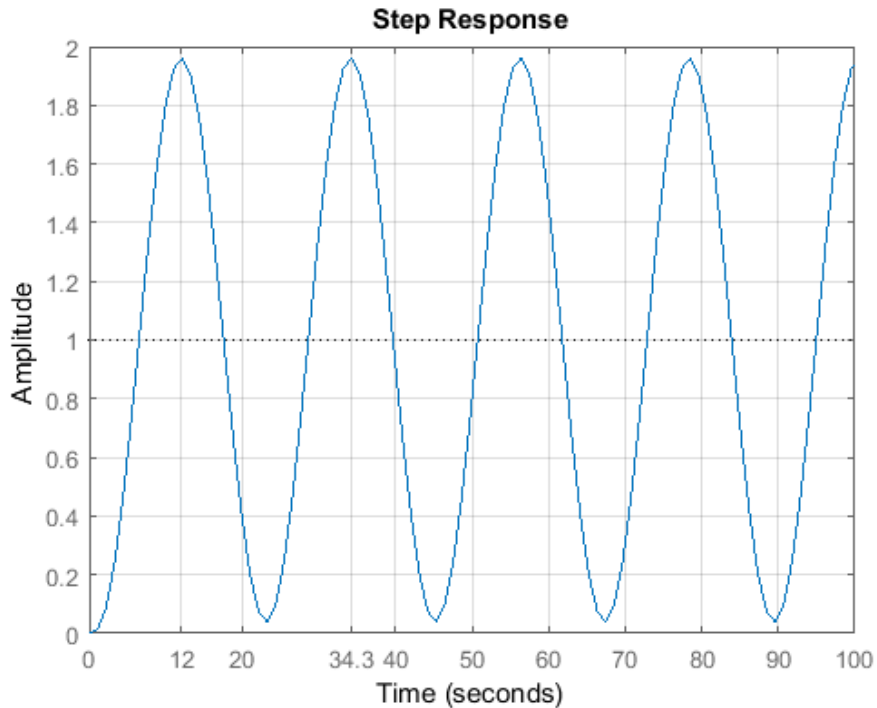
Figure 4.1: sustained oscillation for Pitch angle Transfer function
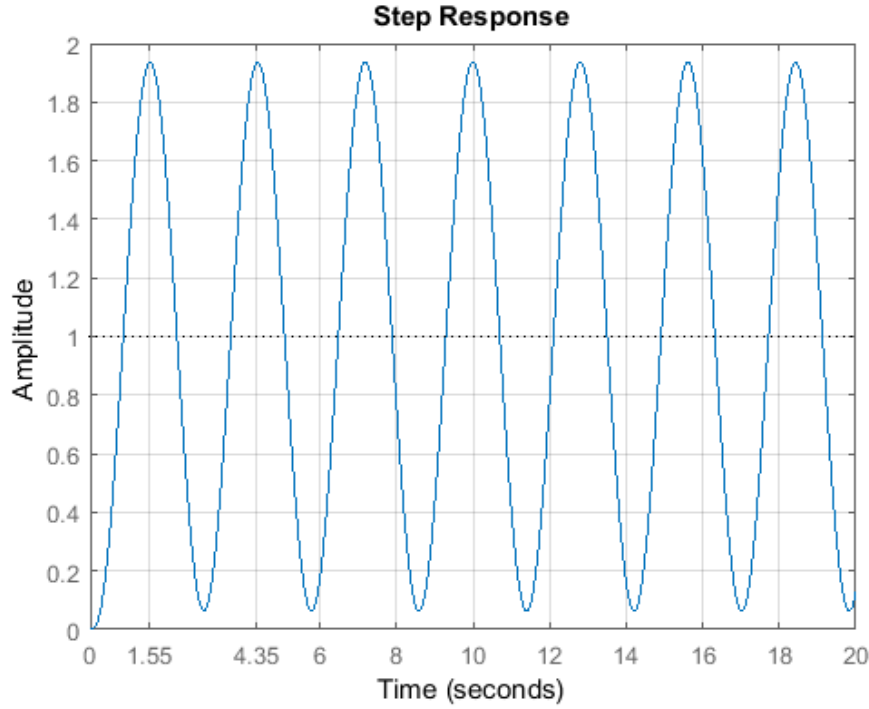
Figure 4.2: Sustained oscillation for yaw angle Transfer function

The same procedure is repeated for yaw angle PID controller.figure 4.2 shows the sustained oscillation obtained for the yaw angle transfer function. The value of T_u yaw angle is obtained as 2.8 (4.35-1.55). proportional constant K_P, Integral constant K_I and derivative constant K_D are calculated using the equations (4.1),(4.2) and (4.3) respectively as: $K_P = 5$ $K_I = 3.5714$ $K_D = 1.75$ for yaw angle PID controller design.

$$K_I = \frac{1.2K_u}{T_u} = 3.5714 \tag{4.4}$$

$$K_D = \frac{3K_u * T_u}{40} = 1.75 \tag{4.5}$$

40

The next Section deals with the analysis of simulation results with PID controller design.

4.3 Simulation results of 2-dof TRMS with PID controller design

Figure 4.3 represents the response of the pitch angle position tracking when a matched disturbance of $0.4sin(0.1t) + 0.4$ is applied with PID controller. The matched disturbance is the disturbance through the input channel. The matched disturbance is given to check how the controller works when the disturbance is applied through input channel. Usually 30 to 40 percent of the input magnitude is applied as the disturbance. Since the input given is unit step, the magnitude of disturbance is taken as 0.4. It is observed that initial overshoot and settling time are very high. There is 60 percent overshoot in pitch angle position tracking and the settling time for pitch is found to be 28 seconds based on 5 percent band (5 percent band is taken for calculating settling time through out this work). It is also noted that the tracking property is lost with the use of PID controller from $t = 50$ second onwards.

Similarly figure 4.4 represents the response of the yaw angle position tracking when a matched disturbance of $0.4sin(0.1t) + 0.4$ is applied with PID controller. There is 50 percent overshoot in yaw angle position tracking with settling time 40 seconds. It is also noted that the tracking property is lost with the use of PID controller from $t = 50$ seconds onwards.
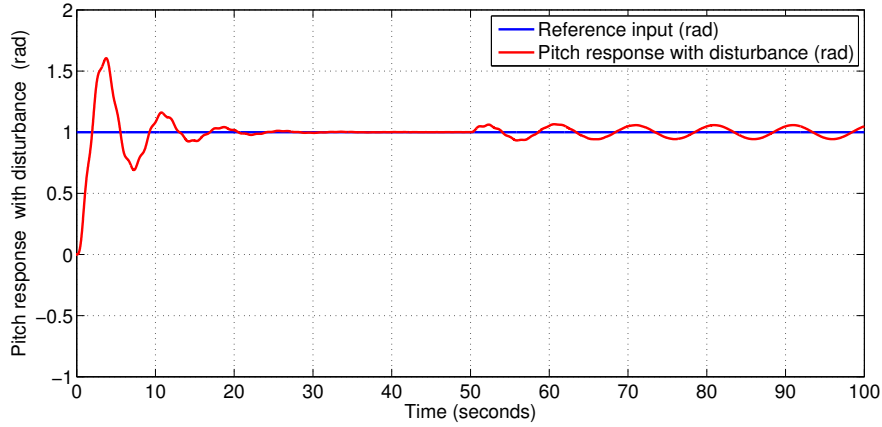
Figure 4.3: Pitch angle position tracking with PID controller design when matched disturbance is applied at 50 sec.
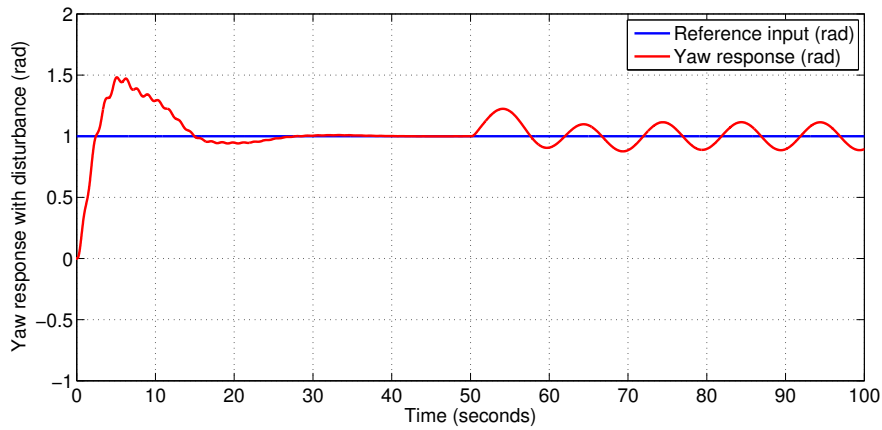
Figure 4.4: Yaw angle position tracking response with PID controller design when disturbance is applied at 50 seconds.

Hence the drawbacks of PID controller are 1)high peak overshoot and settling time. 2)Robustness property of the system is poor with the use of

PID controller as PID is not resilient to the matched disturbance (disturbance through input channel). Referring to the above mentioned draw backs of PID controller, it is required to find a controller which is resilient. The literature review reveals the fact that the above mentioned draw backs can be mitigated to a large extent with the help of sliding mode controller.

4.4   Design of linear sliding surface For Pitch

Considering the above draw backs of PID controller which is explained in Section 4.3, the aim is to identify a highly robust sliding mode controller. The sliding surface has to be designed first and then sliding mode controller. The state space modelling is necessary to design the sliding surface. The state space modelling is derived from transfer function model which is given in equation (3.25). It is observed that there is coupling effect between pitch and yaw of 2-dof TRMS. The coupling effect has been reduced by designing a suitable decoupler. The decoupled transfer function is given in Equation (3.33). Decoupled transfer function is used for the design of linear sliding surface. From the decoupled transfer function model (3.33), the main rotor transfer function is given by:

$$\psi(s) = \frac{1.358}{s^3 + 0.9972s^2 + 0.08017s} u_1(s) \tag{4.6}$$

The phase variable form of state space model can be derived from the transfer function model as:

$$\begin{aligned}
\dot{\psi}_1 &= \psi_2 \\
\dot{\psi}_2 &= \psi_3 \\
\dot{\psi}_3 &= 0\psi_1 - 0.08017\psi_2 - 0.9972\psi_3 + 1.358u_1
\end{aligned} \tag{4.7}$$

The state model in matrix form of equation (4.2) is :

$$
\begin{bmatrix} \dot{\psi}_1 \\ \dot{\psi}_2 \\ \dot{\psi}_3 \end{bmatrix} = \begin{bmatrix} 0 & 1 & 0 \\ 0 & 0 & 1 \\ 0 & 0.08017 & 0.9972 \end{bmatrix} \begin{bmatrix} \psi_1 \\ \psi_2 \\ \psi_3 \end{bmatrix} + \begin{bmatrix} 0 \\ 0 \\ 1.358 \end{bmatrix} u_1
\tag{4.8}
$$

From the state space model obtained in the previous section, the sliding surface is to be calculated for pitch. The relation between sliding surface $S_1(t)$ for pitch and pitch angle state vector $\psi(t)$ is given below as [63]:

$$
S_1(t) = L\psi(t)
\tag{4.9}
$$

where $\psi(t) = [\psi_1(t)\psi_2(t)\psi_3(t)]$ and L is sliding surface matrix for pitch. The system represented by Equation (4.6) is a third order system. Generally, regular form approach is employed to bring down the higher order system. A different set of state variables is considered using $h(t)$ to develop regular form. This $h(t)$ is related to the conventional pitch angle state vector $\psi(t)$ as [63]:

$$
h(t) = T_r\psi(t)
\tag{4.10}
$$

where T_r is the orthogonal matrix used for coordinate transformation. The regular form of equation (4.7) becomes;

$$
\begin{aligned}
\dot{h}_1(t) &= A_{11}h_1(t) + A_{12}h_2(t) + B_1u_1(t \\
\dot{h}_2(t) &= A_{21}h_1(t) + A_{22}h_2(t) + B_2u_1(t)
\end{aligned}
\tag{4.11}
$$

thus the equation (4.11) is written in matrix form as:

$$
\begin{bmatrix} \dot{h_1} \\ \dot{h_2} \end{bmatrix} = \begin{bmatrix} A_{11} & A_{12} \\ A_{21} & A_{22} \end{bmatrix} \begin{bmatrix} h_1 \\ h_2 \end{bmatrix} + \begin{bmatrix} B_1 \\ B_2 \end{bmatrix} u_1
$$

(4.12)

where

$$
A_{11} = \begin{bmatrix} 0 & 1 \\ 0 & 0 \end{bmatrix} A_{12} = \begin{bmatrix} 0 \\ 1 \end{bmatrix} A_{21} = \begin{bmatrix} 0 & -0.08017 \end{bmatrix}
$$

$$
A_{22} = \begin{bmatrix} 0.9972 \end{bmatrix} B_1 = \begin{bmatrix} 0 \\ 0 \end{bmatrix} B_2 = \begin{bmatrix} 1.358 \end{bmatrix}
$$

(4.13)

Now, switching function associated with the in regular form in equation (4.12) is:

$$
S_1(t) = l_1 h_1(t) + l_2 h_2(t)
$$

(4.14)

During sliding motion the switching function will be equal to zero. Hence the equation (4.14)can be rewritten as:

$$
l_1 h_1(t) + l_2 h_2(t) = 0
$$

(4.15)

From equation (4.15) $h_2(t)$ can be obtained as:

$$
h_2(t) = l_2{}^{-1} l_1 h_1(t) = -M_1 h_1(t)
$$

(4.16)

where $M_1 = l_2{}^{-1} l_1$ The calculation of M_1 is detailed below.

4.4.1 Calculation of M_1

The calculation of M_1 is done after the selection of quadratic performance index J. Let the quadratic performance index J be:

$$J = \frac{1}{2} \int_{t_s}^{\infty} \psi^T Q \psi \, dt \qquad (4.17)$$

where t_s is the time at which sliding mode commences, matrix Q is known as performance index matrix. It is selected to minimize the deviation of final state of the system from its desired value. Assume Q as identity matrix

$$Q = \begin{bmatrix} 1 & 0 & 0 \\ 0 & 1 & 0 \\ 0 & 0 & 1 \end{bmatrix} \qquad (4.18)$$

The performance matrix Q is also transformed and partitioned with $h(t)$, where $h(t)$ is a different set of state variables employed for regular form approach [63]. The regular form of the matrix Q is given by:

$$T_r Q T_r^T = \begin{bmatrix} Q_{11} & Q_{12} \\ Q_{21} & Q_{22} \end{bmatrix} \qquad (4.19)$$

where T_r is calculated as 1 as in [63]. and

$$Q_{21} = Q_{12}^T \qquad (4.20)$$

where

$$Q_{11} = \begin{bmatrix} 1 & 0 \\ 0 & 1 \end{bmatrix}, Q_{12} = \begin{bmatrix} 0 \\ 0 \end{bmatrix} \qquad (4.21)$$

and

$$Q_{21} = \begin{bmatrix} 0 & 0 \end{bmatrix} Q_{22} = \begin{bmatrix} 1 \end{bmatrix} \tag{4.22}$$

Now the performance index in coordinate transform becomes:

$$J = \frac{1}{2} \int_{t_s}^{\infty} h_1^T Q_{11} h_1 + 2 h_1^T Q_{12} h_2 + h_2^T Q_{22} h_2 \tag{4.23}$$

The above equation can be rearranged as:

$$\begin{aligned} J =& \frac{1}{2} \int_{t_s}^{\infty} h_1^T \hat{Q} h_1 + \\ & ((h_2 + Q_{22}^{-1} Q_{21} h_1))^T Q_{22} (h_2 + Q_{22}^{-1} Q_{21} h_1) \end{aligned} \tag{4.24}$$

where

$$\hat{Q} = Q_{11} - Q_{12} Q_{22}^{-1} Q_{21} \tag{4.25}$$

Now defining

$$v = h_2 + Q_{22}^{-1} Q_{21} h_1 \tag{4.26}$$

The modified performance index is obtained as:

$$J = \frac{1}{2} \int_{t_s}^{\infty} h_1^T \hat{Q} h_1 + v^T Q_{22} v \tag{4.27}$$

Hence this performance index is to be minimized subject to constraint equation in quadratic form as given below. The constraint equation is the system equation

$$\dot{h}_1(t) = A_{11} h_1(t) + A_{12} h_2(t) \tag{4.28}$$

eliminating the $h_2(t)$ contribution by equation (4.26), the modified constraint equation becomes:

$$\dot{h}_1(t) = \hat{A}_{11} h_1(t) + A_{12} v(t) \tag{4.29}$$

47

where

$$\hat{A} = A_{11} - A_{12}Q_{22}^{-1}Q_{21} \tag{4.30}$$

$\hat{A}$ is calculated to be:

$$\hat{A} = \begin{bmatrix} 0 & 1 \\ 0 & 0 \end{bmatrix} \tag{4.31}$$

The expression for h_2 partition as per [63] is given by:

$$h_2 = -Q_{22}^{-1}(A_{12}^T P + Q_{21})h_1 \tag{4.32}$$

where P is the positive definite matrix . Comparing the equations (4.32) and (4.16) the value of M_1 is calculated as:

$$M_1 = -Q_{22}^{-1}(A_{12}^T P + Q_{21}) \tag{4.33}$$

From the above equation, it is clear that the value of M_1 can be obtained by first calculating the the value of Matrix P. The matrix P can be calculated from ricatti equation.

$$P\hat{A} + \hat{A}^T P - PA_{12}Q_{22}^{-1}A_{12}^T P + \hat{Q} = 0 \tag{4.34}$$

By substituting available values in ricatti equation (4.34), a unique positive definite solution P can be obtained as:

$$P = \begin{bmatrix} 1 & \sqrt{3} \\ \sqrt{3} & 1 \end{bmatrix} \tag{4.35}$$

Substituting all the values of P, Q_{22}^{-1}, A_{12}^T in equation (4.27), M_1 is obtained as :

$$M_1 = \begin{bmatrix} 1 & \sqrt{3} \end{bmatrix} \tag{4.36}$$

Now the switching surface S_1 is given by:

$$S_1 T_r^T = \begin{bmatrix} M_1 & I_m \end{bmatrix} \tag{4.37}$$

where I_m is the identity matrix.

$$S_1 = \begin{bmatrix} M_1 & I_m \end{bmatrix} * T_r \tag{4.38}$$

where I_m is the identity matrix. The value of T_r is calculated as 1 using QR decomposition. Then sliding surface of the pitch angle calculated as:

$$S_1 = \begin{bmatrix} 1 & \sqrt{3} & 1 \end{bmatrix} \begin{bmatrix} \psi_1 \\ \psi_2 \\ \psi_3 \end{bmatrix} \tag{4.39}$$

Equation (4.39) defines the sliding surface for pitch. Now the sliding surface for the yaw is to be obtained.

4.5 Design of linear sliding surface for yaw of 2-dof TRMS

The switching surface for yaw can be calculated in the same way as that of pitch surface. The transfer function model of yaw is obtained from equation(3.35) as:

$$\phi(s) = \frac{3.6}{s^3 + 6s^2 + 5s} u_2(s) \tag{4.40}$$

The phase variable form of the above equation can be written as:

$$\dot{\phi}_1 = \phi_2$$
$$\dot{\phi}_2 = \phi_3 \tag{4.41}$$
$$\dot{\phi}_3 = -5\phi_2 - 6\phi_3 + 3.6u_2$$

Continuing in the same way as that of pitch angle surface design, the switching surface for yaw angle is obtained. From the state space model obtained in equation (4.41), the sliding surface is to be calculated for yaw. The relation between sliding surface $S_2(t)$ for yaw and yaw angle state vector $\phi(t)$ is given below as [62]:

$$S_2(t) = L_1\phi(t) \tag{4.42}$$

where $\phi(t) = [\phi_1(t)\phi_2(t)\phi_3(t)]$ and L_1 is sliding surface matrix for yaw. The system represented by Equation (4.41) is a third order system. Generally, regular form approach is employed to bring down the higher order system. A different set of state variables is considered using $h(t)$ to develop regular form. This $h(t)$ is related to the conventional pitch angle state vector $\phi(t)$ as [63]:

$$h(t) = T_r\phi(t) \tag{4.43}$$

where T_r is the orthogonal matrix used for coordinate transformation. The regular form of equation (4.41) becomes;

$$\dot{h}_3(t) = A_{11}h_3(t) + A_{12}h_4(t) + B_1u_2(t$$
$$\dot{h}_4(t) = A_{21}h_3(t) + A_{22}h_4(t) + B_2u_2(t) \tag{4.44}$$

The equation (4.3) is converted into the matrix form as:

$$\begin{bmatrix} \dot{h_3} \\ \dot{h_4} \end{bmatrix} = \begin{bmatrix} A_{11} & A_{12} \\ A_{21} & A_{22} \end{bmatrix} \begin{bmatrix} h_3 \\ h_4 \end{bmatrix} \\ + \begin{bmatrix} B_1 \\ B_2 \end{bmatrix} u_2 \tag{4.45}$$

where

$$A_{11} = \begin{bmatrix} 0 & 1 \\ 0 & 0 \end{bmatrix} A_{12} = \begin{bmatrix} 0 \\ 1 \end{bmatrix} A_{21} = \begin{bmatrix} 0 & -5 \end{bmatrix} \\ A_{22} = \begin{bmatrix} -6 \end{bmatrix} B_1 = \begin{bmatrix} 0 \\ 0 \end{bmatrix} B_2 = \begin{bmatrix} 3.6 \end{bmatrix} \tag{4.46}$$

Now, switching function associated with the in regular form in equation (4.45) is:

$$S_2(t) = l_3 h_3(t) + l_4 h_4(t) \tag{4.47}$$

During sliding motion the switching function will be equal to zero. Hence the equation (4.47)can be rewritten as:

$$l_3 h_3(t) + l_4 h_4(t) = 0 \tag{4.48}$$

From equation (4.48) $h_3(t)$ can be obtained as:

$$h_4(t) = l_4{}^{-1} l_3 h_3(t) = -M_2 h_3(t) \tag{4.49}$$

where $M_2 = l_4{}^{-1} l_3$ The calculation of M_2 is detailed below.

4.5.1 Calculation of M_2

The calculation of M_2 is done after the selection of quadratic performance index J_1. Let the quadratic performance index J_1 be:

$$J_1 = \frac{1}{2} \int_{t_s}^{\infty} \phi^T Q \phi dt \qquad (4.50)$$

where t_s is the time at which sliding mode commences, matrix Q is known as performance index matrix. It is selected to minimize the deviation of final state of the system from its desired value. Assume Q as identity matrix

$$Q = \begin{bmatrix} 1 & 0 & 0 \\ 0 & 1 & 0 \\ 0 & 0 & 1 \end{bmatrix} \qquad (4.51)$$

The performance matrix Q is also transformed and partitioned with $h(t)$, where $h(t)$ is a different set of state variables employed for regular form approach [62]. The regular form of the matrix Q is given by:

$$T_r Q T_r^T = \begin{bmatrix} Q_{11} & Q_{12} \\ Q_{21} & Q_{22} \end{bmatrix} \qquad (4.52)$$

where T_r is calculated as 1 as in [62]. and

$$Q_{21} = Q_{12}^T \qquad (4.53)$$

where

$$Q_{11} = \begin{bmatrix} 1 & 0 \\ 0 & 1 \end{bmatrix}, Q_{12} = \begin{bmatrix} 0 \\ 0 \end{bmatrix} \qquad (4.54)$$

and

$$Q_{21} = \begin{bmatrix} 0 & 0 \end{bmatrix} Q_{22} = \begin{bmatrix} 1 \end{bmatrix} \tag{4.55}$$

Now the performance index in coordinate transform becomes:

$$J_1 = \frac{1}{2} \int_{t_s}^{\infty} h_3^T Q_{11} h_3 + 2h_3^T Q_{12} h_4 + h_4^T Q_{22} h_4 \tag{4.56}$$

The above equation can be rearranged as:

$$J_1 = \frac{1}{2} \int_{t_s}^{\infty} h_3^T \hat{Q} h_3 + \tag{4.57}$$
$$((h_4 + Q_{22}^{-1} Q_{21} h_3))^T Q_{22} (h_4 + Q_{22}^{-1} Q_{21} h_3)$$

where

$$\hat{Q} = Q_{11} - Q_{12} Q_{22}^{-1} Q_{21} \tag{4.58}$$

Now defining

$$v = h_4 + Q_{22}^{-1} Q_{21} h_3 \tag{4.59}$$

The modified performance index is obtained as:

$$J_1 = \frac{1}{2} \int_{t_s}^{\infty} h_3^T \hat{Q} h_3 + v^T Q_{22} v \tag{4.60}$$

Hence this performance index is to be minimized subject to constraint equation in quadratic form as given below. The constraint equation is the system equation

$$\dot{h}_3(t) = A_{11} h_3(t) + A_{12} h_4(t) \tag{4.61}$$

eliminating the $h_4(t)$ contribution by equation (4.61), the modified constraint equation becomes:

$$\dot{h}_3(t) = \hat{A}_{11} h_1(t) + A_{12} v(t) \tag{4.62}$$

where

$$\hat{A} = A_{11} - A_{12}Q_{22}^{-1}Q_{21} \tag{4.63}$$

$\hat{A}$ is calculated to be:

$$\hat{A} = \begin{bmatrix} 0 & 1 \\ 0 & 0 \end{bmatrix} \tag{4.64}$$

The expression for h_4 partition as per [63] is given by:

$$h_4 = -Q_{22}^{-1}(A_{12}^T P_1 + Q_{21})h_3 \tag{4.65}$$

where P_1 is the positive definite matrix . Comparing the equations (4.65) and (4.49) the value of M_2 is calculated as:

$$M_2 = -Q_{22}^{-1}(A_{12}^T P_1 + Q_{21}) \tag{4.66}$$

From the above equation, it is clear that the value of M_2 can be obtained by first calculating the the value of Matrix P_1. The matrix P_1 can be calculated from ricatti equation.

$$P_1\hat{A} + \hat{A}^T P_1 - P_1 A_{12}Q_{22}^{-1}A_{12}^T P_1 + \hat{Q} = 0 \tag{4.67}$$

By substituting available values in ricatti equation (4.67), a unique positive definite solution P_1 can be obtained as:

$$P_1 = \begin{bmatrix} 1 & \sqrt{3} \\ \sqrt{3} & 1 \end{bmatrix} \tag{4.68}$$

Substituting all the values of P_1, Q_{22}^{-1}, A_{12}^T in equation (4.67), M_2 is obtained as :

$$M_2 = \begin{bmatrix} 1 & \sqrt{3} \end{bmatrix} \tag{4.69}$$

Now the switching surface S_2 is given by:

$$S_2 T_r^T = \begin{bmatrix} M_2 & I_m \end{bmatrix} \tag{4.70}$$

where I_m is the identity matrix.

$$S_2 = \begin{bmatrix} M_2 & I_m \end{bmatrix} * T_r \tag{4.71}$$

where I_m is the identity matrix. The value of T_r is calculated as 1 using QR decomposition. Then sliding surface of the given system available in (4.40) is defined as:

$$S_2 = \begin{bmatrix} 1 & \sqrt{3} & 1 \end{bmatrix} \begin{bmatrix} \phi_1 \\ \phi_2 \\ \phi_3 \end{bmatrix} \tag{4.72}$$

Thus the sliding surfaces for both pitch and yaw of 2-dof TRMS are obtained. Now, the design of the controller is to be done which is discussed in next Section.

4.6 Design of state feedback controller for pitch and yaw of 2-dof TRMS

In the above Section, the design of linear surfaces for both pitch and yaw are carried out. The next important step towards achieving the expected system performance lies in the design of controllers. Generally the state feedback linearization technique is employed for design of controller [63]. In state feedback linearization, controller is designed so that the output tracks the reference signal. Unit step signal is taken as reference signal.

$$r_1(t) = 1 \tag{4.73}$$

The error signal which is the difference between output and reference is given by:

$$
\begin{aligned}
e_1 &= \psi_1 - r_1 \\
e_2 &= \psi_2 - \dot{r}_1 \\
e_3 &= \psi_3 - \ddot{r}_1
\end{aligned}
\tag{4.74}
$$

The state space model of this equation is given by:

$$
\begin{aligned}
\dot{e}_1 &= e_2 \\
\dot{e}_2 &= e_3 \\
\dot{e}_3 &= 0\psi_1 - 0.08017\psi_2 - .9972\psi_3 + 1.358u_1 - \dddot{r}_1
\end{aligned}
\tag{4.75}
$$

Then the state feedback pitch control u_p is given by

$$
u_p = \frac{1}{1.358}(\dddot{r}_1 - \dot{e}_3 - k_1 e_1 - k_2 e_2) + K_1 sign(S_1)
\tag{4.76}
$$

Substituting the values of $\dot{e}_3$ in equation (4.75) in equation (4.76) the pitch control u_p becomes:

$$
\begin{aligned}
u_p = \frac{1}{1.358}(0\psi_1 + 0.08017\psi_2 \\
+0.9972\psi_3 + \dddot{r}_1 - k_1 e_1 - k_2 e_2) + K_1 sign(S_1)
\end{aligned}
\tag{4.77}
$$

where $K_1 = 3.5$. Similarly the yaw control is designed using state feedback linearization. The reference signal for yaw control is taken as

$$
r_2(t) = 1
\tag{4.78}
$$

The procedure explained above is repeated for design of yaw angle control signal. The error signal which is the difference between the output and

reference is given by:

$$
\begin{aligned}
e_4 &= \phi_1 - r_2 \\
e_5 &= \phi_2 - \dot{r}_2 \\
e_6 &= \phi_3 - \ddot{r}_2
\end{aligned}
\tag{4.79}
$$

The state space model is given by:

$$
\begin{aligned}
\dot{e}_4 &= e_5 \\
\dot{e}_5 &= e_6 \\
\dot{e}_6 &= 0\phi_1 - 5\phi_2 - 6\phi_3 + 3.6u_1 - \dddot{r}_2
\end{aligned}
\tag{4.80}
$$

The state feedback yaw control u_y is given by

$$
u_y = \frac{1}{3.6}(\dddot{r}_2 - \dot{e}_6 - k_3 e_4 - k_4 e_5) + K_2 sign(S_2)
\tag{4.81}
$$

$$
u_y = \frac{1}{3.6}(5\phi_2 + 6\phi_3 + \dddot{r}_2 - k_3 e_4 - k_4 e_5) + K_2 sign(S_2)
\tag{4.82}
$$

where $K_2 = 5$,

In the state feed back control law, shown in equation (4.76) and (4.81), the values of K_1, and K_2 are obtained by trial and error method. Next Section deals with the performance of 2-dof TRMS with linear sliding surface (LSS)design.

4.7 Simulation results of 2-dof TRMS with Linear surface design

The MATLAB simulation has been done for 100 seconds by taking the unit step as the reference input and the results are plotted for 2-dof TRMS. Figure 4.5 shows the pitch control signal as derived in equation(4.77). It is evident

from the figure that the magnitude of pitch control signal is $2V$, which is within the prescribed control limit $-2.5V$ and $2.5V$ [1]. Similarly figure 4.6 shows the yaw control signal. It is also noticed that the magnitude of yaw control signal is $0.2V$ which is well within the prescribed control limit $-2.5V$ and $2.5V$. Thus it is proved that the above control signals for pitch and yaw are acceptable for the 2-dof TRMS.

Figures 4.7 and 4.8 show the pitch angle and yaw angle linear sliding surfaces respectively. It is understood from the these figures that during sliding mode the state vectors for pitch and yaw angles slide along the designed sliding surface while keeping the tracking error to a minimum value.
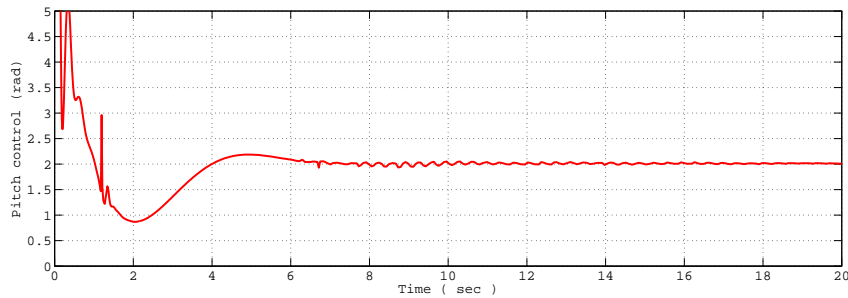
Figure 4.5: Pitch control with linear sliding surface design
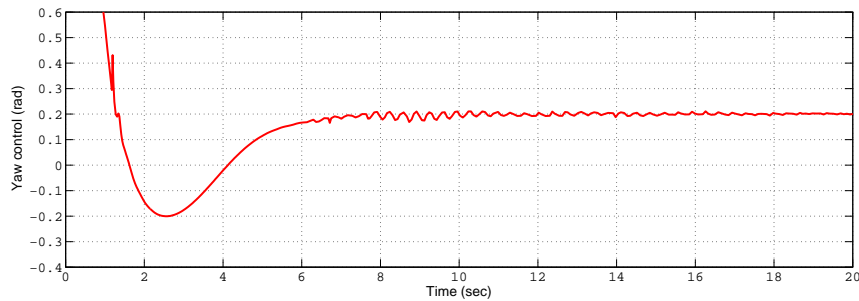
Figure 4.6: Yaw control with linear sliding surface design
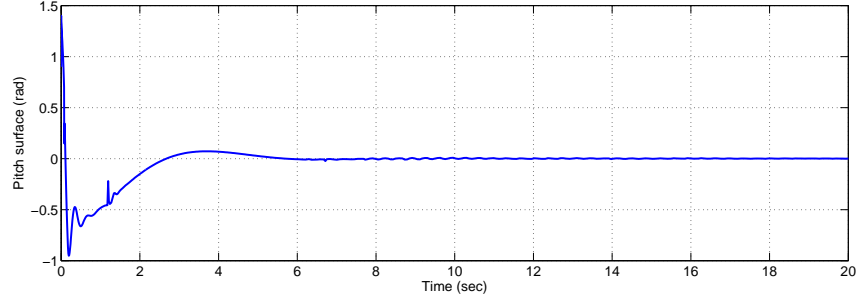
Figure 4.7: Pitch surface with linear sliding surface design
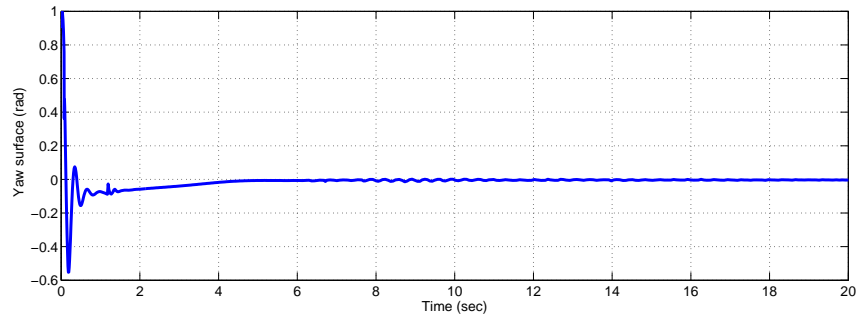
Figure 4.8: Yaw surface with linear sliding surface design

The position tracking responses of the Pitch and Yaw for unit step input reference are provided in figure 4.9 and 4.10 respectively. It is noticed that the settling time for pitch is 8 seconds and for yaw the settling time is 10 seconds. It is also noted that there is 12 percent overshoot in pitch angle tracking response and 5 percent overshoot in yaw angle tracking response.

The disturbance of $(0.4+0.4\sin(0.1t)$ is given at t=50 seconds for checking its dynamic performances of the system with the designed sliding surface. Figures 4.11 and 4.12 show the pitch angle and yaw angle tracking responses respectively when the disturbance is given at t= 50 seconds. The disturbance of $0.4sin(.1t) + 0.4$ is given to both pitch and yaw through input channel (matched disturbance). When the disturbance is applied, both pitch and
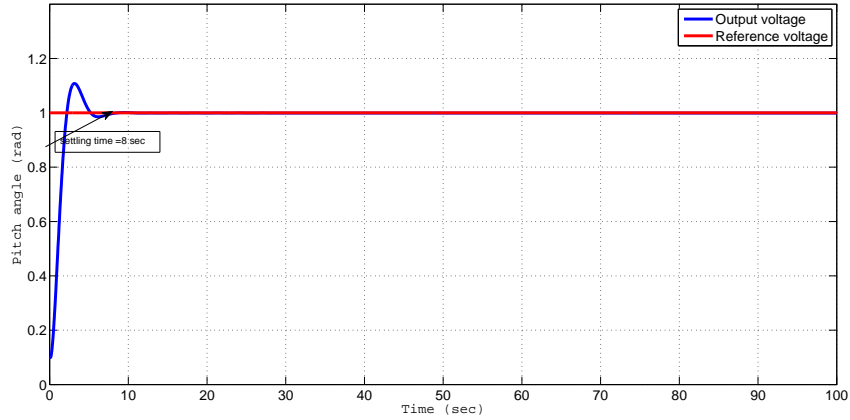
Figure 4.9: Pitch angle position tracking response with linear surface design
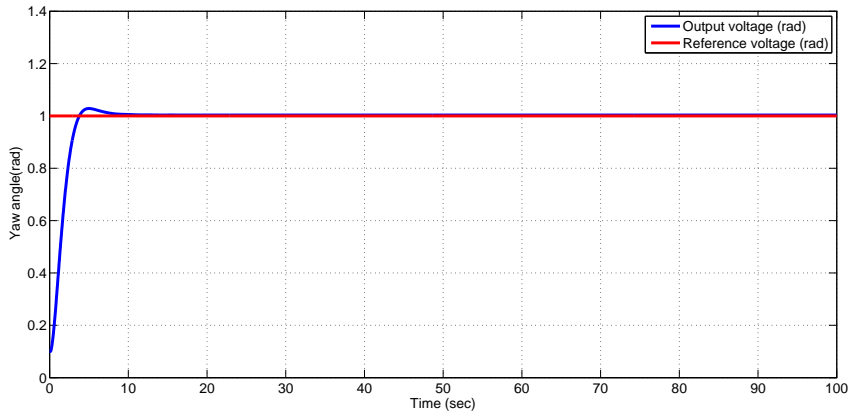
Figure 4.10: yaw angle position tracking with linear sliding surface design

yaw angle position track the corresponding reference inputs.

Hence It is clear that the pitch angle and yaw angle tracking responses for 2-dof TRMS are not affected by the matched disturbances given to the system as the state trajectory slides along the designed LSS. This explains invariance (Robustness) property of the designed linear sliding surface (LSS).
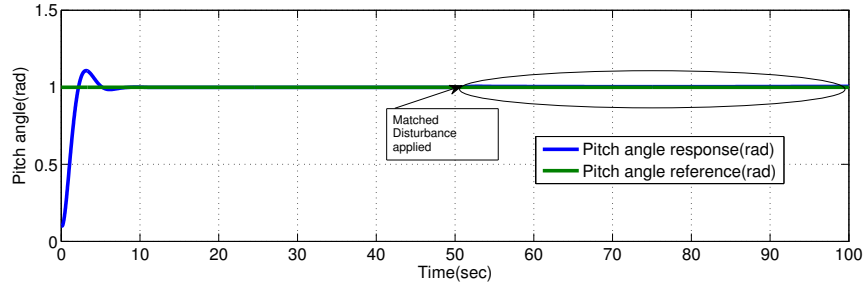
Figure 4.11: pitch angle position tracking response with linear sliding surface design when disturbance at 50 seconds is given
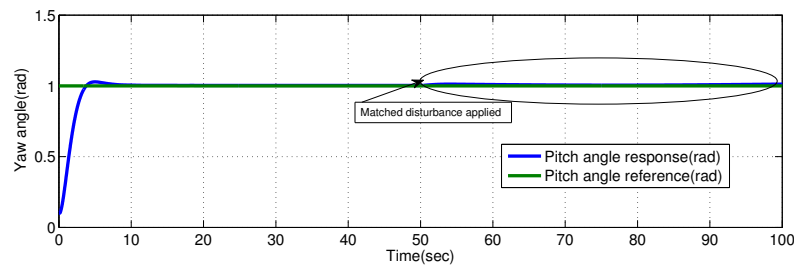
Figure 4.12: Yaw angle position tracking with linear sliding surface design when disturbance at 50 seconds is given

The next Section deals with the comparison between LSS and PID design.

4.8 Comparison

The table 4.1 shows performance comparison between the LSS design and PID controller design for the 2-degree of freedom Twin rotor MIMO system (2-dof TRMS). It is found that when the PID Controller is employed the settling time is 28 seconds for pitch and 40 seconds for yaw. Also the peak overshoot is 60 percent for pitch angle tracking and 50 percent for yaw angle tracking. The settling time for pitch angle reduced to 8 seconds and for yaw the settling time is reduced to 10 seconds respectively with the use of LSS.

Also the peak over shoot is reduced to 12 percent for pitch angle tracking and 5 percent for yaw angle tracking with the use of LSS. Moreover, a disturbance of $0.4sin(0.1t) + 0.4$ is applied through the input channel at 50 seconds. It is found that the tracking property is lost when PID controller is used. The system becomes insensitive to the matched disturbance of $0.4sin(0.1t) + 0.4$ with the use of LSS design. Thus it is inferred that the system become robust with the use of LSS design.

Table 4.1: Performance comparison for 2-dof TRMS with Linear sliding surface design and PID Controller design

Description	LSS	PID Controller
Settling time for Pitch angle position	8 sec	28 sec
Settling time for Yaw angle position	10 sec	40 sec
Overshoot for Pitch angle position	12 percent	60 Percent
Overshoot for yaw angle position	5 percent	50 Percent
Robustness	Robust	Not robust
Chattering	low	low

4.9   Analysis of Results

In this chapter two controllers are designed for 2-dof TRMS. 1) The nonlinear controller with LSS design and 2) PID controller. The simulation result show that the initial overshoot is reduced to 12 percent for pitch and 5 percent for yaw. Also the settling time is reduced to 8sec for pitch and 10 seconds for yaw with the use of linear sliding surface design and nonlinear sliding mode controller. It is verified in simulation. The robustness of the designed LSS for 2-dof TRMS is demonstrated by applying a matched disturbance of $0.4sin(0.1t)+0.4$. It is verified that the robustness is improved with the use of LSS.

4.10   Conclusion

This chapter deals with the performance of the 2-dof TRMS with the design of LSS and PID controller. The simulation result validate the design of LSS with satisfactory tracking performance. It also is robust to the matched disturbance. In addition to that the comparisons with the PID included to show that the LSS design perform better in control aspects and robustness aspects. it is verified that the LSS design become more appropriate than the design of controller using PID for systems like 2-dof TRMS. The draw back of the design using LSS is that the complexity of the design is high as compared with the existing PID controller design.

The Performance of the system can be further improved if LSS is replaced with non-linear sliding surface and non-linear sliding mode controller with the application of super-twisting control instead of feedback controller. Hence next chapter deals with the design of non-linear sliding surface and non-linear sliding mode control with super-twisting control employed for 2-dof TRMS.

Chapter 5

Design of Non-linear Sliding Surface for 2-dof Twin Rotor MIMO system

5.1   Introduction

Chapter 4 dealt with the design and application of linear sliding surface (LSS) for pitch and yaw of 2-dof TRMS. When carrying LSS and PI controller, LSS has better transient performance In the above context, research has been carried out to check the performance of the system using non-linear sliding surface (NLSS). The employability of the NLSS also motivated in the technical scenario which is given below. That is in Pitch and Yaw angle position, it is observed that as the settling time decreases the overshoot increases. Hence, the interest of research is to reduce both settling time and overshoot simultaneously. This problem is mitigated with the NLSS design using the concept of variable damping ratio [[64]. The idea is that the initial low value of damping will produce quick response during starting and later high value of damping that reduces the overshoot. Here the controller applied is non-linear sliding mode control (NSMC) [64].

Sliding mode control (SMC) always produces chattering. Chattering in the control signal of 2-dof TRMS may produce heat and mechanical vibration of the system which eventually results into mechanical damage in real time application. Therefore this work it is proposed to apply super-twisting control (STC) in non-linear SMC (NSMC)to reduce chattering. The super-twisting controller available in [69] is applied in this chapter.

This chapter is organised as follows: Section 5.2 deals with design of NLSS for pitch angle of 2-dof TRMS using variable damping ratio concept. Section 5.3 deals with design of NLSS for Yaw of 2-dof TRMS. Stability analysis of designed surface using Lyapunov method is given in Section 5.4. Section 5.5 explains the design of NSMC with super-twisting control and discussion on simulation result for 2-dof TRMS. In Section 5.6 the discussion on real time implementation of the NLSS and controller is given. Section 5.7 deals with the design of third order STC and discussion on simulation results for 2-dof TRMS. The performance of 2-dof TRMS with NLSS design is compared with the results obtained through third order STC which is given in Section 5.8. The analysis of results is gien in Section 5.9. Finally conclusion is given in Section 5.10

5.2   Design of non-linear sliding surface for pitch angle of 2-dof TRMS

The aim of this Section is to develop a non-linear sliding surface with high robustness as well as simultaneous reduction in both settling time and peak overshoot. The 2-dof TRMS has to deliver expected performance in terms of the settling time and overshoot for both Pitch and Yaw. This is achieved with the design of NLSS with the concept of variable damping ratio. The controller design of 2-dof TRMS involves the design of sliding surfaces for both pitch and yaw angles. The design of NLSS in both above mentioned

cases are synthesized using the approach mentioned in [64].

From the decoupled transfer function model given by equation (3.34), the main rotor transfer function for linear part of 2-dof TRMS is given by:

$$\psi(s) = \frac{1.358}{s^3 + 0.9972s^2 + 0.08017s}u_1(s) \qquad (5.1)$$

Where $\psi(s)$ represent the pitch angle position in laplace domain and u_1 is the control signal applied to the pitch of the system. For writing the state model of pitch, the non-linearity n_2 associated with the pitch angle is added with the linear part of the pitch. Then the state model of the pitch is given by:

$$
\begin{bmatrix} \dot{\psi}_1 \\ \dot{\psi}_2 \\ \dot{\psi}_3 \end{bmatrix} = \begin{bmatrix} 0 & 1 & 0 \\ 0 & 0 & 1 \\ 0 & -0.08017 & -0.9972 \end{bmatrix} \begin{bmatrix} \psi_1 \\ \psi_2 \\ \psi_3 \end{bmatrix} + \begin{bmatrix} 0 \\ 0 \\ 1.358 \end{bmatrix} u_1
$$
$$
+ \begin{bmatrix} 0 \\ 0 \\ 1 \end{bmatrix} n_2 \qquad (5.2)
$$

The output equation for pitch is given by:

$$y_1 = \psi_1 \qquad (5.3)$$

The switching function for pitch is given by:

$$NS_1(t) = NL^T \psi(t) \qquad (5.4)$$

where $\psi(t) = [\psi_1(t)\psi_2(t)\psi_3(t)]$ and NL^T is non-linear sliding surface matrix. The NS_1 is the non-linear sliding surface. The transfer function model of the system represented by the equation(3.34) is a third order system. Generally,

regular form approach is employed to bring down the higher order system to low order system for simplicity. For the system considered, different sets of state variables are employed using $h(t)$ to apply regular form approach. This $h(t)$ is related to the conventional pitch angle state vector $\psi(t)$ as:

$$h(t) = T_r \psi(t) \tag{5.5}$$

where T_r is the orthogonal matrix used for coordinate transformation. Now, the regular form of the (5.2) becomes:

$$\dot{h}_1(t) = A_{11} h_1(t) + A_{12} h_2(t) + B_1 u(t)$$
$$\dot{h}_2(t) = A_{21} h_1(t) + A_{22} h_2(t) + B_2 u(t) + n_2(h(t)) \tag{5.6}$$

Equation(5.6) is different from equation (4.6) as non-linear element n_2 is added to equation (4.6).

where

$$A_{11} = \begin{bmatrix} 0 & 1 \\ 0 & 0 \end{bmatrix} A_{12} = \begin{bmatrix} 0 \\ 1 \end{bmatrix} A_{21} = \begin{bmatrix} 0 & -0.08017 \end{bmatrix}$$
$$A_{22} = \begin{bmatrix} -0.9972 \end{bmatrix} B_1 = \begin{bmatrix} 0 \\ 0 \end{bmatrix} B_2 = \begin{bmatrix} 1.358 \end{bmatrix} \tag{5.7}$$

n_2 is the non-linearity associated with pitch. $h_1 = [\psi_1 \psi_2]$ and $h_2 = \psi_3$. The associated switching function in regular form can be expressed as:

$$NS_1(t) = l_1 h_1(t) + l_2 h_2(t) \tag{5.8}$$

where
$$l_1 = M_1 - y(\psi) A_{12}^T F \tag{5.9}$$

The value of l_1 is calculated as in [56]. Here l_1 consists of two parts. The linear and non-linear part. The M_1 is linear part of non-linear sliding sur-

face (NLSS) which is already designed in the previous chapter. The term $y(\psi)A_{12}^T F$ is the one corresponding to non-linear part of the surface The non-linear sliding surface matrix NL^T is written as:

$$NL^T = [I_1 l_2] \tag{5.10}$$

where l_2 is taken as 1 as in [64]

$$NL^T = [I_1 1] \tag{5.11}$$

Now the non-linear pitch sliding surface for the 2-dof TRMS can be represented as:

$$NS_1 = NL^T h(t) = \begin{bmatrix} M_1 - y(\psi)A_{12}^T F & 1 \end{bmatrix} \begin{bmatrix} h_1 \\ h_2 \end{bmatrix} \tag{5.12}$$

The value of M_1 is the linear part of the surface calculated using the quadratic minimization technique which is already explained in the previous chapter. The value of M_1 as obtained in equation(4.36) as:

$$M_1 = \begin{bmatrix} 1 & \sqrt{3} \end{bmatrix} \tag{5.13}$$

The value of F can be calculated from the Lyapunov theorem:$A^T P + PA = -Q$. By applying this theorem in the design procedure, the equation becomes:

$$((A_{11} - A_{12}M_1)^T F + F(A_{11} - A_{12}M_1)) = -W \tag{5.14}$$

Where $A = (A_{11} - A_{12}M_1, P = F$ and $Q = W$.

The W is a positive definite matrix and is selected as:

$$W = 0.34 \begin{bmatrix} 0 & 1 \\ 1 & 0 \end{bmatrix} \tag{5.15}$$

By substituting all the values of A_{11}, A_{12}, A_{21}, A_{22} and W in the equation (5.14), F has calculated as:

On simplification, F becomes:

$$F = \begin{bmatrix} 0.4904 & 0.17 \\ 0.17 & 0.196 \end{bmatrix} \tag{5.16}$$

Then for the design of NLSS the next parameter to be obtained is $y(\psi)$. The $y(\psi)$ is selected for Pitch as detailed below.

5.2.1   Selection of non-linear function for Pitch angle

The $y(\psi)$ represents the pitch angle non-linear function and $y(\phi)$ represents the yaw angle non-linear function. The non-linear function is employed to change the systems closed loop damping ratio of the system from its initial low value to final high value as the output varies from its initial and approaches final value [56]. The non-linear function should satisfy the following properties
1) It should change from 0 to $-\epsilon_1$ as the output approaches the set point (final value) from its initial value where $\epsilon_1 > 0$.
2) It should be differentiable with respect to ψ to ensure the existence of sliding mode.
The possible choice of $y(\psi)$ to satisfy the above two conditions as in paper[56] is:

$$y(\psi) = -\epsilon_1 e^{-k\psi^2} \tag{5.17}$$

where k and ϵ_1 are positive constants. To ensure a small initial value of $y(\psi)$, k should have a large value. Substituting all the available values in Equation (5.12), the pitch non-linear sliding surface is obtained in terms of

phase variables ψ_1, ψ_2, ψ_3 as:

$$NS_1 = [1 - 8.5e^{-100\psi_1^2}]\psi_1$$
$$+[\sqrt{(3)} - 9.8e^{-100\psi_1^2}]\psi_2 + \psi_3 \tag{5.18}$$

5.3   Design of non-linear sliding surface for yaw angle of 2-dof TRMS

From decoupled transfer function model (3.35) the tail transfer function for linear part of 2-dof TRMS is given by:

$$\phi(s) = \frac{3.6}{s^3 + 6s^2 + 5s}u_2(s) \tag{5.19}$$

where $\phi(s)$ represent the yaw angle position in laplace domain and u_2 is the control signal applied to the tail rotor of the system. The non-linearity n_5 is added to the linear part of the yaw. Then the state model of the pitch is given by:

$$\begin{bmatrix} \dot{\phi}_1 \\ \dot{\phi}_2 \\ \dot{\phi}_3 \end{bmatrix} = \begin{bmatrix} 0 & 1 & 0 \\ 0 & 0 & 1 \\ 0 & -5 & -6 \end{bmatrix} \begin{bmatrix} \phi_1 \\ \phi_2 \\ \phi_3 \end{bmatrix} + \begin{bmatrix} 0 \\ 0 \\ 3.6 \end{bmatrix} u_2$$
$$+ \begin{bmatrix} 0 \\ 0 \\ 1 \end{bmatrix} n_5 \tag{5.20}$$

The output equation for yaw is given by:

$$y_2 = \phi_1 \tag{5.21}$$

The switching function for yaw is given by:

$$NS_2(t) = NL^T \phi(t) \tag{5.22}$$

where $\phi(t) = [\phi_1(t)\phi_2(t)\phi_3(t)]$ and NL^T is non-linear sliding surface matrix. The transfer function model of the system represented by the equation(3.35) is a third order system. Here also regular form approach is given. The $h(t)$ is related to the conventional yaw angle state vector $\phi(t)$ as:

$$h(t) = T_r \phi(t) \tag{5.23}$$

where T_r is the orthogonal matrix used for coordinate transformation. proceeding in the same way as that of pitch angle surface the yaw angle surface can be calculated.

5.3.1 Selection of non-linear function for yaw angle

Similarly the non-linearity function $y(\phi)$ for yaw is given by:

$$y(\phi) = -\epsilon_2 e^{-k\phi^2} \tag{5.24}$$

The procedure which is adopted for the design of non-linear pitch angle sliding surface is same as that adopted for the design of non-linear yaw angle sliding surface. The equation (5.12) can also apply for the calculation of yaw angle surface. M_1 will be replaced by M_2. but the same values are obtained for M_1 and M_2 and it is explained in Section 4.3 and Section 4.4. Hence the equation for NS_2 and NS_1 will be same. But the phase variables will be different. The non-linear sliding surface for yaw angle is obtained in terms of phase variables ϕ_1, ϕ_2, ϕ_3 as:

$$NS_2 = [1 - 8.5e^{-100\phi_1^2}]\phi_1$$
$$+[\sqrt{(3)} - 9.8e^{-100\phi_1^2}]\phi_2 + \phi_3 \tag{5.25}$$

Thus in this Section , the selection of non-linear sliding surface for both pitch and yaw are carried out. The next aim is to check the stability of the designed non-linear sliding surface for pitch and yaw of 2-dof TRMS.

5.4 Stability of non-linear sliding Surface for 2-dof TRMS using Variable Damping Ratio Concept

In the Section 5.2 and 5.3 the non-linear sliding surfaces for both pitch and yaw angles are calculated by selecting the non-linear function. The next objective is to check whether the selected non-linear sliding surfaces are stable in the sense of lyapunov or not. As per the Lyapunov first theorem of asymptotic stability, If $V(h)$ is positive definite and $\dot{V}(h)$ is negative definite then the system is said to be asymptotically stable.

Proof: Let the positive definite Lyapunov function be:

$$V(h) = h_1{}^T(t)Fh_1(t) \tag{5.26}$$

where F is a positive definite matrix and it is chosen based on the condition satisfying the Lyapunov equation. The derivative of Lyapunov function $V(h)$ becomes:

$$\dot{V}(h) = \dot{h_1^T}(t)Fh_1(t) + h_1{}^T(t)F\dot{h}_1(t) \tag{5.27}$$

substituting for $\dot{h}_1(t)$ in equation (5.27) $\dot{V}(h)$ becomes:

$$\dot{V}(h) = (A_{11}h_1 + A_{21}h_2)^T Fh_1 + h_1{}^T F((A_{11}h_1 + A_{21}h_2) \tag{5.28}$$

But during sliding mode, sliding surface function is equal to zero. The equation (5.12) becomes:

$$(M_1 - y(\psi)A_{12}^T F)h_1 + h_2 = 0 \tag{5.29}$$

then

$$h_2 = -(M_1 - y(\psi)A_{12}^T F)h_1 \tag{5.30}$$

Replacing $h_2(t)$ in terms of $h_1(t)$, in equation (5.28), $\dot{V}(h)$ becomes:

$$\dot{V}(h) = h_1{}^T((A_{11} - A_{12}M_1)^T F + F(A_{11} - A_{12}M_1))h_1(t) \\ +2y(\psi)h_1^T(t)FA_{12}A_{12}^T Fh_1(t) \tag{5.31}$$

The equation(5.31) is further reduced as:

$$\dot{V}(h) = h_1{}^T((A_{11} - A_{12}M_1)^T F + F(A_{11} - A_{12}M_1) \\ +2y(\psi)h_1^T(t)FA_{12}A_{12}^T F)h_1(t) \tag{5.32}$$

Now, substituting the Lyapunov equation $((A_{11} - A_{12}M_1)^T F + F(A_{11} - A_{12}M_1)) = -W$ in equation(5.32), $\dot{V}(h)$ becomes:

$$\dot{V}(h) = h_1{}^T(-W + 2y(\psi)h_1^T(t)FA_{12}A_{12}^T F))h_1(t) \tag{5.33}$$

Here the $y(\psi)$ is negative definite by definition and $FA_{12}A_{12}^T F$ is positive definite matrix. Then the term $2y(\psi)h_1^T(t)FA_{12}A_{12}^T F$ becomes negative semi-definite matrix. Adding the term $2y(\psi)h_1^T(t)FA_{12}A_{12}^T F$ with negative definite matrix $-W$ always results in the negative definite matrix. Therefore we can write $\dot{V}(h)$ is less than zero. Thus the designed pitch angle non-linear sliding surface for 2-dof TRMS is stable in the sense of Lyapunov. The stability of yaw angle non-linear sliding surface can also be proved by the same procedure.

5.5 Design of non-linear sliding mode Controller with super-twisting control applied for 2-dof TRMS

The non-linear sliding mode controller for 2-dof TRMS is designed based on the method available in [56]. Pitch and yaw control inputs have to be calculated for 2-dof TRMS. The non-linear pitch control for 2-dof TRMS u_1 is given in [56] is re-stated as:

$$u_1 = -B_2^{-1}(NL^T Ah + kNS_1 + O_1 sign(NS_1) - \dot{y}(\psi)A_{12}^T Fh_1) \qquad (5.34)$$

where u_1 is the sliding mode control signal applied to pitch:

$$B_2 = \begin{bmatrix} 1.358 \end{bmatrix},$$

$$NL = \begin{bmatrix} l_1 \\ l_2 \end{bmatrix}, \text{ and}$$

$$A = \begin{bmatrix} 0 & 1 & 0 \\ 0 & 0 & 1 \\ 0 & -0.08017 & -0.9972 \end{bmatrix}$$

The main problem of sliding mode control is chattering in control signal. High chattering affects the mechanical part of the system in real time. To reduce such chattering, the higher order sliding modes are introduced. The main disadvantage of using higher order sliding mode is the difficulty in gathering information of derivatives in real time. But the super-twisting control does not require the information regarding the derivatives. This super-twisting control is a continuous control ensuring all properties of first order sliding mode control. The non-linear SMC for 2-dof TRMS is designed adopting the control structure envisaged in [64] but with a modification. Instead of the signum function used in [64] super-twisting control is adopted in this work to reduce chattering. In the existing non-linear SMC mentioned in literature [64], a super-twisting controller [69] is incorporated which is

explained below. The non-linear control applied to pitch is given by;

$$u_1 = -B_2^{-1}(NL^T Ah + kNS_1 + O_1 u_{S1} - \dot{y}(\psi)A_{12}^T Fh_1)$$
(5.35)

Here NS_1 is the non-linear sliding surface for pitch angle position of TRMS. The O_1 is the term that contain equation for non-linear sliding mode controller n_{2max}. Then to obtain the value of O_1, n_{2max} is to be calculated. The value of n_{2max} is obtained as 0.875 as discussed in Section 3.2. The control signal to the yaw will be in tune only if it satisfies the condition that $n_{2max} < O_1$. Hence the value of O_1 is chosen to be $O_1 = 0.9$ which is slightly greater than $n_{2max}(0.875)$.

The u_{S1} is the super-twisting controller which is given by:

$$u_{S1} = -\gamma_1(NS_1)^{\frac{1}{2}} sign(NS_1) - \gamma_2 \int sign(NS_1)$$
(5.36)

The γ_1 and γ_2 are positive gains. The parameters γ_1 and γ_2 are calculated using the equation:

$$\gamma_1 = 1.5R^{\frac{1}{2}}$$
(5.37)

$$\gamma_2 = 1.1R$$
(5.38)

With sufficient convergence conditions,

$$\gamma_2 > R$$
(5.39)

and

$$\frac{2(\gamma_2 + R)}{\gamma_1^2(\gamma_2 - R)} < 1$$
(5.40)

The value of R is selected such that the maximum bound of system matrix $f(x) < R$.

The value chosen for k, γ_1, and γ_2 are $k = 5$. $\gamma_1 = 6$, $\gamma_2 = 4$ respectively.

Substituting all available values in equation(5.35), u_1 becomes:

$$u_1 = -1/1.38(5NS_1 + 0.9u_{s1} - \dot{y}(\psi)[0.17\psi_1 + 0.196\psi_2]) \tag{5.41}$$

Similarly non-linear sliding mode control with super-twisting algorithm for yaw is given by:

$$u_2 = -B_2^{-1}(NL^T Ah + kNS_2 + O_2 u_{s2} - \dot{y}(\phi)A_{12}^T Fh_1) \tag{5.42}$$

where
$$u_{S2} = -\gamma_3(NS_2)^{\frac{1}{2}} sign(NS_2) - \gamma_4 \int sign(NS_2) \tag{5.43}$$

u_2 is the non-linear sliding mode control signal applied to pitch: $B_2 = \begin{bmatrix} 3.6 \end{bmatrix}$,

$NL = \begin{bmatrix} l_1 \\ l_2 \end{bmatrix}$, and

$A = \begin{bmatrix} 0 & 1 & 0 \\ 0 & 0 & 1 \\ 0 & -5 & -6 \end{bmatrix}$

The O_2 is the term that contain equation for non-linear sliding mode controller n_{5max}. Then to obtain the value of O_2 n_{5max} is to be calculated. The value of n_{5max} is obtained as 1.68 as discussed in Section 3.2. The control signal to the yaw will be in tune only if it satisfies the condition that $n_{5max} < O_2$. Hence the value of O_2 is chosen to be $O_2 = 1.7$ which is slightly greater than $n_{5max}(1.68)$. The value for k γ_3, γ_4 is chosen to be $k = 5$, $\gamma_3 = 6$, $\gamma_4 = 4$. Substituting all available values in equation(5.38)u_2 is calculated as:

$$u_2 = -1/3.6(5NS_2 + 1.7u_{S2} - \dot{y}(\phi)[0.17\phi_1 + 0.196\phi_2]) \tag{5.44}$$

Thus non-linear sliding mode control with STC for both pitch and yaw are obtained. Further the real time performance of 2-dof TRMS with the above control signal is to be investigated.

5.5.1 Simulation Results and Discussion with non-linear sliding surface design

The MATLAB simulation has been done for 100 seconds by taking the unit step as the reference input and the results are plotted for 2-dof TRMS. Figure 5.1 shows the pitch control signal. It is evident from the figure that the magnitude of pitch control signal is in between $1V$ and $2.5V$, which is well within the prescribed control limit $-2.5V$ and $2.5V$ [21]. Similarly figure 5.2 shows the yaw control signal. It is noticed that the magnitude of yaw control signal is in between $-0.5V$ and $-1V$. From the simulation results obtained in figure 5.1 and 5.2, it is ensured that these control signals can be applied to 2-dof TRMS as the value of the control signal is within the limit prescribed by manufactures. Also it is noticed that the chattering is reduced with the use of super-twisting control in non-linear SMC.

Figure 5.1: Pitch control signal using non-linear SMC with super-twisting control and non-linear sliding surface design

Figures 5.3 and 5.4 show the pitch angle and yaw angle non-linear sliding surfaces respectively. During sliding mode, the state vectors for pitch and yaw angles will slide along the designed sliding surface and keep the tracking error to a minimum value. Also, the pitch angle and yaw angle responses are not be affected by the disturbances given to the system since the state trajectory slides along this surface designed. This explains in-variance (Robustness) property of the designed surface.
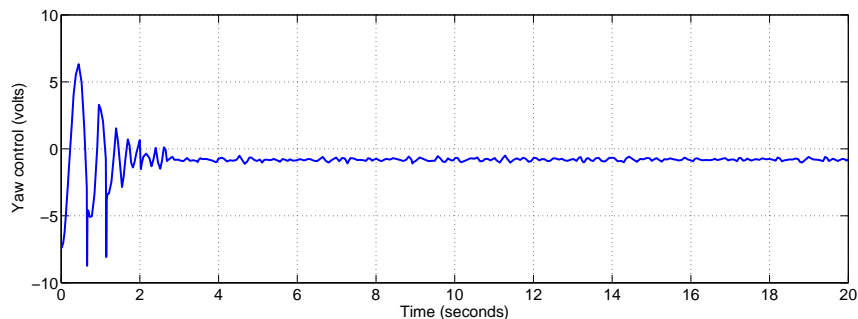
Figure 5.2: Yaw control signal using non-linear SMC with super-twisting control and non-linear sliding surface design

Figure 5.3: Pitch angle non-linear sliding surface using non-linear SMC with super-twisting control and non-linear sliding surface design

Figures 5.5 and 5.6 show the pitch angle and yaw angle position tracking responses respectively when the above control signals are applied. Here the reference signal is taken as unit step. It is found that the response of both pitch angle and yaw angle position track the unit step signal and this ensures the tracking property of non-linear sliding mode control with NLSS design. The initial conditions for pitch is given as 0.1 rad and for yaw 0.4 rad. Pitch response settles in 8 seconds and yaw response settles in 7 seconds. It is noted that there is no initial over shoots and under shoots in both pitch and yaw angle responses.

79
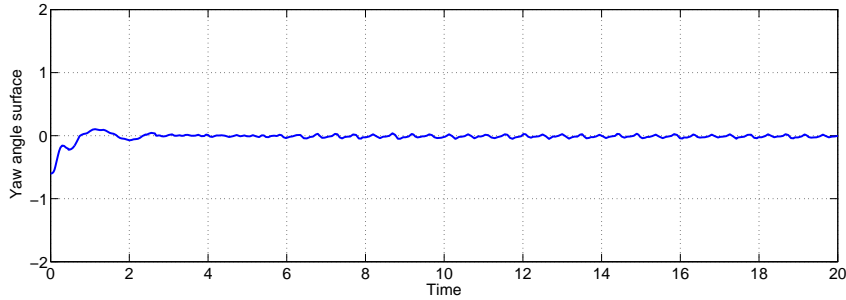
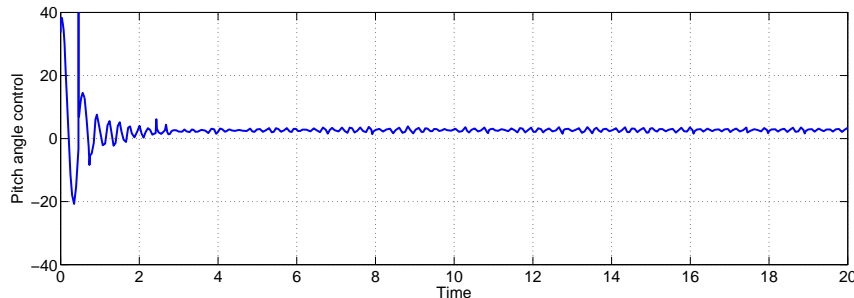Figure 5.4: Yaw angle non-linear sliding surface with non-linear SMC with super-twisting control and non-linear sliding surface design

Figures 5.7 and 5.8 show the pitch angle and yaw angle position tracking responses respectively when the disturbance is given at 50 seconds. The disturbance of $0.4sin(.1t) + 0.4$ is given to both pitch and yaw through input channel (matched disturbance). Even when the disturbance is applied, both the outputs track the corresponding reference inputs. This verifies the invariance property of the designed sliding surface.
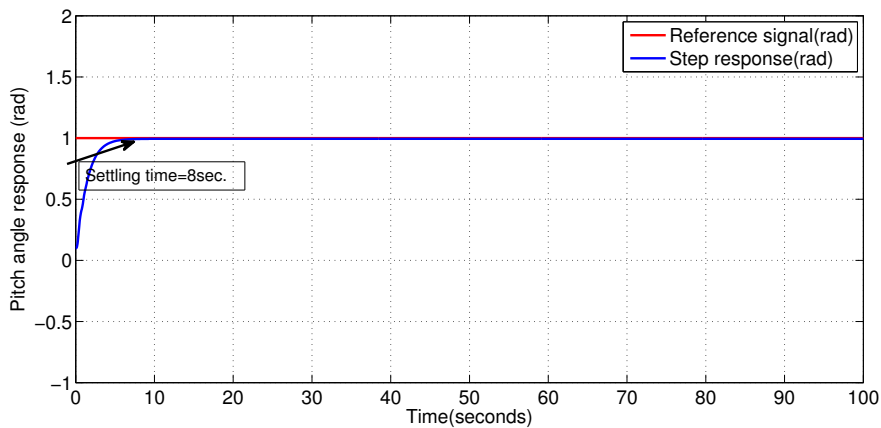
Figure 5.5: Pitch angle position tracking using non-linear SMC with super-twisting control applied and non-linear sliding surface design
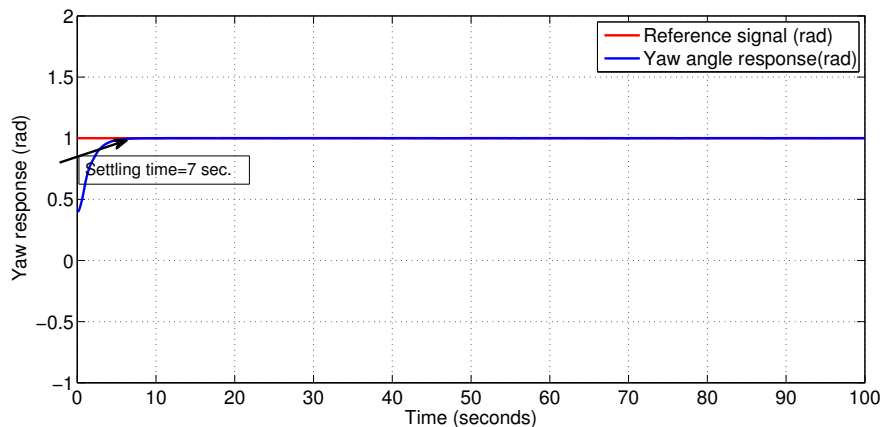
Figure 5.6: Yaw angle position tracking using non-linear SMC with super-twisting control applied and non-linear sliding surface design
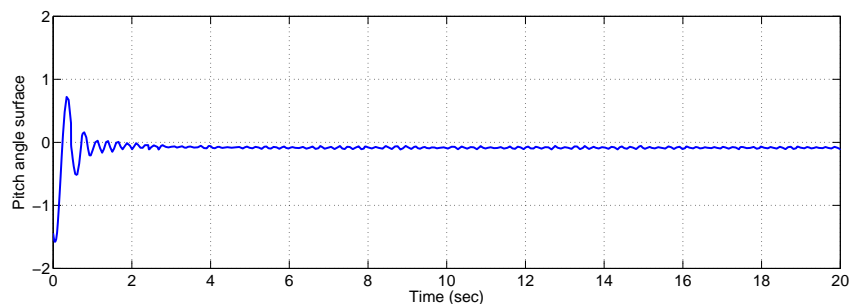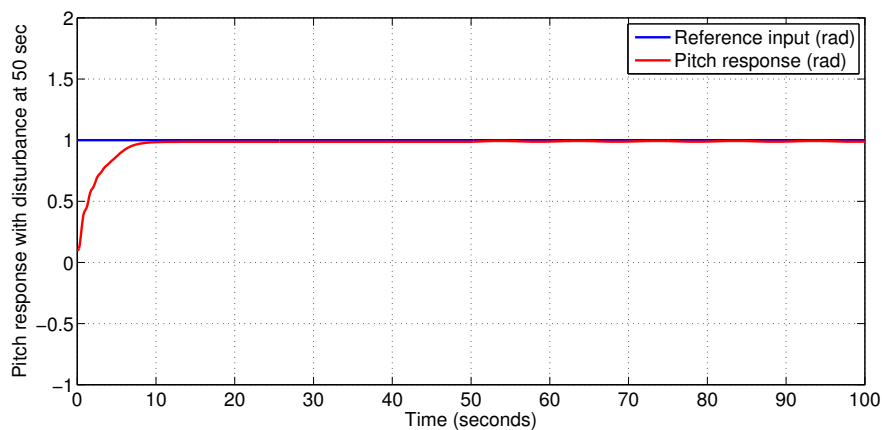

Figure 5.7: Pitch angle position tracking using non-linear SMC with super-twisting control and non-linear sliding surface design when matched disturbance is applied at 50 sec.

Figures 5.9 and 5.10 show the pitch angle and yaw angle position tracking respectively when zero initial condition is given. Even when the initial conditions are changed, the responses for both pitch and yaw track the corre-

81
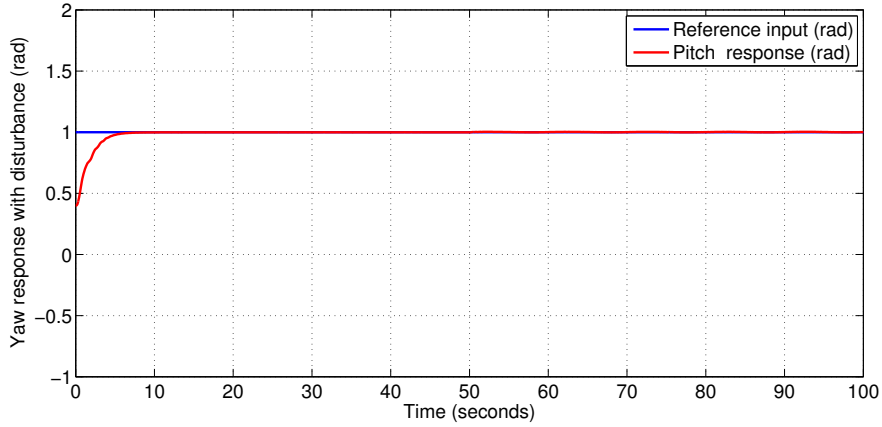
Figure 5.8: Yaw angle position tracking using non-linear SMC with super-twisting control and non-linear sliding surface design when matched disturbance is applied at 50 sec.

sponding reference inputs. this will verify the robustness property of designed sliding surface.
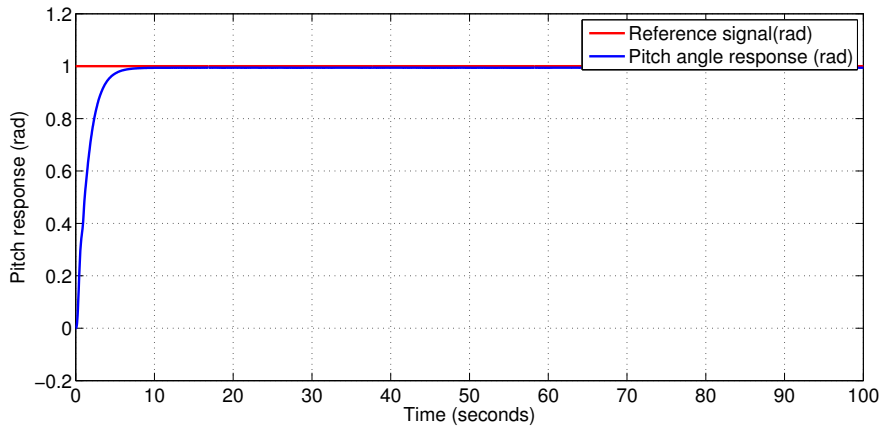
Figure 5.9: Pitch angle position tracking (zero initial condition) using non-linear SMC with super-twisting control and non-linear sliding surface design
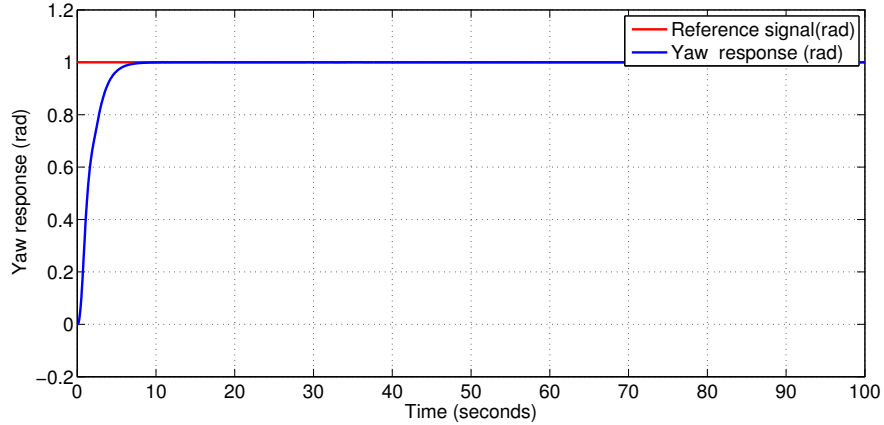
Figure 5.10: Yaw angle position tracking (zero initial condition) using non-linear SMC with super-twisting control and non-linear sliding surface design

Thus it is concluded that the generated control signal has good tracking ability and the designed NLSS is invariant to the disturbance. The MATLAB simulation results seen to be quite satisfactory. Since the control inputs generated for both pitch and yaw are within the control limit prescribed by the manufacturer of 2-dof TRMS [21]. The next Section deals with implementation of NLSS and non-linear SMC with the application of super-twisting control.

5.6 Real time implementation for 2-dof TRMS

Figure 5.11 shows the block diagram of real time implementation with the designed NLSS and non-linear SMC (NSMC) with super-twisting control applied for 2-dof TRMS by using Advantech PCI1711 interfacing card. This card reads the 16 bit data from encoders. There are two blocks in the figure shown. They are encoder (Analogue to digital) and decoder (digital to analogue) blocks. The encoder block has two outputs which are position of rotor in radians in the vertical and horizontal planes [21]. The control

signals for pitch and yaw are given to the digital to analogue block. These encoder and decoder serves as an interface between the PC and external environment. The sensors senses the real time pitch and yaw angle positions. these real time angle positions sensed by the sensors and are given to the encoders. The encoder delivers the discrete values corresponding to the interrupt service routine(ISR). The control algorithm operate according to the pulses distributed by the clock and the clock delivers the interrupt service routine.

Since the system constraints are too high, the operating regions for pitch and yaw are to be fixed prior to the real time implementation. The operating region in radian 43] for pitch is $\begin{bmatrix} -0.51 & 1.2 \end{bmatrix}$ and for yaw is $\begin{bmatrix} -1.2 & 1.2 \end{bmatrix}$ as explained in [43]. In this work the maximum limit is not applied as it may cause system failure. Hence a lower values, (0.2 radian for pitch and 0.8 radian for yaw) are applied in order to ensure safety working of the 2-dof TRMS. Here the operating region is fixed in accordance with the value of operating region considered in [43].
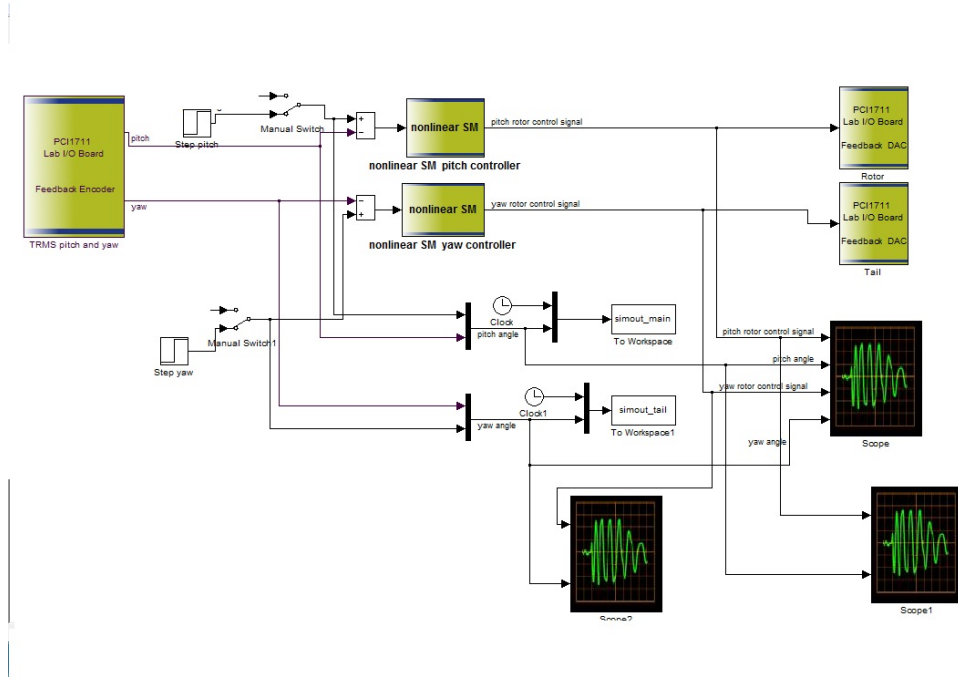
Figure 5.11: Block diagram for real time implementation of non-linear SMC with super-twisting control and non-linear sliding surface design

5.6.1 Real time implementation results and discussion for 2-dof TRMS

Figure 5.12 shows the real time implementation set-up for pitch and yaw angle control of 2-dof TRMS. Figure 5.13 shows the real time pitch angle and yaw angle position tracking and control signals given to pitch and yaw of 2-dof TRMS.

85

Figure 5.12:   Real time setup for 2-dof TRMS using non-linear SMC with super-twisting control and non-linear sliding surface design
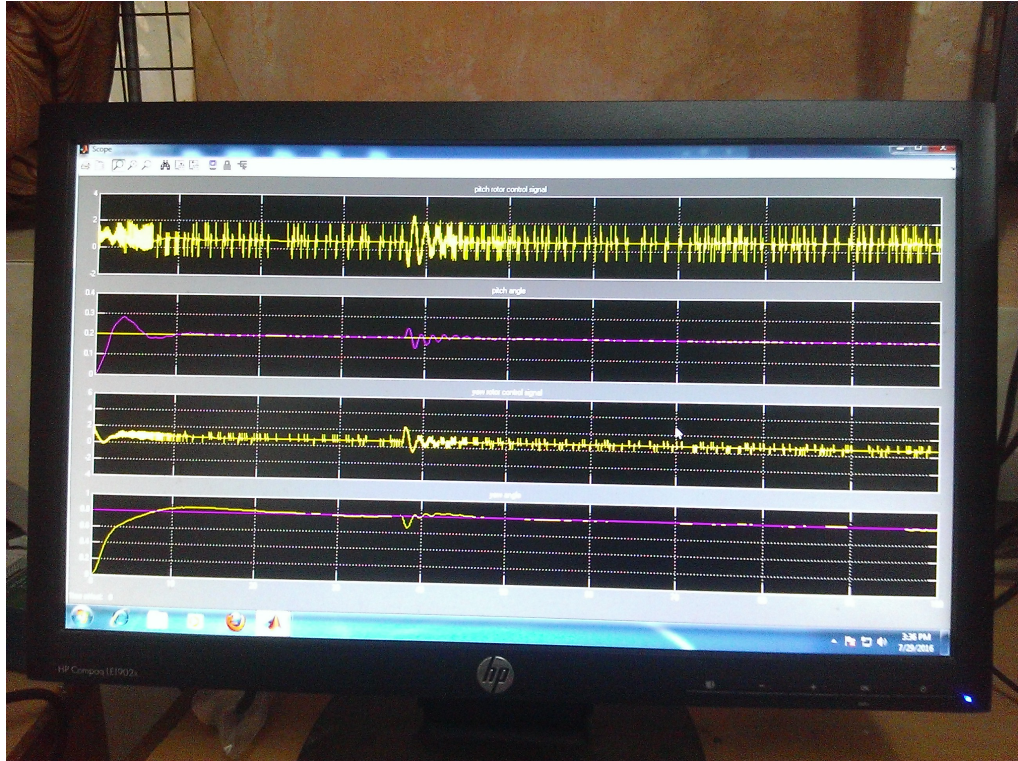
Figure 5.13: Real time implementation results of tracking responses of both pitch and yaw of 2-dof TRMS using non-linear SMC with super-twisting control and non-linear sliding surface design
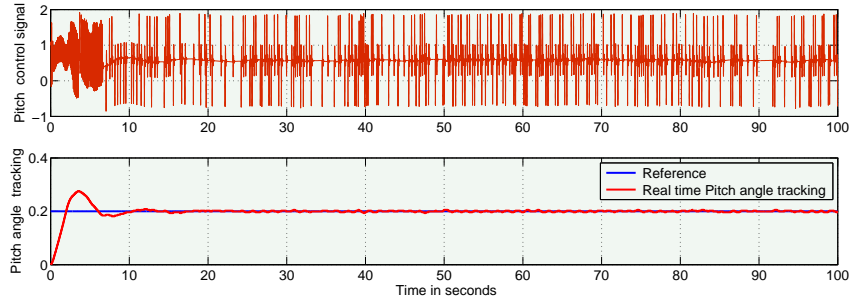
Figure 5.14: Real time implementation result of pitch angle position tracking response of 2-dof TRMS using non-linear SMC with super-twisting control and non-linear sliding surface design
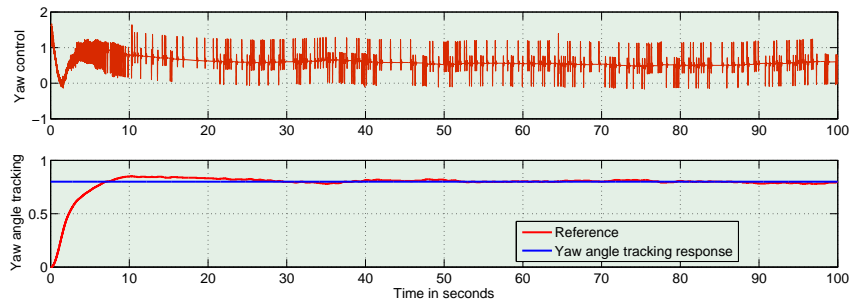
Figure 5.15: Real time implementation result of yaw angle position tracking response of 2-dof TRMS using non-linear SMC with super-twisting control and non-linear sliding surface design
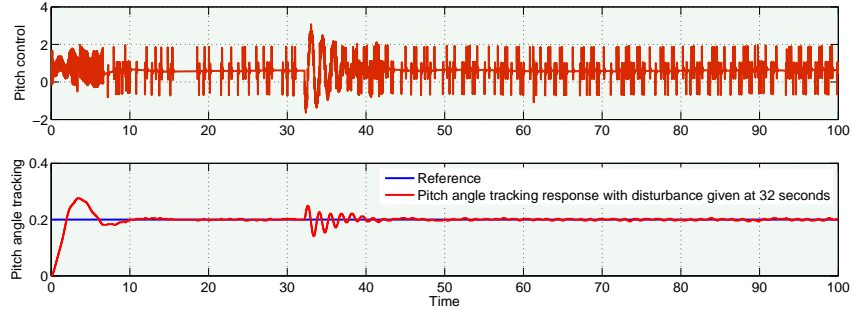
Figure 5.16: Real time implementation result of pitch angle position tracking response of 2-dof TRMS using non-linear SMC with super-twisting control and non-linear sliding surface design when an external disturbance is applied at 32 sec.
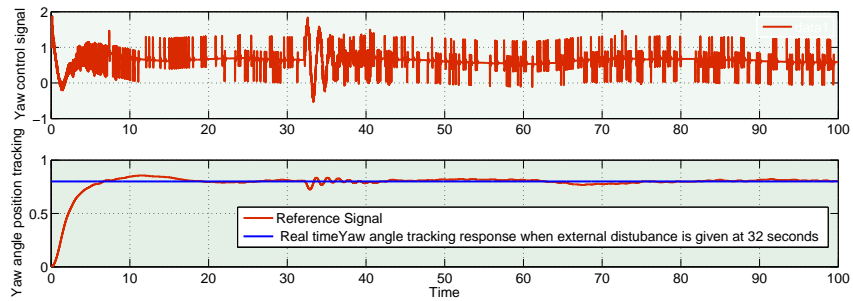
Figure 5.17: Real time implementation result of yaw angle position tracking response OF 2-dof TRMS using non-linear SMC with super-twisting control and non-linear sliding surface design when an external disturbance is applied at 32 sec.

Figures 5.14 and 5.15 show pitch angle and the yaw angle position tracking responses respectively in real time implementation. It is observed that both responses for pitch and yaw track the reference inputs with small amount of over shoots at starting. The settling time for pitch is found to be 13 seconds

89

and settling time for yaw is found to be 15 seconds. It is also noted that in real time system there is an overshoot of 40 percent in the pitch angle tracking and an overshoot of 6 percent in yaw angle tracking. This may be due to high moment of inertia of TRMS system.

Figures 5.16 and 5.17 show the pitch and yaw angle position tracking responses respectively in real time implementation with external disturbance. An external disturbance (A force equivalent to 100 gram) is applied to the beam. It is observed that both responses for pitch and yaw track the reference inputs. Here the external disturbance is applied at 32 seconds The system performance has undershoots and overshoots and settles in 10 seconds.

Thus it is concluded that the generated control signal through non-linear sliding mode control with super-twisting algorithm applied has a good tracking ability and the designed non-linear sliding surface is invariant to the external disturbance also.

5.7 Design of Third order Super-twisting control for 2-dof TRMS

The main problem of sliding mode control is chattering. The higher order sliding modes can solve this problem. The main disadvantage of using higher order sliding mode is the increasing information demand. The increase in information demand is explained below . If the sliding order is r, then surface S, and derivatives of the surface are $\dot{S}$,$\ddot{S}$ upto $(r-1)$. These derivatives are to be calculated. In this context, the solution lies in super-twisting control (STC). This is because the STC needs only measurement of surface S.

The super-twisting control is a continuous control ensuring all properties of first order sliding mode control. For higher order systems, first order sliding surfaces will result the asymptotic convergence of the system. Hence, in order to get the finite time convergence the design of higher order super-twisting is needed. Since the system under consideration is third order, a

third order super-twisting control has to be designed for both pitch and yaw of 2-dof TRMS to get finite time convergence. The third order super-twisting control is given by [65] as:

$$u_{pitch} = -c_1(\zeta_1)^{(\frac{1}{2})} sign(\zeta_1) - c_3 \int sign(\zeta_1) \qquad (5.45)$$

The parameter ζ_1 is obtained from where

$$\zeta_1 = \psi_2 + c_2 \psi_1^{\frac{2}{3}} sign(\psi_1) \qquad (5.46)$$

Here c_1, c_2 and c_3 are constants. $\psi_1, \psi_2,$ and ψ_3 are the state variables corresponding to pitch. and

$$u_{yaw} = -c_4(\zeta_2)^{(\frac{1}{2})} sign(\zeta_2) - c_6 \int sign(\zeta_2) \qquad (5.47)$$

where
$$\zeta_2 = \phi_2 + c_5 \phi_1^{\frac{2}{3}} sign(\phi_1) \qquad (5.48)$$

Here c_4, c_5, c_6 are constants. Also $\phi_1, \phi_2,$ and ϕ_3 are state variables corresponding to yaw.

Thus the third order STC is designed for the 2-dof TRMS. Next Section deals with the simulation results of 2-dof TRMS with Third order STC.

5.7.1 Results and Discussion of Third order Super-twisting control for 2-dof TRMS

Fig. 5.18 shows the pitch control signal when third order super -twisting control (Third order STC) is employed. It is evident from the figure that the magnitude of pitch control signal is in between $2V$ and which is within the prescribed control limit $-2.5V$ and $2.5V$ [21]. Similarly figure 5.19 shows the yaw control signal. It is noticed that the magnitude of yaw control signal is $-0.75V$ which is within $-2.5V$ and $2.5V$ [21]. It is also observed that

the pitch angle and yaw angle control signals are continuous that is free of chattering.
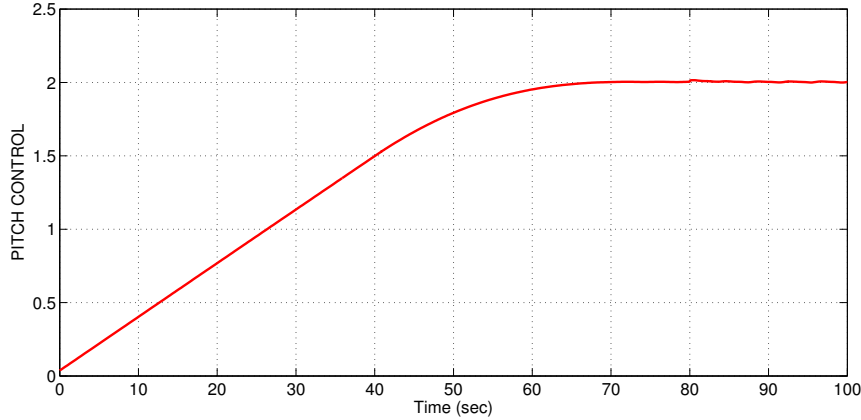
Figure 5.18: Pitch control signal with third order Super-twisting control design
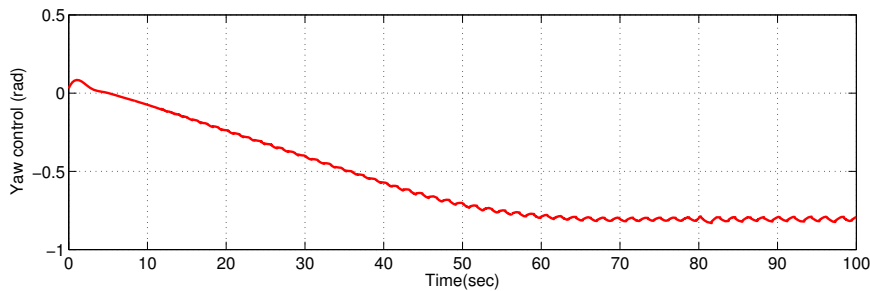
Figure 5.19: Yaw control signal with third order Super-twisting control design

Figures 5.20 and 5.21 show the pitch angle and yaw angle sliding surfaces respectively when third order super-twisting control is used. During sliding mode the state vectors for pitch and yaw angles slide along the designed sliding surface and keeps the tracking error to be minimum.
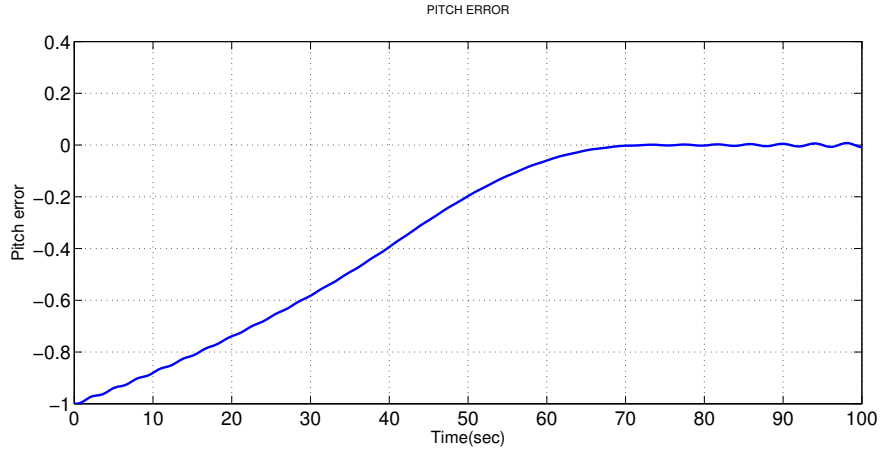
Figure 5.20: Pitch error surface with third order Super-twisting controller design
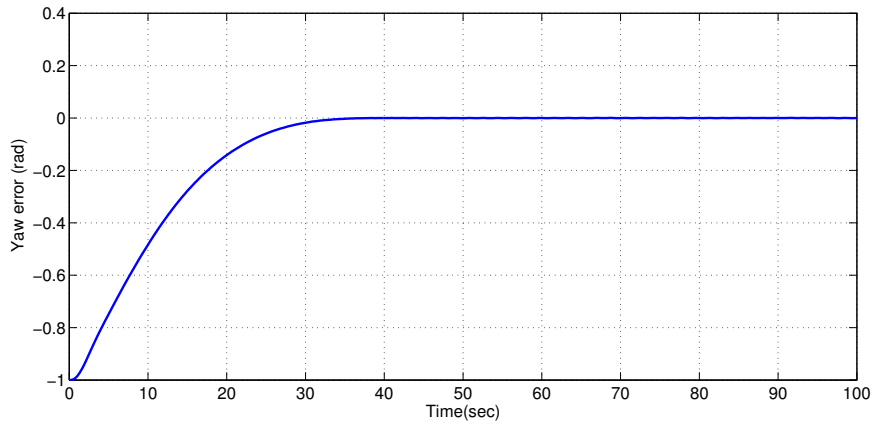
Figure 5.21: Yaw error surface with third order Super-twisting controller design

Figures 5.22 and 5.23 show the pitch angle and yaw angle position tracking responses respectively when third order super-twisting control is used. The initial conditions for pitch is given as 0.1 rad and for yaw 0.4 rad. Pitch response settles in 70 seconds and yaw response settles in 35 seconds. It is

noted that there is no initial over shoots and under shoots in both pitch and yaw angle responses.
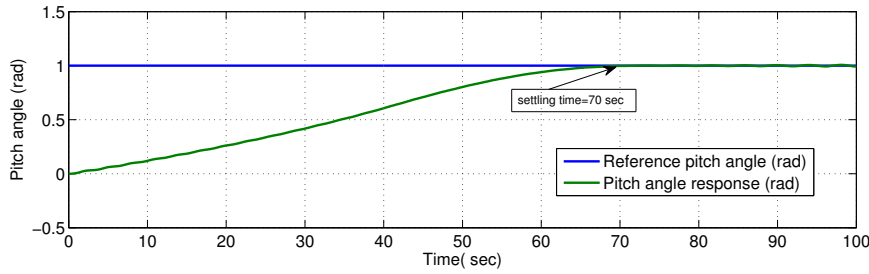
Figure 5.22: Pitch angle position tracking response with third order Super-twisting controller design
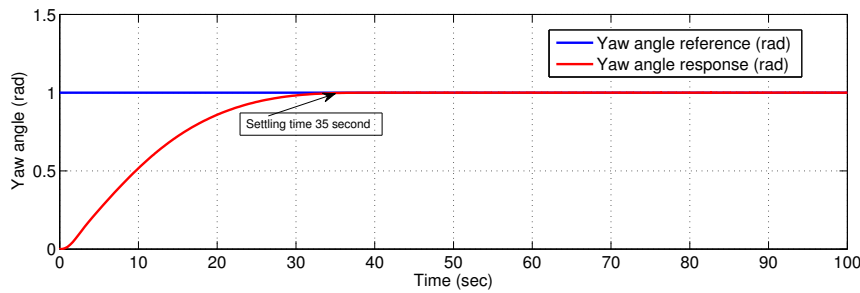
Figure 5.23: Yaw angle position tracking response with third order Super-twisting control design

Figures 5.24 and 5.25 show the pitch angle and yaw angle position tracking responses respectively when the disturbance is given at 80 seconds. The disturbance of $0.4sin(.1t) + 0.4$ is given to both pitch and yaw through input channel (matched disturbance). When matched disturbance is applied there is a small deviation in the pitch angle position tracking. The explains the robustness of the system reduces with the use of third order super-twisting control.
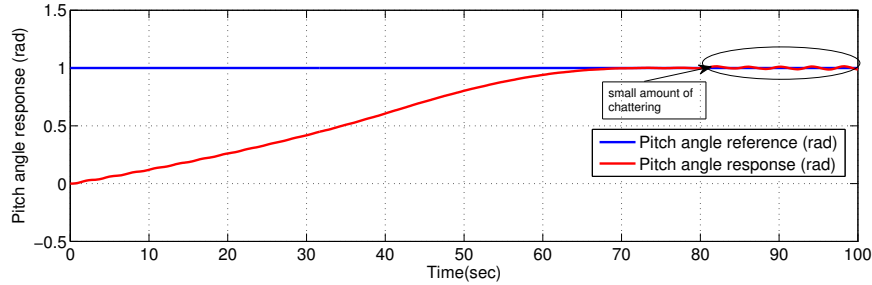
Figure 5.24: Pitch angle position tracking response with third order Super-twisting controller design when a disturbance is applied at 80 sec.
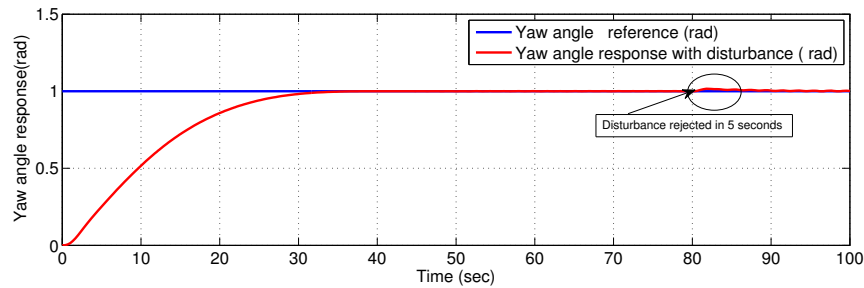
Figure 5.25: Yaw angle position tracking response with third order Super-twisting control design when a disturbance is applied at 80 sec.

5.8 Comparison

Table 5.1 shows the comparison between non-linear sliding surface (NLSS) and, real time implementation using NLSS and third order super-twisting control (Third order STC)design for 2-dof TRMS. Pitch angle position tracking response settles in 8 seconds and yaw angle position tracking response settles in 7 seconds with the NLSS design. The robustness of the system is also improved with the use of NLSS design. The non-linear sliding surface is capable of withstanding a matched disturbance of $0.4 + 0.4sin(0.1t)$ as well as external disturbance in real time implementation without the loss of

tracking efficiency. The pitch angle position tracking response settles in 70 seconds and yaw angle position tracking response settles in 35 seconds when third order STC is used. The robustness property of the system is slightly lost with the use of third order super-twisting control.

Thus it is concluded that even though the chattering is reduced, the robustness property is affected with the use of third order STC for the 2-dof TRMS.

Table 5.1: Performance comparison for 2-dof TRMS with simulation real time implementation of Non-linear surface design and Third order super-twisting controller design

Description	NLSS	Real time NLSS	Third order STC
Settling time for Pitch angle position	8 sec	13 sec	70 sec
Settling time for Yaw angle position	7 sec	15 sec	35 sec
Overshoot for Pitch angle position	Nil	40 percent	Nil
Overshoot for yaw angle position	Nil	6 percent	Nil
Robustness	Robust	Robust	Less robust
Chattering	low	high	low

Table 5.2: Performance comparison for 2-dof TRMS with simulation real time implementation of Non-linear sliding surface design and Linear sliding surface design

Description	NLSS	Real time NLSS	LSS
Settling time for Pitch angle position	8 sec	13 sec	8 sec
Settling time for Yaw angle position	7 sec	15 sec	10 sec
Overshoot for Pitch angle position	Nil	40 percent	12percent
Overshoot for yaw angle position	Nil	6 percent	5 percent
Robustness	Robust	Robust	Robust
Chattering	low	high	low

5.9   Analysis of Results

In this chapter a non-linear sliding mode control with super-twisting control and third order super-twisting control have been designed for highly non-linear 2-dof TRMS. The performance of 2-dof TRMS is compared with the non-linear sliding mode controller using NLSS and that with the third order STC. With the newly designed non-linear sliding surface as per[56],it is verified that the system becomes more robust with the use of NLSS. Also there is simultaneous reduction in overshoot and settling time for pitch and yaw of the 2-dof TRMS. The settling time for pitch is reduced to 8 seconds and for yaw it is reduced to 7 seconds. There is no overshoot in both pitch and yaw of 2-dof TRMS. Also the non-linear surface is proved to be stable in the sense of Lyapunov stability analysis. There is a significant reduction in chattering with the application of super-twisting controller. The non-linear sliding mode control with NLSS for 2-dof TRMS has been tested in real time with the use of MATLAB tool box and PCI1711 card. The performance comparison between the non-linear sliding mode controller with non-linear sliding surface and the third order super-twisting control has been made for 2-dof TRMS. In real time implementation of NLSS in 2-dof TRMS, it is noted that there is an overshoot of 40 percent in pitch angle position tracking and 6 percent overshoot in yaw angle position tracking. This high variation in simulation result and real time implementation may be due to the high moment of inertia of the 2-dof TRMS. The other reason may be due to the incorrect damping ratio constant given by the manufacturer.

5.10   Conclusion

This chapter deals with the performance of 2-dof Twin Rotor MIMO system with the design of non-linear sliding surface and non-linear sliding mode controller. The super-twisting controller is included in the non-linear sliding mode controller to reduce chattering. The simulation result validate the

design using non-linear sliding surface has good tracking performance and also robust to the matched disturbance. The simultaneous reduction of peak overshoot and settling time has also been noticed from the simulation result. The real time implementation validates the robustness of the system with the application of NLSS. In addition to that the comparisons with the third order super-twisting and LSS have been provided to show that the NLSS design perform better in control aspects and robustness aspects. it is verified that the NLSS design becomes more appropriate than the design of controller using LSS and third order super-twisting for systems like 2-dof TRMS. The draw back of the design using NLSS is that the complexity of the design is high as compared with the existing PID, LSS and third order super-twisting.

Chapter 6

Design,Simulation and Comparison of Various Controllers for Dual Input Buck Boost Converter

6.1   Introduction

In chapter 5, it is seen that for electro mechanical system (2-dof TRMS) the non-linear sliding mode controller with super-twisting control and non-linear sliding surface have given an excellent performance with simultaneous reduction of settling time, initial overshoot and chattering. And also there is an improvement in robustness of the system. In the present chapter, it is proposed to use various controllers for an electrical system and analyse through extensive simulation. The electrical system considered here is dual input buck boost converter (DIBB).

The different modes of operations and corresponding state space modelling of DIBB is explained in Section 2.2.2. The equation for transfer function for DIBB shown in figure 2.3 can be obtained using the equation which is

available in [66] as:

$$G(s) = \frac{V_1}{RC}\frac{D}{(1-D)^2}\frac{s - \frac{R(1-D)^2}{LD}}{s^2 + \frac{1}{RC} + \frac{(1-D)^2}{LC}} \tag{6.1}$$

Where V_1 is the input voltage applied to the DIBB, D is the duty ratio. C is the capacitance of DIBB,L is the inductance of DIBB, and R is the load resistance. The transfer function for DIBB is obtained by substituting the values of DIBB parameters as in table 8.2 of Appendix 8, $D = 0.75$, $R = 100$, $C = 450 * 1e - 6$, $L = 3.75 * 1e - 3, and V_1 = 12$

$$G(s) = 3200\frac{s - 2222}{s^2 + 22.22s + 3.7 * 10^4} \tag{6.2}$$

The corresponding root locus obtained using MATLAB-9 is shown below in figure 6.1.

From the root locus it is clear that there is one zero lying on the right side of s plane and two complex poles on the left side of the s plane. Since one zero is on the right side of the s plane the system becomes a non-minimum phase system. The following controllers are designed for dual input buck boost converters:

1)PI Controller

2) A conventional sliding mode control

in cascaded structure 3) super-twisting control

4) Integral sliding mode control with discontinuous control

5) Integral sliding mode control with super-twisting control algorithm.

The main motivation of this chapter has come from the work carried out by K.Sundaresan and et.al. The purpose is to find out the degree of acceptance of the performance when each controller is employed in DIBB. It is obvious that the pure electrical system of DIBB is very much faster compared to TRMS. Certain algorithm give noticeable improvement while some others are not effective.
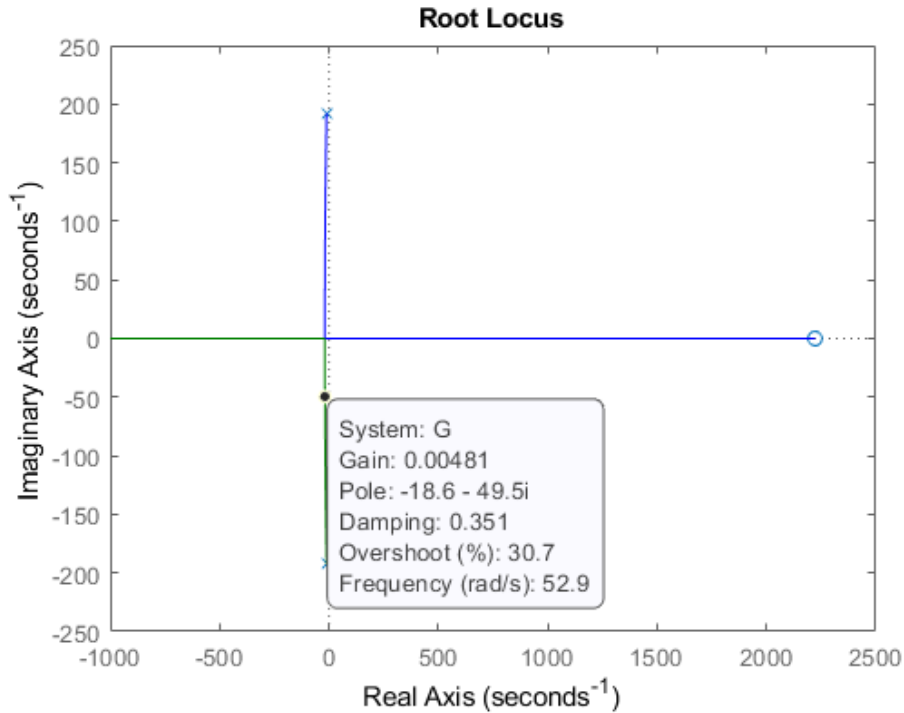
Root Locus

Figure 6.1:   Root locus of Buck Boost converter's linearized Transfer function

The performance improvement of DIBB under various control strategies is measured in terms of chattering in output signal, initial transients and robustness of the system. The robustness of the system is measured by making changes in input voltage, load current and change in reference voltage.

This chapter is organised as follows: Section 6.2 deals with design of PI controller using *Damped − Oscilation* method for DIBB. Section 6.3 deals with design of conventional sliding mode control in cascaded structure for DIBB. Design of super-twisting control is given in Section 6.4. Section 6.5 explains the design of discontinuous control in integral sliding mode control (ISMC) for DIBB. The design of super-twisting control in ISMC for DIBB is given in Section 6.6. The performance comparison of DIBB with various controllers is given in Section 6.7. Analysis of results is detailed in Section

6.8. Finally conclusion is given in Section 6.9.

6.2 Design of PI controller parameters

From the root locus of the DIBB system, it is clear that no sustained oscillation is possible for the system as the two poles are not on the imaginary axis. Hence $Damped-oscillation$ method of PID tuning is used [67]. This method is slightly modified method of zeiglers ultimate gain method. By setting $T_I = $ inf and T_d=0, as in case of zeiglers ultimate gain method the value of K_p is increased from minimum value until ratio of a_1 to a_2 is 0.25 where a_1 and a_2 are first two continuous peaks. The corresponding step response is obtained in figure 6.2 . Now the decay ratio is obtained as 0.25 for $K_P = 0.0049$. The period is taken between two consecutive positive peaks as $T_d = 0.147$.

The value of K_I is obtained as:

$$K_I = 1.5\frac{K_P}{T_d} = 0.0516 \tag{6.3}$$

Figure 6.3 shows the block diagram for the Proportional Integral control (PI control) for DIBB . The reference voltage is compared with the output voltage. The error signal thus obtained is passed through the PI controller. The PI controlled signal is compared with 25KHZ signal. The resulting signal is given as the triggering signal to the DIBB.

The values of proportional constant K_P, integral constant K_I are obtained as $K_P = 0.0049$. and $K_I = 0.0516$.
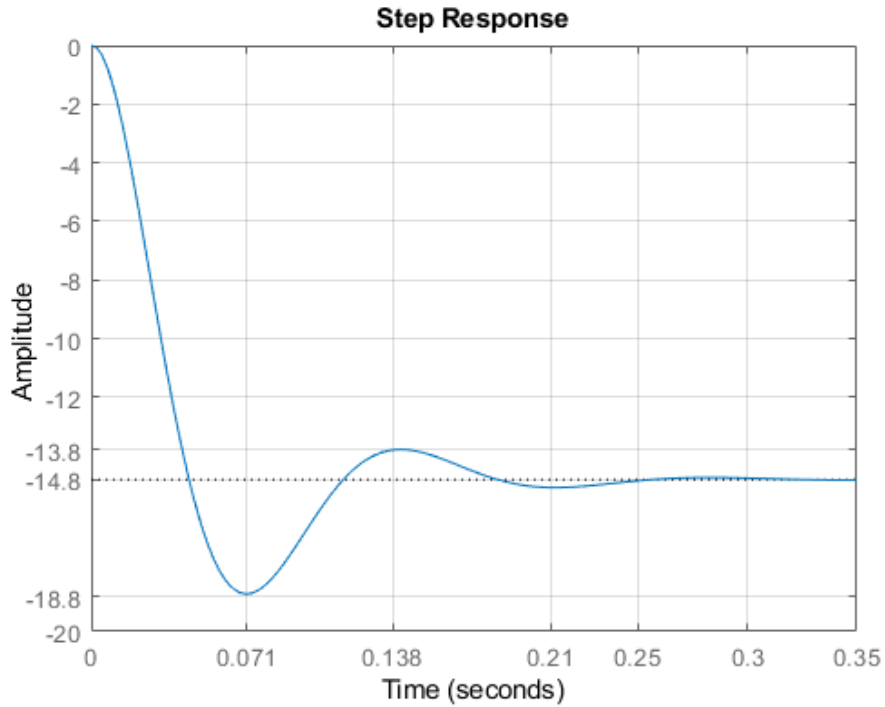
Figure 6.2: PI parameter tuning using $Damped - OScln - Test$

6.2.1 Simulation Results and discussion of the DIBB under PI control

The performance of DIBB using above values for K_p and K_I are given in figures (6.4) to (6.8). Figure 6.4 shows the output voltage of dual input buck boost (DIBB) converter when PI controller is used. It is obvious that there is no initial overshoots or undershoots. It becomes steady from $13 seconds$ sec on wards. Hence it is concluded that the settling time is high when PI controller is used.

Figure 6.5 chattering in output voltage of DIBB when PI control is used.

103
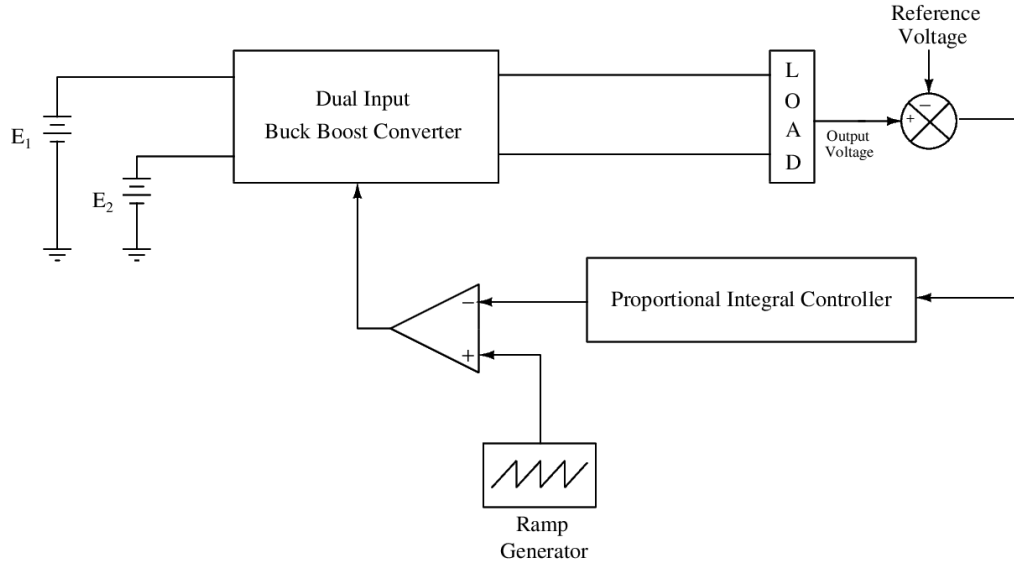
Figure 6.3:   Block Diagram of DIBB with PI control.

There exists a ripple voltage of $0.25V$ which is within the tolerable limit.
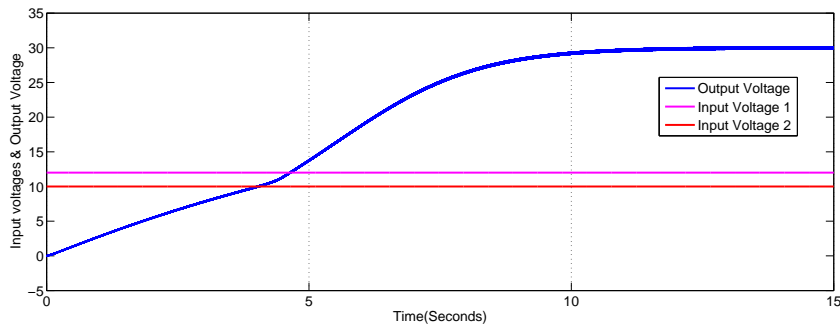
Figure 6.4:   Output voltage of DIBB with PI control

The next step is to check the robustness of the DIBB under the PI control. The robustness is checked by making sudden changes in input voltage,load current and reference voltage

Figure 6.6 shows the variation of output voltage with the change in input
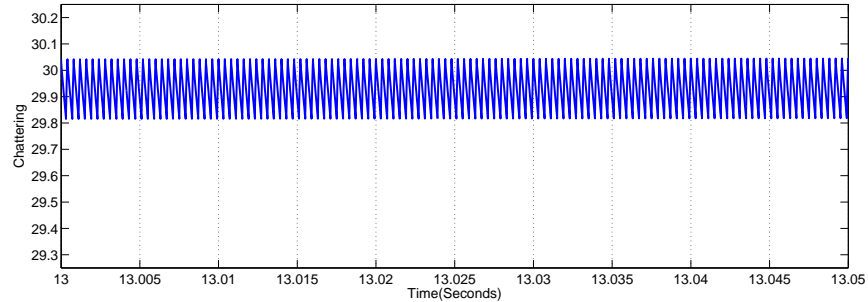
Figure 6.5: Chattering in output voltage of DIBB with PI control
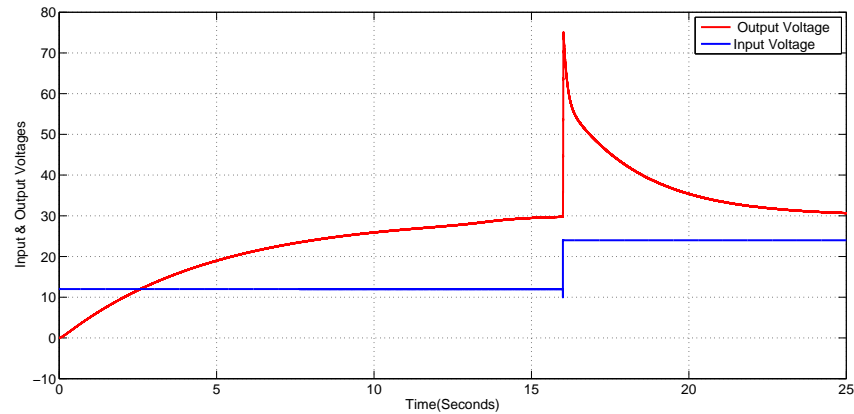
Figure 6.6: Output voltage response of DIBB with PI control when one of the input voltage changes from 12V to 24V

voltage1 (V_1) when PI controller is employed. The change in input voltage from 12V to 24V occurs at 16 sec. It is noted that there is an overshoot in the output voltage of DIBB at the time of sudden change in one of the input voltage of DIBB and settles in 8 seconds

Figure 6.7 (a) shows the change in load current at 16 seconds. Figure 6.7(b) shows the response of DIBB with PI control when load current is changed at 16 seconds. It is noticed that there is no change in output voltage of DIBB. Figure 6.8 shows the output voltage of DIBB when the reference is changed from 30V to 40V. Here it is seen that the output voltage is also

105
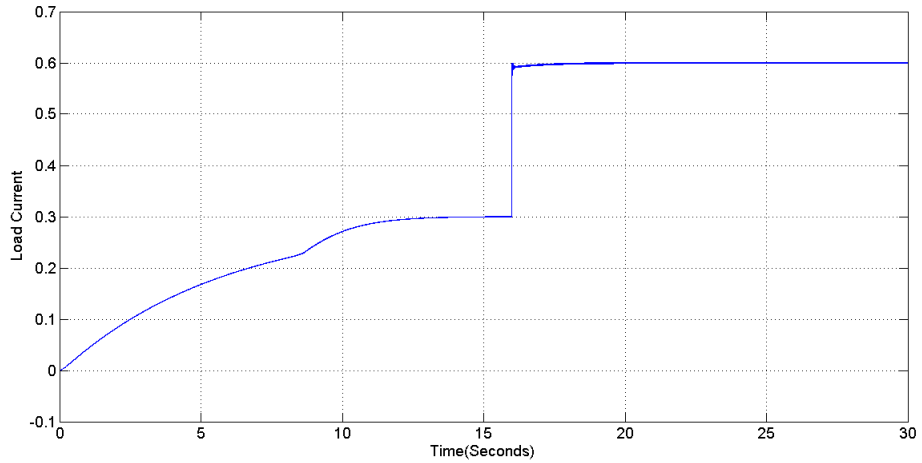
(a) Load Current
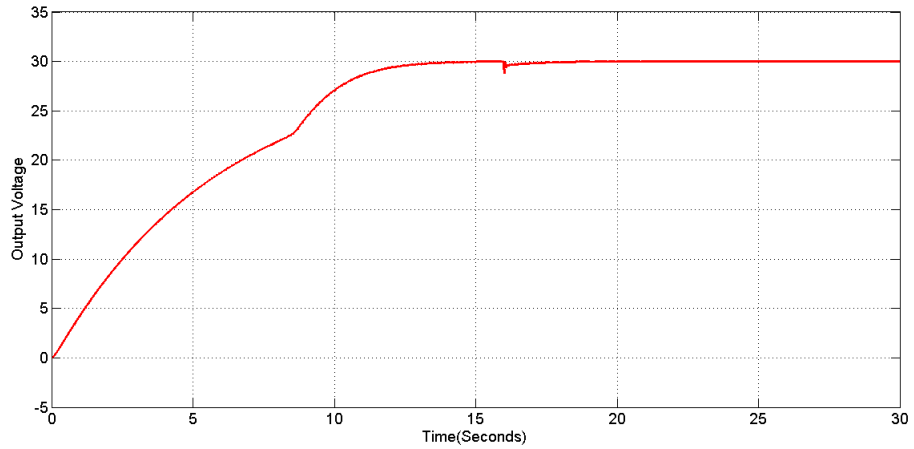
(b) Output Voltage

Figure 6.7: Response with Load Variation

changing from 30V to 40V by taking a time delay of 0.3 seconds.

Hence it is concluded that the settling time and chattering are high with the use of PI control. Also overshoot at the time of change in input voltage
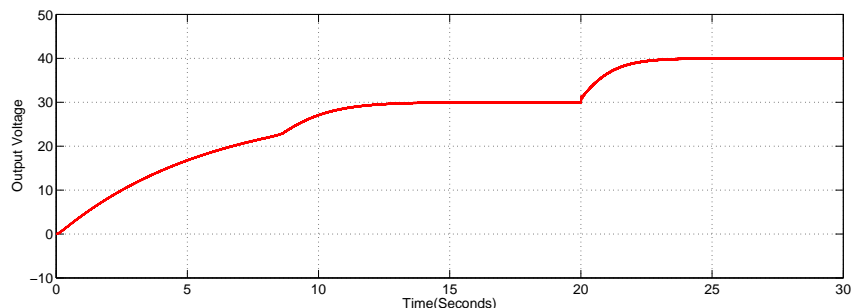
Figure 6.8: output voltage of DIBB when reference changes from 30V to 40V with PI control

is high for DIBB when PI controller is employed. The drawbacks of the PI control are reduced with the use of sliding mode control (SMC) [68] as the sliding mode control is insensitive to the parametric variation and external disturbance. The next Section deals with the design of conventional sliding mode control[69] for DIBB

6.3   Design of Conventional sliding mode control in cascaded structure for DIBB

The general procedure for designing a sliding mode controller is to develop a state space model of the converter. For a system defined by state space variables $x_1, x_2, x_3......x_n$ the sliding function S can be expressed in the following form [59] as::

$$S = \alpha_1 x_1 + \alpha_2 x_2 + \alpha_3 x_3........... + \alpha_n x_n. \tag{6.4}$$

Where $\alpha_1, \alpha_2, \alpha_3......\alpha_n$ are sliding coefficients. The second step is to find the sliding mode control u. It is necessary to ensure that the sliding function is confined to the sliding surface $S = 0$. This is achieved by applying the

107

existence condition given by:

$$lim_{S->0}S\dot{S} < 0 \tag{6.5}$$

The control signal u is calculated as per [59] as:

$$u = 0.5(1 - sign(S)) \tag{6.6}$$

The chattering may result when SMC is used. Thus in order to reduce the chattering problem sliding mode control in cascaded structure has been developed [59]. The design of conventional sliding mode control in cascaded structure for DIBB is detailed in next Section.

Fig 6.9 shows the block diagram of conventional SMC applied to DIBB. Here the two loops are employed as the system is non-minimum phase system. The conventional SMC for DIBB using cascaded structure requires two control loops. These are inner current loop and outer voltage loop. Generally for most converters, motion rate of current is much faster than the motion rate of voltage. Because of this reason, SMC is applied in inner current loop and proportional integral (PI) controller is given in outer voltage loop.

6.3.1 Outer voltage loop

1) Outer voltage loop : In figure. 6.9, the output voltage of the dual input buck boost converter is compared with the reference voltage V_d and the resulting signal is fed through PI controller, the output of PI controller is referred to as i_c. This current signal is now added with the feed forward inductor current i_d. Then the resultant current is i^* termed as:

$$i^* = i_d + i_c \tag{6.7}$$

The resultant current thus obtained is the overall reference current to the inner loop. Now the overall reference current to the inner current loop is i^*.
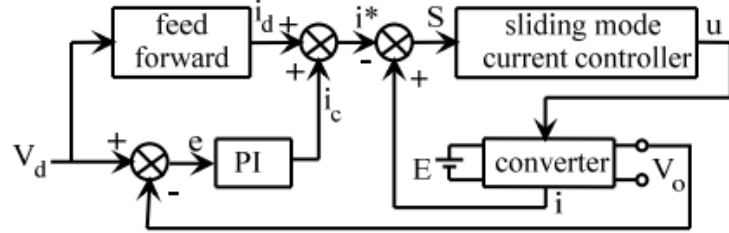
Figure 6.9: Block Diagram of Conventional Sliding Mode control applied to DIBB.

6.3.2 Inner Current Loop

The buck boost output current i is compared with the reference current i^* and the sliding surface S is designed. As per [59], the sliding surface is obtained as

$$S = i - i^*$$ (6.8)

Where i is the dual input buck boost output current and i^* is the reference current to inner current loop. The state of the system will slide along this sliding surface during sliding mode irrespective of the system. Thus even if parameters of the system is varied it will not affect response of the system during sliding mode.

The next step is to design controller value. The control signal given to the switch of dual input buck boost converter should be such that the switch should either open or close according to the duty ratio. For dual input buck boost converter the sliding mode control scheme as per [69] is:

$$u = 0.5(1 - sign(S))$$ (6.9)

6.3.3 Simulation Results and discussion of the DIBB under conventional sliding mode control

The conventional sliding mode controller is applied to DIBB. The performance of DIBB under conventional sliding mode control is given in figures 6.10 to 6.16. Figure 6.10 shows the two input voltages and regulated output voltage during boost operation of dual input buck boost (DIBB) converter when conventional sliding mode control is used. It is obvious from the figure that there is an overshoot of 16.6 percent. It becomes steady from 0.2 second on-wards.

Figure 6.11 shows the chattering in the output voltage of DIBB when conventional control is applied. There exists a ripple with magnitude of $0.02V$ in the output voltage of DIBB which is within the tolerance limit. Hence it is concluded that the chattering is reduced with the use of conventional sliding mode control in cascaded structure.

Figure 6.12 shows the error surface of DIBB when conventional sliding mode control is applied. The error between the reference voltage and the output voltage becomes zero in 0.2 seconds. Hence it is concluded that the settling time is reduced with the use of conventional sliding mode control. It is already observed that the settling time taken for DIBB is 0.5 seconds with the PI control.

The next step is to check the robustness of the DIBB under conventional SMC. The robustness is checked by making sudden changes in input voltage,load current and reference voltage

Figure 6.13 shows the DIBB response using conventional sliding mode control when there is a change in load current at 1.5 seconds. It is observed that there is small change in output voltage at the time of change in load current and attains the steady value within 0.2 seconds. Figure 6.14 shows the load current change at time 1.5 sec.

Figure 6.15 shows the variation of output voltage with the change in input voltage1 V_1 when conventional sliding mode control is applied. The change
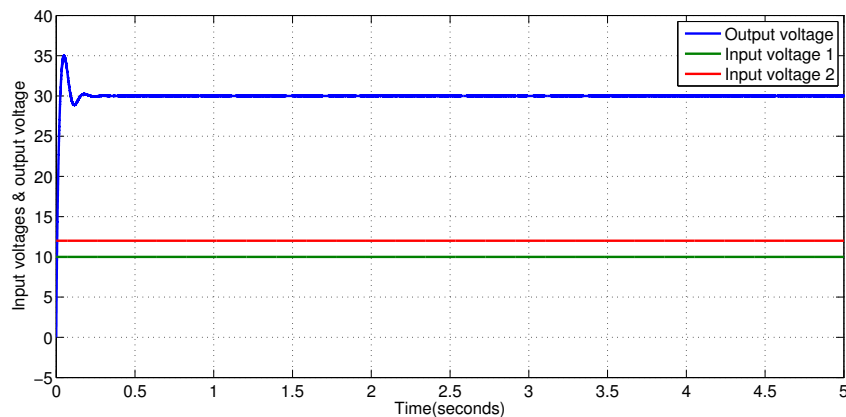
Figure 6.10:   Output voltage response of DIBB with conventional sliding mode control
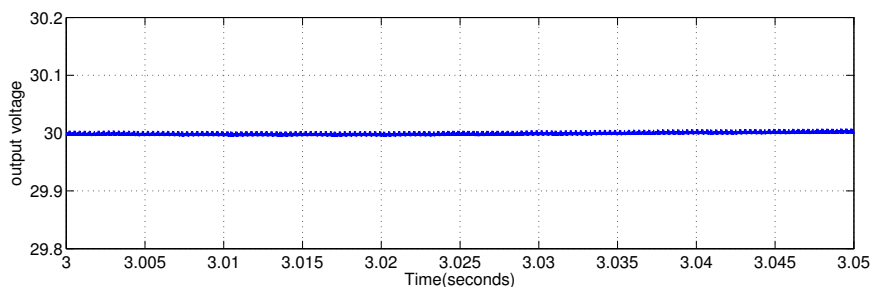
Figure 6.11:   Chattering in output voltage response of DIBB with conventional sliding mode control

in input voltage from $12V$ to $24V$ occurs at 1.5 sec. It is noted that there is small overshoot at the time of sudden change in input voltage and attains the steady state value within 0.1 second and this explains the robustness of the conventional sliding mode control. Hence it is concluded that the over shoot and settling time is reduced with the use of super-twisting control.

Figure 6.16 shows the output voltage when the reference is changed from 30V to 40V. The change occurs within 0.05 sec. The change from 30V to
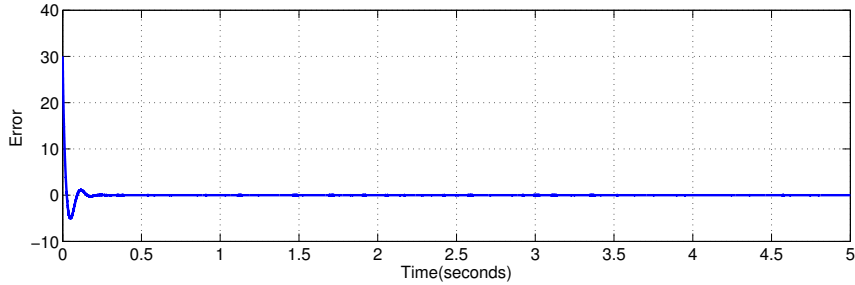
Figure 6.12:   Error with conventional sliding mode control for DIBB

40V occurs at 0.05 seconds.
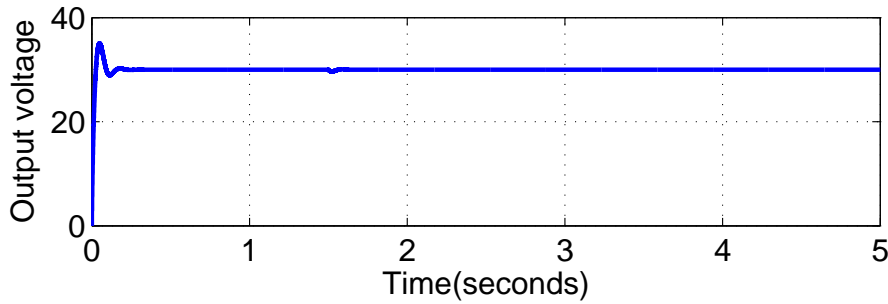
Figure 6.13:   Output voltage response of DIBB with conventional sliding mode control when the load current changes

Although the magnitude of chattering is reduced with the use of conventional SMC, the frequency of chattering is found to be more. So this control cannot be applied in real time implementation as the high frequency of the control signal damage the switch used. But the super-twisting control can solve this problem. The next Section deals with the application of super-twisting control in DIBB.

112
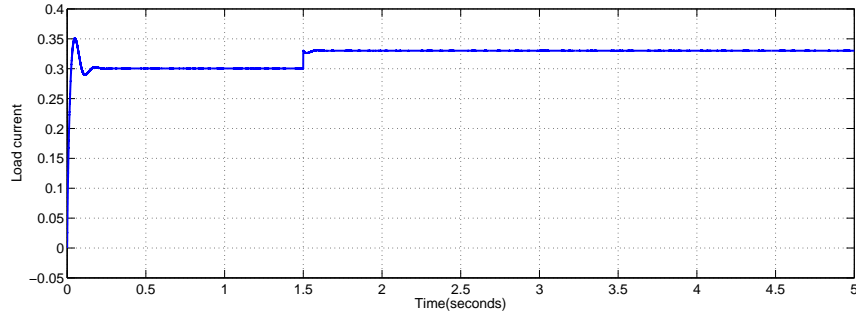
Figure 6.14:   Load current with conventional sliding mode control of DIBB

Figure 6.15:   Output voltage response of DIBB with conventional sliding mode control when one of the input voltage changes from 12V to 24V

Figure 6.16: Output voltage of DIBB with conventional sliding mode control when reference voltage changes from 30V to 40V

6.4   Design of super-twisting control for DIBB

The conventional SMC generates high frequency switching in control signal which is also known as chattering problem. In order to avoid chattering problem in control signal, super-twisting control (STC) algorithm is used [69]. There are two parts in the super-twisting control algorithm. One is continuous control part and other one is discontinuous control part. The continuous control part reduces the chattering effect and discontinuous control part stabilizes the system.
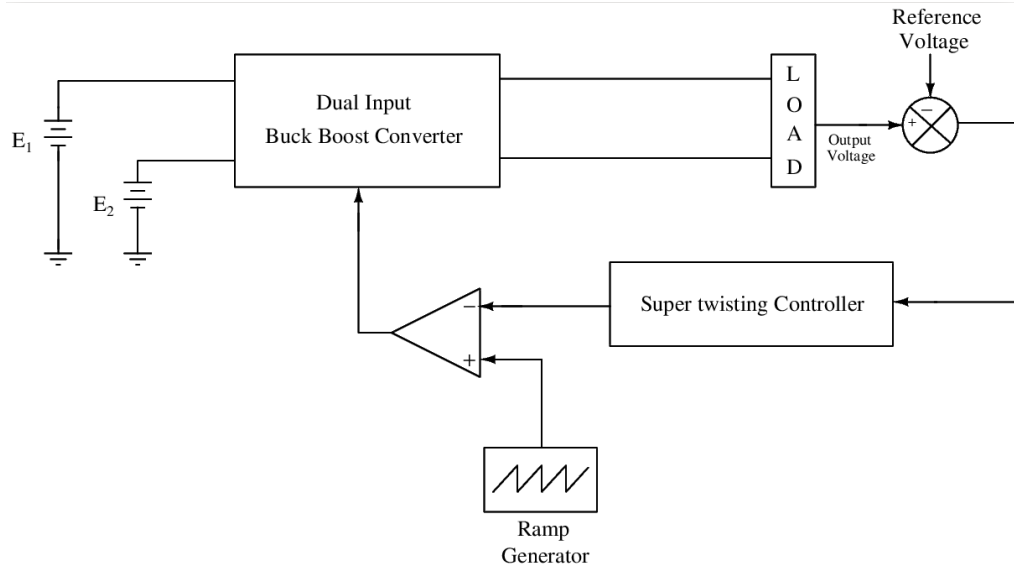
Figure 6.17: Block Diagram of DIBB with Super-twisting control

Figure 6.17 shows the block diagram for DIBB under super-twisting algorithm. Here the reference voltage is compared with the output voltage and the difference between the reference voltage and actual voltage is taken as the error signal. The error signal is passed through the super-twisting controller. the signal thus obtained is compared with the ramp signal. The output of the comparator is taken as the control signal which can be used to

114

trigger the DIBB.

super-twisting control as given in [59] can be written as:

$$u_S = -\gamma_1(e)^{\frac{1}{2}} sign(e) - \gamma_2 \int sign(e) \tag{6.10}$$

Where e is the error between the output and reference signal. The γ_1 and γ_2 are positive gains. The parameters γ_1 and γ_2 are calculated using the equation:

$$\gamma_1 = 1.5R^{\frac{1}{2}} \tag{6.11}$$

$$\gamma_2 = 1.1R \tag{6.12}$$

With sufficient convergence conditions,

$$\gamma_2 > R \tag{6.13}$$

and

$$\frac{2(\gamma_2 + R)}{\gamma_1^2(\gamma_2 - R)} < 1 \tag{6.14}$$

The value of R is selected such that the maximum bound of system matrix $f(x) < R$.

6.4.1 Simulation Results and discussion of the DIBB under Super-Twisting Control

The performance of DIBB under super-twisting control is given in figures 6.18 to 6.24. Figure 6.18 shows the two input voltages and regulated output voltage during boost operation of dual input buck boost (DIBB) converter when super-twisting control is used. It is obvious that there is no initial overshoot or undershoot.

figure 6.19 shows the chattering in output voltage of DIBB. There exists a ripple voltage of 0.1V which is within the tolerance limit. The frequency of the chattering is reduced to large extent.

Figure 6.20 shows the error signal of DIBB with super-twisting control. It is noted that the error attains zero value in 0.1 second which explains the efficiency of the super-twisting control.
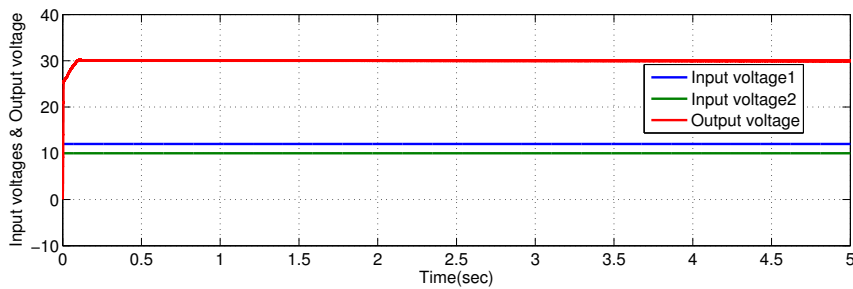
Figure 6.18: Output voltage of DIBB with super- twisting control during boost operation
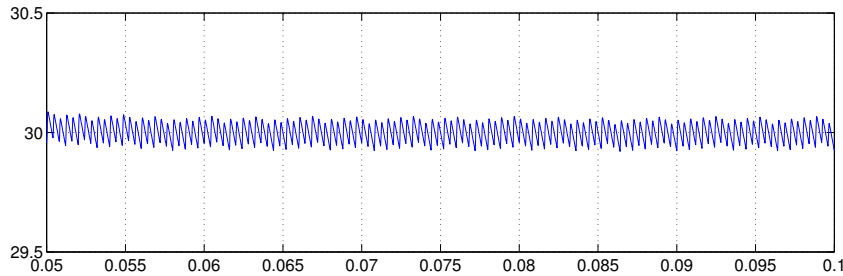
Figure 6.19: Chattering in output voltage response of DIBB with super-twisting control

The next step is to check the robustness of the DIBB under super-twisting control. The robustness is checked by making sudden changes in input voltage,load current and reference voltage.

Figure 6.21 shows the output voltage of DIBB whenever there is change
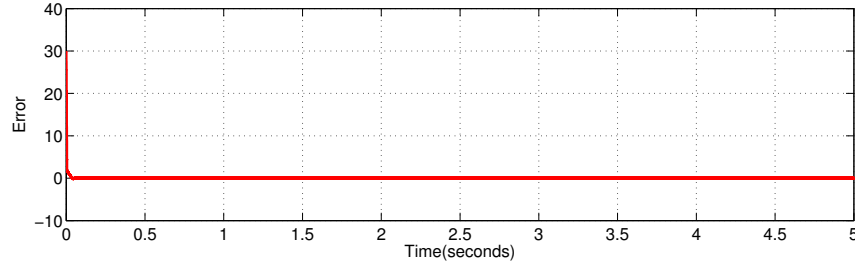
Figure 6.20:   Error of DIBB with super-twisting control

in load current with super-twisting control. It is observed that there is no change in output voltage at the time of change in load current. Figure 6.22 shows load current change at 1.5 seconds.

Figure 6.23 shows the variation of output voltage with the change in input voltage1 V_1 when super-twisting control is applied. The change in input voltage from 12V to 24V occurs at 1.5 sec. It is noted that there is small overshoot at the time of change in input voltage and attains the steady state value within 0.2 second. This explains the robustness of the super-twisting control.

Figure 6.24 shows the regulated output voltage of DIBB when the reference is changed from 30V to 40V at 1.5 seconds. It is observed that there is no overshoot during the step change in the reference voltage and the output attains the desired value in 0.1 second.

It is noted that the performance of DIBB under super-twisting control is good in terms of chattering and robustness. The performance will be more better if we reduce the reaching time. Integral sliding is used to reduce reaching time. Next Section deals with the application of Integral sliding mode control in DIBB

117
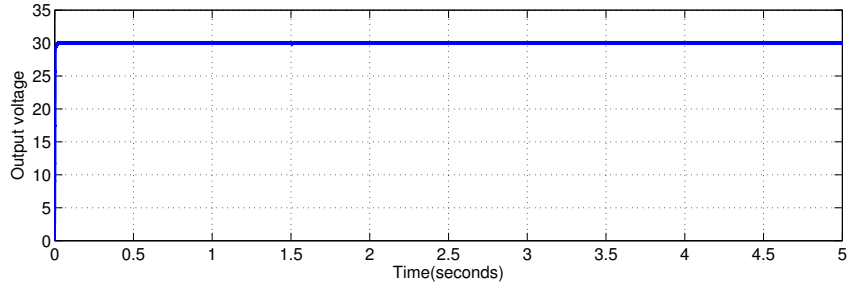
Figure 6.21:   Output voltage response of DIBB with super-twisting control
when there is step change in load current at 1.5 second
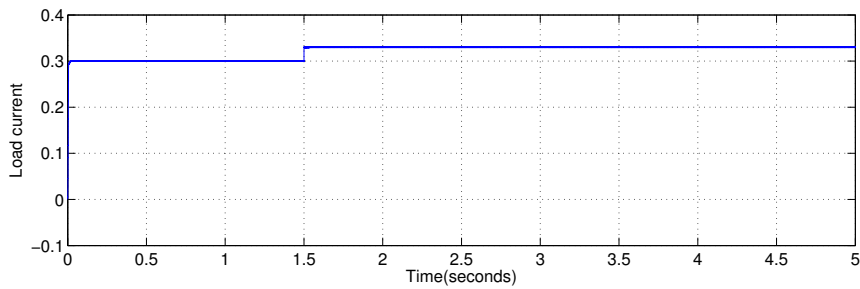
Figure 6.22: Load current change of DIBB with super-twisting control
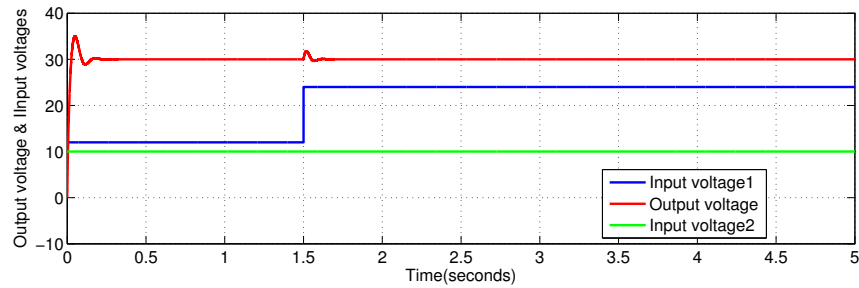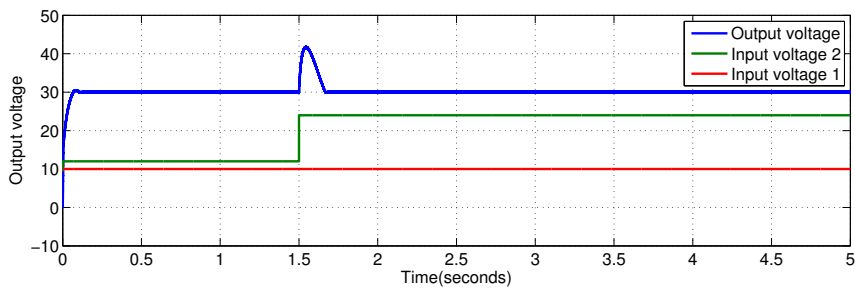

Figure 6.23:   Output voltage response of DIBB with super-twisting control
when one of the input voltage changes from 12V to 24V

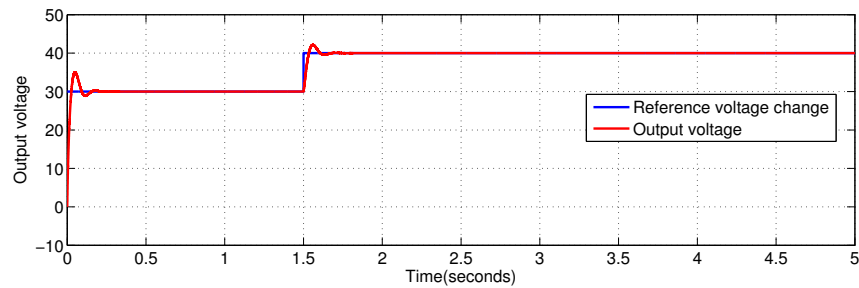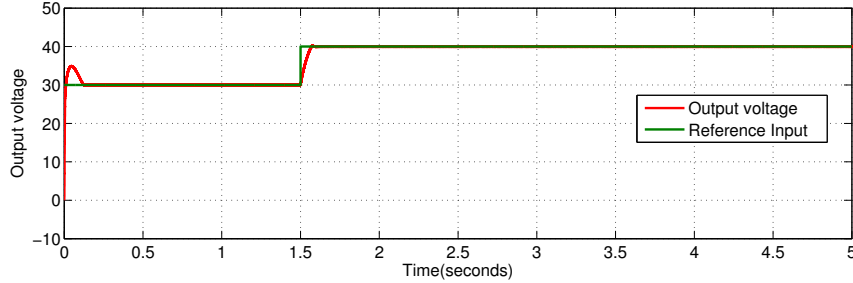Figure 6.24: Output voltage of DIBB with super-twisting control when reference changes from 30V to 40V

6.5 Design of discontinuous control in Integral Sliding Mode Control for DIBB

There are two phases in sliding mode control. First one is reaching phase and second is sliding phase. The reaching phase is one in which the system states are driven from any initial state to reach the sliding manifold. Sliding phase is one in which system induces into sliding manifold. The robustness comes into action only after the occurrence of sliding mode. The robustness cannot be guaranteed during reaching phase. Integral sliding mode controller (ISMC) is the best solution to eliminate the reaching phase [70]. Finite time stabilization without disturbances are studied by Bhatt and Berstein, using chain of integrators [71]. This control is not able to reject matched disturbance (Disturbance through input channel).

In order to reject matched disturbance, a discontinuous control is added with the nominal control. But this may result in chattering problem at the output. As discussed in previous chapters the higher order sliding mode control can reduce chattering. The most popular higher order sliding mode control techniques are twisting algorithm and super-twisting algorithm. In twisting algorithm, the real time measurement of switching variable derivative is required. But in some real time applications the measurement of

derivative of switching variable is not possible. Such issues do not occur in super-twisting algorithm. Hence the integral sliding mode control with super-twisting algorithm is the best solution to reduce chattering effect as well as to eliminate the reaching phase.

The system in equation (2.10)can be written in the following form as:

$$\dot{x} = f(x)x + g(x)u \tag{6.15}$$

Where $f(x)$ and $g(x)$ are the system matrix and input matrix respectively. If a disturbance d which is equivalent to sudden change in input voltage and current respectively are applied to the system, the system equation now becomes:

$$\dot{x} = f(x)x + g(x)u + d \tag{6.16}$$

The integral sliding mode control is added with either the discontinuous control or continuous control (super-twisting algorithm) to make the system robust. The integral control is designed using nominal control as discussed below. The nominal control u_N is designed using finite time stabilizing control by Bhatt and Berstein as per [71] and is given by:

$$u_N = -\beta(e)^{\frac{1}{2}} sign(e) \tag{6.17}$$

where β is the nominal control gain and e is the error between the actual value of the output voltage and reference value. This control is unable to reject matched disturbance entering through control channel. So in order to reject such disturbance some authors designed additional discontinuous control [71]. The discontinuous control is used to make the system robust which is given by:

$$u_D = -\epsilon sign(e) \tag{6.18}$$

Where ϵ is the discontinuous controller gain and e is the error.

The control signal obtained by adding the nominal control and discontinuous control is given by:

$$u_1 = u_N + u_D \tag{6.19}$$

Now if the control given to the system is selected as [61]:

$$u = \frac{1}{g(x)}(-f(x) + u_1) \tag{6.20}$$

By applying equations (6.20) and (6.19) in (6.16), the system becomes

$$\dot{x} = u_N + u_D + d \tag{6.21}$$

Thus the system equation is modified in terms of nominal control, discontinuous control and disturbance. The sliding surface as in [72] is reproduced here: The sliding surface S is given by:

$$S = x - x_0 - \int u_N \tag{6.22}$$

where x_0 is the initial condition. Also, the derivative of sliding surface is:

$$\dot{S} = \dot{x} - u_N \tag{6.23}$$

Substituting equation (6.21) in equation (6.23)

$$\dot{S} = u_N + u_D + d - u_N \tag{6.24}$$

When the system is in sliding mode, the equivalent value of control is calculated by equating derivative of sliding surface to zero.

$$u_N + u_D + d - u_N = 0 \tag{6.25}$$

Hence,

$$u_D = -d \tag{6.26}$$

This means that the disturbance can be rejected when the system is on sliding mode and the magnitude of disturbance is equal to the magnitude of discontinuous control.

6.5.1   Results and discussion for DIBB under discontinuous control in Integral Sliding Mode Control

Figure 6.25 shows the input voltages and regulated output voltage during boost operation of dual input buck boost converter when discontinuous control in combination with integral sliding mode control (ISMC). It is obvious that there is an initial overshoot of 20 percent with settling time of 0.05 seconds.

Figure 6.26 shows chattering in output voltage. There exists a ripple voltage of $0.4V$ which is not within the tolerance limit. This high value of chattering is due to the discontinuous control.

Figure 6.27 shows the error with respect to time. It is observed that the error attains zero value within 0.04 seconds. This is because of the elimination of reaching phase.
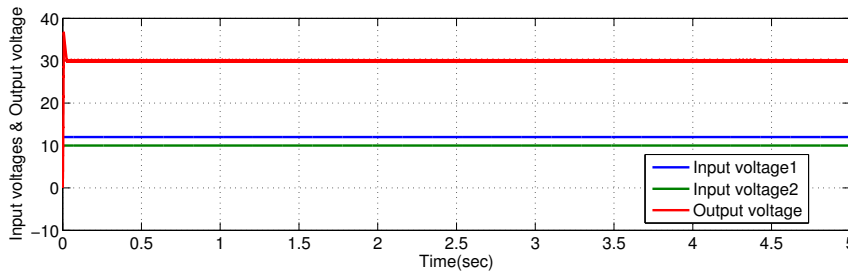
Figure 6.25:   Output voltage of DIBB with discontinuous control in ISMC during boost operation.

Figure 6.28 shows the output voltage response of DIBB with discontinuous control in ISMC when there is change in load current. It is observed that there is no change in output voltage at the time of step change in load.

Figure 6.26:   Chattering in Output voltage of DIBB with discontinuous control in ISMC during boost operation.
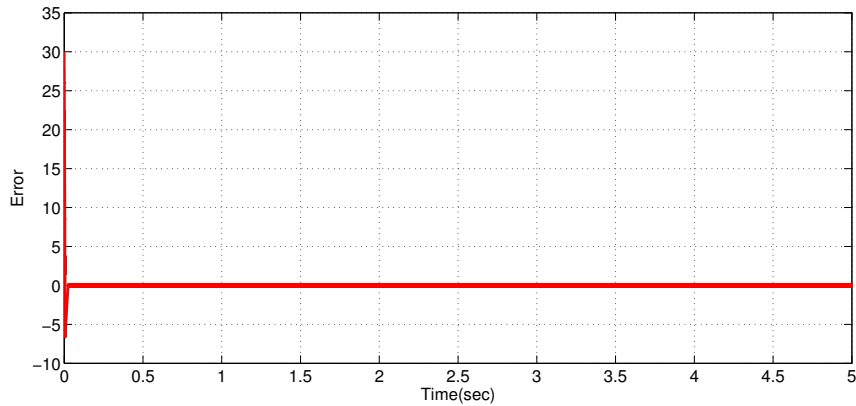
Figure 6.27: The error signal of DIBB with discontinuous control in ISMC.

Figure 6.29 shows the variation of output voltage with the change in input voltage1 (V_1) when integral sliding mode with discontinuous control is applied. The change in input voltage from $12V$ to $24V$ occurs at 1.5 sec.

Figure 6.30 shows the regulated output voltage of dual input buck boost converter when the reference is changed from $30V$ to $40V$ at 1.5 seconds. It is observed that there is no overshoot during the change in the reference

123

voltage and the output attains the desired value in 0.01 seconds.
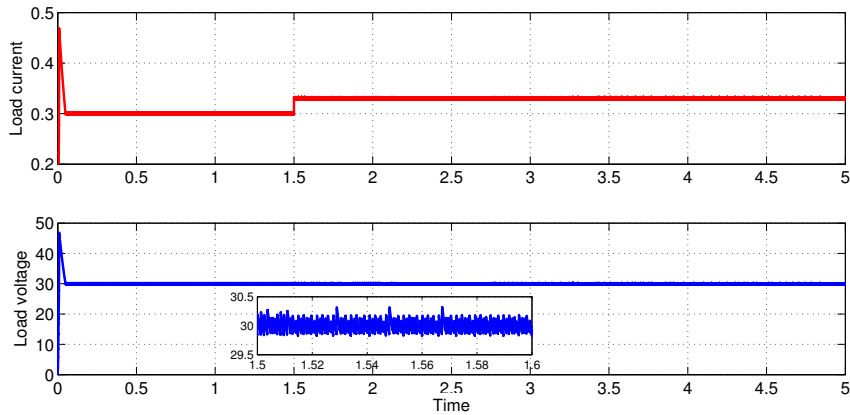
Figure 6.28: Output voltage response of DIBB with discontinuous control in ISMC when there is step change in load current.

Figure 6.29: Output voltage response of DIBB with discontinuous control in ISMC when one of the input voltage changes from 12V to 24V

The performance of DIBB is improved with the use of discontinuous control in ISMC. But the magnitude of chattering is increased with the use of discontinuous control in integral sliding. To reduce this effect of chattering super-twisting control is applied instead of discontinuous control. Hence the next Section deals with the the application of super-twisting control in ISMC.
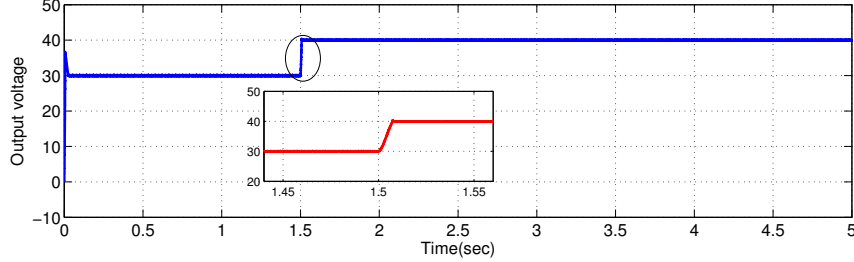
Figure 6.30: Output voltage of DIBB with discontinuous control in ISMC when reference is changed from 30V to 40V

6.6 Design of Super-twisting control in ISMC applied for DIBB

The integral sliding mode controller with super-twisting control applied is given in [72] as :

$$u_1 = u_N + u_S \tag{6.27}$$

where u_N is the nominal control and u_s is the super-twisting control. The nominal control is given by:

$$u_N = -\beta(e)^{\frac{1}{2}} sign(e) \tag{6.28}$$

Here β is the nominal controller gain, and e is the error between the actual value of the output voltage and reference value. The,u_s being the super-twisting control u_S is given by [62]:

$$u_S = -\gamma_1(e)^{\frac{1}{2}} sign(e) - \gamma_2 \int sign(e) \tag{6.29}$$

Where γ_1 and γ_2 are positive gains. The parameters γ_1 and γ_2 are calculated using the equation (6.11) to (6.14):

125

Defining the sliding surface S as:

$$S = x - x_0 - \int u_N \qquad (6.30)$$

where x_0 is the initial condition. Taking the derivatives of the surface $\dot{S}$ becomes:

$$\dot{S} = \dot{x} - u_N \qquad (6.31)$$

Then the control signal consisting of nominal control and super-twisting control is given by:

$$u_1 = u_N + u_S \qquad (6.32)$$

Proceeding in the similar fashion as explained for discontinuous control in ISMC, the system equation becomes:

$$\dot{x} = u_N + u_S + d \qquad (6.33)$$

When the system is on sliding surface, the equivalent value of control is calculated by substituting derivative of sliding surface equal to zero. Hence it can be shown as:

$$u_N + u_s + d + -u_N = 0 \qquad (6.34)$$

Thus,

$$u_S = -d \qquad (6.35)$$

This means that the disturbance is rejected when the system is on sliding mode.

6.6.1 Simulation Results and Discussion of DIBB with Super-twisting control in ISMC applied for DIBB

The performance of DIBB using super-twisting control in ISMC is given in figures 6.31 to 6.36. Figure 6.31 shows the two input voltages and regulated output voltage during boost operation of dual input buck boost converter when Integral sliding with super-twisting control applied is used. It is obvious that there is no overshoot and becomes steady within 0.06 second onwards.

Figure 6.32 shows chattering in output voltage. It is obvious that there exists a ripple voltage of $0.15V$ in the output voltage which is within the tolerance limit.

Figure 6.33 shows the error between the reference voltage and the output voltage of DIBB with super-twisting control in ISMC. It is observed that error become zero in 0.01 seconds this is due to the reduction in reaching phase.
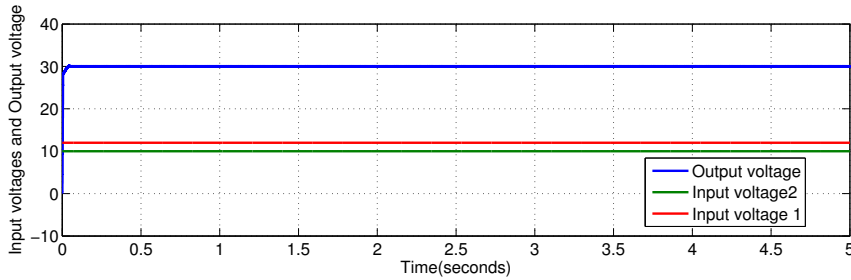
Figure 6.31: Output voltage response of DIBB with super-twisting control in ISMC

The robustness is checked by making sudden changes in input voltage, load current and change in reference voltage. Figure 6.34 shows the output voltage response of DIBB with super-twisting control in ISMC when there is a change in one of the input voltage. It is observed that there is small overshoot during the change in the input voltage and the output attains the desired value in 0.1 seconds.
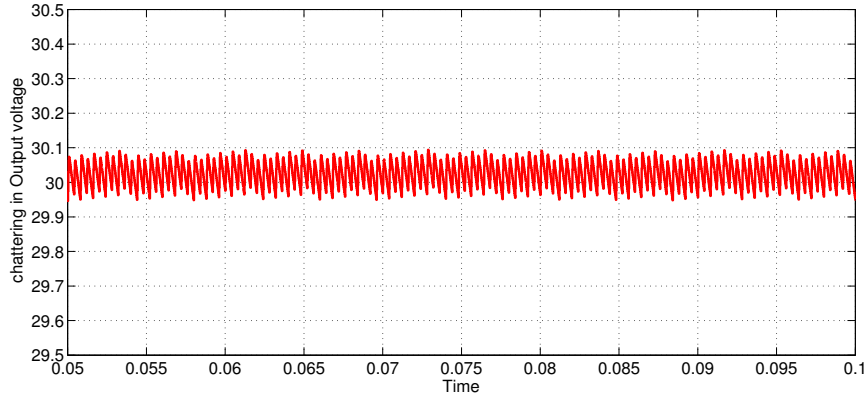
Figure 6.32: Chattering in Output voltage of DIBB with super-twisting control in ISMC during boost operation
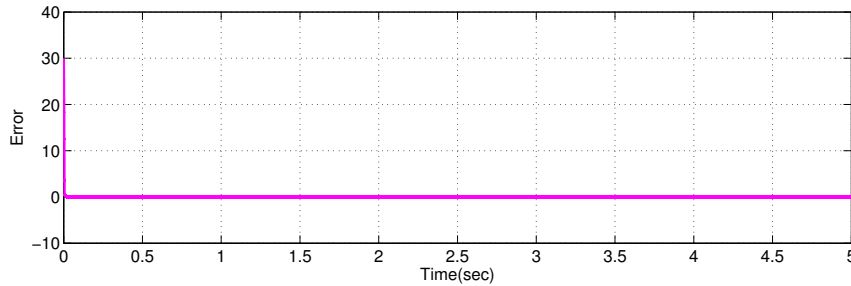
Figure 6.33: Error in DIBB with super-twisting control in ISMC

Figure 6.35 shows the output voltage response of dual input buck boost converter with super-twisting control in ISMC when there is a change in load current at 1.5 seconds . It is observed that there is no change in output voltage at the time of change in load.
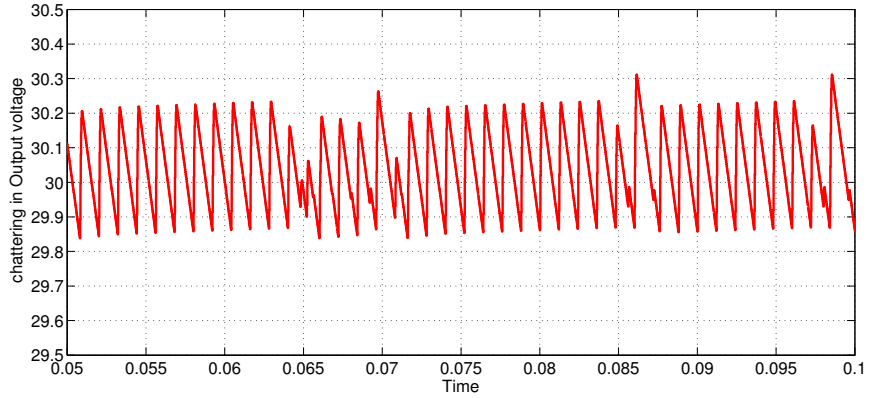
Figure 6.36 shows the regulated output voltage of DIBB when the reference is changed from $30V$ to $40V$ at 1.5 seconds. It is observed that there is no overshoot during the change in the reference voltage and the output attains the desired value in 0.1 seconds.

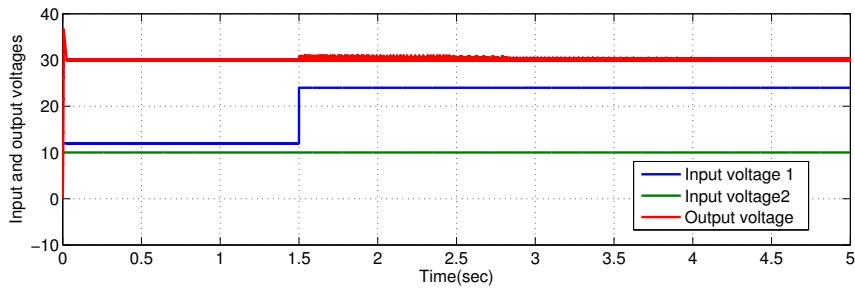Thus it is inferred that the settling time as well as the chattering is
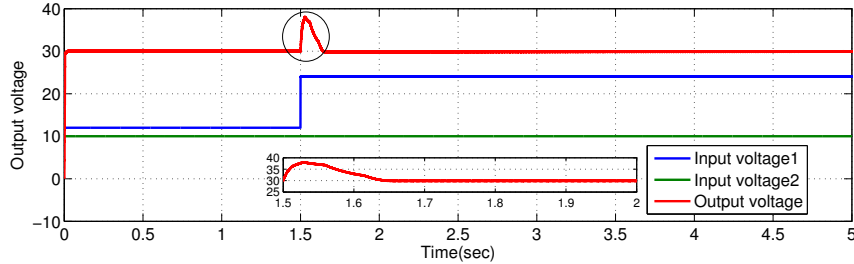
Figure 6.34: Output voltage response of DIBB with super-twisting control in ISMC when one of the input voltage changes from 12V to 24V
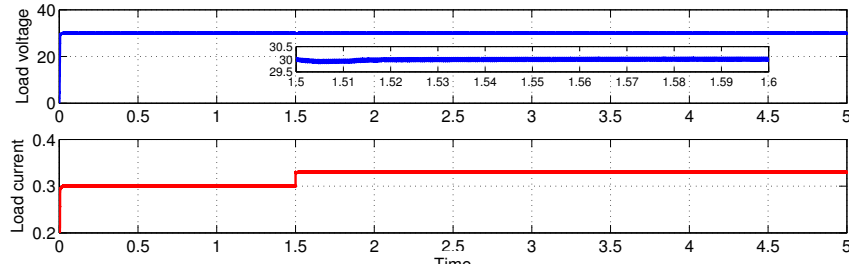
Figure 6.35: Output voltage response of DIBB with super-twisting control in ISMC when there is load current change at 1.5 seconds
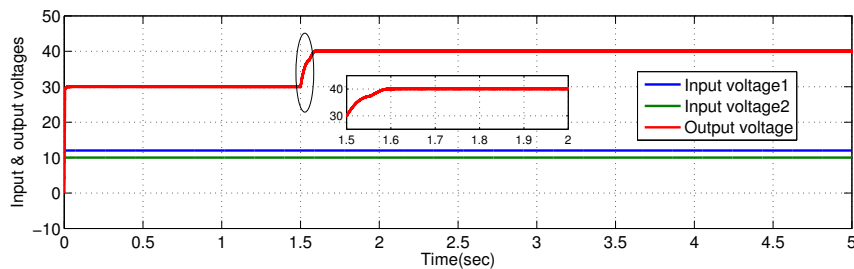
Figure 6.36: Output voltage of DIBB with super-twisting in ISMC when reference is changed from 30V to 40V

reduced by using integral sliding mode control with super-twisting control applied.

129

6.7   Comparison

Table 6.1 shows the performance comparison of DIBB with various control strategies. The magnitude in chattering, frequency in chattering and robustness of the system with various controllers are shown in this table. The robustness is checked by making sudden changes in input voltage, load current and reference voltage. Table 6.2 shows the initial transients performance of the DIBB with various controllers.

Table 6.1:   Performance Comparison of DIBB with various control strategies

Description	Mag. of Chattering	Robustness
PI Control	0.25V	slightly Robust
conventional sliding	0.02V	Robust
super-twisting control	0.1 V	Robust
Discontinuous control in ISMC	0.4 V	Robust
super-twisting control in ISMC	0.08 V	Robust

Table 6.2:   Initial Transients comparison of DIBB with various control strategies

Description	Over shoot	Settling time
PI Control	Nil	13 seconds
conventional sliding	16.6 percent	0.2 second
super-twisting control	Nil	0.1 second
Discontinuous control in ISMC	20 percent	0.04 second
super-twisting control in ISMC	Nil	0.06 second

6.8   Analysis of Result

The focus of the chapter is to apply sliding mode controller to dual input Buck boost converter. Firstly, the design of PI controller is done. It is observed that the settling time is 13 seconds. The chattering is 0.25 V in the output response. Moreover it is noted that the changes in input voltages,

load current or reference voltage take high value of settling time in the output response. The system becomes less robust with the use of PI controller. In order to reduce the settling time, the design of sliding mode controller has been done. The conventional sliding mode control is tried first. Since the system is non-minimum phase system as described in Section 6.1, two loop control is used. It is found that the frequency of chattering is very high due to the application of discontinuous part of conventional sliding mode controller in the current loop of the DIBB. In order to reduce chattering a continuous controller known as super-twisting controller is applied to the system. It is found that the chattering is reduced to 0.1V with the design of super-twisting control in the DIBB system. Moreover an integral sliding mode controller is designed for DIBB to eliminate the reaching time. The integral sliding mode with super-twisting control produces an output response with 0.08V chattering and less reaching time. The simulation results of DIBB for its responses to sudden change in load current, sudden change in input voltage and sudden change in reference voltage are compared for all the control strategies applied for DIBB. The results show that the effectiveness of modified integral sliding mode controller with super-twisting control as continuous part in ISMC. The control signal obtained using super-twisting control and super-twisting control in ISMC for DIBB can be used in real time application.

6.9 Conclusion

This chapter analyses the performance of DIBB with the design of PI control, conventional sliding mode control, super-twisting control, integral sliding mode control with super-twisting control, Integral sliding mode with discontinuous control. The simulation result validate the design using super-twisting control and design of ISMC with super-twisting control has good tracking performance and is robust to the matched disturbance. In addition

to that the comparisons with the conventional sliding mode control and PI control have been provided to show that the STC and STC with ISMC design perform better in control aspects and robustness aspects. it is verified that the STC design become more appropriate than the design of controller using PI for systems like DIBB.

Chapter 7

Conclusions and Future Work

7.1 Introduction

Two different types of systems are considered in this research work. The performance analysis of the 2-dof TRMS is carried out first with PID control, linear sliding surface with non-linear control , non-linear sliding surface with the combination of super-twisting and non-linear sliding mode control and third order super-twisting control. In the second case, the research work includes the performance of DIBB when applied with PI control, conventional sliding mode control, super-twisting control and super-twisting control in combination with integral sliding mode control.

The state space modeling of 2-dof TRMS is done using the dynamics which is available in the manual. Therefore, the modeling has been done by including all system related non-linearities since the system is highly non-linear. The transfer function derived from state space analysis has coupling term. In order to eliminate the coupling effect a decoupler is designed using minimal-di method. The decoupler thus obtained nullifies the cross-coupling effect between pitch and yaw of the TRMS system.

The performance of the 2-dof TRMS with the design of LSS is investigated in chapter 4. The simulation results validate the design using LSS has

satisfactory tracking performance and is robust to the matched disturbance. In addition to that the comparison with the PID has been provided to show that the LSS design perform better in control aspects and robustness aspects.

The performance of 2-dof Twin Rotor MIMO system with the design of non-linear sliding surface and non-linear sliding mode control is investigated in chapter 5. The super-twisting controller is included in the non-linear sliding mode controller to reduce chattering. The simulation results validate the design using non-linear sliding surface which has good tracking performance and also robust to the matched disturbance. The simultaneous reduction of peak overshoot and settling time has also obtained and it is validated using simulation. The real time implementation validates the robustness of the system with the application of NLSS. In addition to that the comparison with the third order super-twisting and LSS has been provided to show that the NLSS design perform better in control aspects and robustness aspects. It is verified that the NLSS design becomes more appropriate than the design of controller using LSS and third order super-twisting for systems like 2-dof TRMS. The draw back of the design using NLSS is that the complexity of the design is high as compared with the existing PID, LSS and third order super-twisting. The applicability of the designed non-linear sliding surface with STC employed in non-linear controller has been tested both in simulation and in real time.

The performance of DIBB with the design of conventional sliding mode control, super-twisting control, integral sliding mode control with super-twisting control, Integral sliding mode with discontinuous control is investigated in chapter 6. The simulation results validate the design using super-twisting control and design of ISMC with super-twisting control has good tracking performance and also robust to the matched disturbances. In addition to that the comparison with the conventional sliding mode control and PI control has been provided to show that the STC and STC with ISMC design perform better in control aspects and robustness aspects. It is verified

134

that the STC design become more appropriate than the design of controller using PI for systems like DIBB.

7.2   Major Research Contributions

The main contributions of the thesis can be summarized as:

- Developed a mathematical model for the 2-dof TRMS considering all system-relevant non-linearities and coupling effects. The non-linearities include the parabolic variation of torques of yaw angle and trigonometric and parabolic variations torques of pitch angle.

- The developed decoupler is capable of eliminating coupling effects between pitch and yaw angles of 2-dof TRMS. The decoupler is designed based on minimal-di method which guarantees the expected performance without the poles and zeros of the system getting cancelled against each other.

- The linear sliding surface is designed for linear part of 2-dof TRMS using optimal design procedure. Also a non-linear controller is designed for 2-dof TRMS. The performance validation of the controller is done using simulation.

- Using the concept of variable damping ratio, a non-linear sliding surface is designed for 2-dof TRMS by considering all non-linearities associated with the system. The simultaneous reduction in both peak overshoot and settling time is noted in the simulation results. Also, a non-linear sliding mode controller with super-twisting algorithm is designed. The controller performance is validated by both simulation and real time implementation. The use of super-twisting algorithm helps to reduce the chattering in control signal given to pitch and yaw of TRMS.

- The use of third order super-twisting algorithm helped to reduce the chattering in control signal given to both pitch and yaw of of TRMS and validation through simulation is also done for the 2-dof TRMS.

- PID controller is designed for dual input buck boost converter using *Damped − Oscilation* method as the system is non-minimum phase system. The performance is validated through simulation.

- The sliding mode controller is designed for Dual input buck boost converter (DIBB) and is validated through simulation.

- Super- twisting controller is designed for DIBB to reduce chattering. Also validation is done through simulation.

- The combination of super-twisting control and integral sliding mode control is designed for DIBB. The performance is validated through simulation.

In nutshell, the performance of the sliding mode controllers on systems with high time constant (Electro mechanical systems) and low time constant (Electrical system) are analysed. It is found that both systems perform well with sliding mode control. Super-twisting controller gives chattering free responses in both systems. Also it is noticed that the non-linear sliding surface with variable damping ratio makes the electromechanical system (2-dof TRMS) more robust and to reduce the settling time. The application of super-twisting control instead of signum function in non-linear sliding mode control reduces the chattering in control signal.

7.3   Scope and Future Work

The thesis work concentrated on two MIMO systems. These are 2-dof TRMS and DIBB. The following are the scope and future work.

136

There are 3-dof MIMO and higher dof MIMO systems. The investigations of the performance of these systems with linear and non-linear sliding surfaces with relevantly designed sliding mode controllers is very needed. This can be taken as future work.

In this work the decoupler is designed for linearized model of the system. But for non-linear part the decoupler design is not carried out. Hence this also may be the scope for the researchers as a future work.

The objective of the algorithm considered is limited to asymptotic stability of the system and the finite time stabilization of the system is not considered at all. This is yet another scope for future work

The expected performance is obtained for the above mentioned 2-dof TRMS and double input buck boost converter. It is not verified for other mechanical , electromechanical, electronic systems. Hence same could be considered for future work.

Bibliography

[1] Y. Wu and Y. zhou " A stable time in variant controller for an open loop unstable systems," International Journal of Control, Vol.77, no.1, pp. 9-18, 2004.

[2] Y. Wu and Y. zhou " Output feed back control for MIMO non-linear systems with unknown sign of the high frequency gain matrix," International journal of Control, Vol.77, no.1, pp.9-18, 2004.

[3] W. Lin and C. Quian " Semi-global robust stabilization of MIMO non-linear systems in semi-strict feedback forms," Automatica, Vol.37, pp. 1305-1321, 2001.

[4] X. Liu, G. Gu and k.zhou " Robust stabilization of MIMO non-linear systems by back stepping," Automatica, Vol.35, pp. 987-992, 1999.

[5] Yaote Chang, " Block back stepping control of MIMO systems," IEEE transaction on Automatic control, Vol.56, no.5, pp. 1191-1197, 2011.

[6] R. Isermaan, K. H. Lachman, and D. Matco, Adaptive control systems, Prentice hall Newyork 1992.

[7] J.K.Tar,I.J. Rudas, K.R. Kozlowski and C. Pozna "A novel approach to the model reference adaptive control of MIMO systems", International workshop on robotics in andria Danube region RADD June pp.(23-25), 2010.

[8] J.k. Tar, J.J Rudas, S. Preti and R.E Pecup "An SVD based modification of Adaptive inverse dynamics controller," Proceeding. of 5 th international Symposium on applied computational Intelligence and Informatics , Timisoara Romania, 2009, pp. 193-198, 2009.

[9] Y.Zhang, W.Xie, and Z.Li, " Model predictive direct power control of a PWM rectifier with duty cycle optimization," IEEE Transaction Power Electronics, Vol.28, no.11, pp. 5343-5351, 2013.

[10] Rivera V. Yaramase, A.Liar J. Rodriguez, B.Wu, and M. Fadel " Digital predictive control of a three phase four leg inverter," IEEE Transaction Industrial Electronics, Vol.60, no.11, pp. 4903-4912, 2013.

[11] P. Cortes, A. Wilson and S.Kouro, " Model predictive control of multi level Cascaded H- Bridge inverter," IEEE Transaction on Industrial Electronics, Vol. 57, No.8, pp.2691-2699, 2010.

[12] K.V.Ling, S.P. Yue and J.M. Maciejowshi, " FPGA implementation of model predictive control," Proceedings of the American control conference M, Miniapolis Minisotta USA, June (14-16), 2006.

[13] Sajin Gopi, V.M. Vaidyan and M.V. Vaidyan "Implementation of FPGA based model predictive control for MIMO systems, " IEEE Conference on Systems , Process and control (13-15,) kulalampur Malaysia, December 2013.

[14] X. Ye, " Decentralised adaptive regulation with unknown high frequency gain signs," IEEE Transaction Automatic Control, Vol.44, no.11, pp. 2072-2076, 1999.

[15] X.Ye, " Decentralised adaptive adaptive stabilization of large scale nonlinear time delay systems with unknown high frequency -gain signs," IEEE Transaction on Automatic control, Vol.56, no.6, pp. 1473-1478, 2011.

[16] C.Chen, Lulu song, ZhiLiu " Asymptotic fuzzy-approximation based control of MIMO systems with unknown input non-linearities and control direction," in Proceedings of 3rd international conference on informative and cybernetics for computational social systems, 2016.

[17] W.He and S.S.Ge," Vibration control of flexible beam with output constraint," IEEE Transaction on Industrial Electronics, Vol. 62, no.8, pp.5023-5030, August 2015.

[18] J.Yang, W.X. Zheng , S. Li, B.Wu, and M.Cheng " Design of prediction accuracy enhanced continuous time MPC for disturbed system via disturbance observer," IEEE transaction on Industrial Electronics, Vol. 62, no.9 pp.5807-5816 September 2015.

[19] C. Pukdeboon, A.S. A.S. Zonober and M. W.L.Thenin " Quasi continuous higher order sliding mode for space craft. attitude tracking maneuvers," IEEE Transaction on Industrial Electronics, Vol.57, no.4, pp.1436-1444 April 2010.

[20] Bin Xu and Ying Xin Shou, "Composite learning control of MIMO systems with applications," IEEE Transactions on Industrial Electronics, Vol. 65, no.8, pp.6414-6424 August 2010.

[21] TRMS 33-949S User Manual, Feedback Instruments Ltd., East Sussex,U.K., 2006.

[22] K.Sunderesan, Hariprasad B., Kiran S., Kuruvina shetti,P.Sankar, "Output voltage control of Dual Input Buck Boost converter," IEEE IGST 2013.

[23] R. A. Krohling, H. Jaschek, and J. P. Rey, "Designing PI/PID controllers for a motion control system based on genetic algorithms," in Proceedings of 12th IEEE International Symposium Intell. Control, Istanbul, Turkey, pp. 125-130, 1997.

141

[24] A. Odwyer, Hand book of PI and PID controller Tuning Rules,London U.K.Imperial College Press 2003.

[25] M. T. Huang and J. G. Juang, "Application of GA and PID control to nonlinear TRMS, in Proceedings of Artificial. Intelligence. Application Conference, Taichung, Taiwan, pp. 734-739, 2002.

[26] M.T. Huang and J. G. Juang, "Application of GA and PID control to non-linear TRMS," in proceedings of Arif.Intell.Application, conference.,Taichung, Taiwan. pp.734-739, 2002.

[27] Jih-Gau Juang, Ming-Te Huang, and Wen-Kai Liu, "Control using pre-searched genetic algorithm," IEEE Trans. on systems,man, and cyberneticsPART C: Applications and reviews, Vol. 38, No. 5, 2008.

[28] J. L. Meza, V.Santi banez, R.Soto, and M A Llama " FuzZY Self tuning PID semi global Regulator for Robot Manipulators control using pre-searched genetic algorithm," IEEE Transactions on Industrial Electronics on systems,man, and cyberneticsPART C: Applications and reviews, Vol. 59, No. 6, 2012.

[29] Keyu Li, " PID tuning for optimal closed loop performance with specified gain and phase margins," IEEE Transaction on control systems Technology Vol. 21, No. 3, 2013.

[30] Eranda Harinath, George K.I Mann, "Design and tuning of Standard additive Model based fuzzy PID controllers for Multi variable process systems," IEEE Transaction on systems, man, and cyberneticsPART C: Applications and reviews, Vol. 38, No. 3, 2008.

[31] Lucfola Campestrini , Louiz Carlos, Stevanatto Filho, and Aleandre Sanfelice Bazanella, "Tuning of multi variable decentrlized controllers through the ultimate point method," IEEE Transactions on Control systems Technology performance, Vol. 17, No. 6, 2009.

[32] V. Utkin, " Variable structure sliding systems with sliding modes," IEEE Transactions Automatic control. AC-22 no.2, pp. 212-222. April 1977.

[33] J. P. Su, C. Y. Liang, and H. M. Chen, Robust control of a class ofnon-linear systems and its application to a TRMS," in Proceedings of IEEE International Conference on Industrial Technology, Bangkok, Thailand, pp. 1272-1277, 2002.

[34] C.S.Liu, L.R. Chen, B.Z.Li.,S.K.Chen. " Improvement of Twin -rotor MIMO system tracking and transient response using fuzzy control technology," in proceedings of IEEE Congr. Industrial Electronics Application. pp.1-6, 2006.

[35] C.W. Tao.J.S. Taur and M.l. Chan, " Adaptive fuzzy terminal sliding mode controller for linear systems with mismatched time varying uncertinities," IEEE Transaction .Systems. Man, Cybernatics, vol.34, no.1, pp.255-262, feb. 2004.

[36] C.K.Lin, " Nonsingular terminal sliding mode control of robot manipulators using fuzzy wavelet networks," IEEE Transaction .Systems. Fuzzy. Systems., Vol.14, no.6, pp. 849-859, December 2006.

[37] Y.H. chang C.W. Chang . J.S. Taur and C.W. Tao." Fuzzy swing-up and fuzzy sliding mode balance control for planetary gear -up type invered pendulam," IEEE Transaction Industrial. Electronics. Cybern, vol.56, no.9, pp.3751-3761, September 2009.

[38] chin Wang Tao, Jin-shiuh Taur, " A novel Fuzzy sliding and fuzzy integral sliding controller for Twin Rotor Multi- input-Multi Output System," IEEE Transactions on Fuzzy systems. Vol.18, no.5, OCTOBER 2010.

[39] Alison silva, Walmir Caminhas, Andre Lemos and Fernando Gomide, " Real time Nonlinear modeling of a Twin Rotor MIMO system using

Evolving Nuero -Fuzzy Network," IEEE symposium on Computational Intelligence in Control and Automation, 2014.

[40] Lydiya John and Mija S, " Robust H-infinity control algorithm for Twin Rotor MIMO system," IEEE international conference on Advanced communication control and computing Technology, pp.168-173, 2014.

[41] Emmanuael Prempain, Andrea Lecchini " Dynamic Analysis of a Twin Rotor MIMO system and control design," 12 th international conference on control sheffield, UK, september 2018.

[42] S. Ajwad, M. Ullah, B. Kheltia and J Iqbal, " A comprehensive state of art on control of Industrial articulated robots," Journal of Balkan Trobological Association vol.20, no.4 pp. 499-521,2014.

[43] Syed Humayoon Shah, Said G Khan, Jamshed Iqbal Mathkar Aharthi " " Robust control of Twin Rotor MIMO system," 2019 international conference on robotics and automation in industry, October 2019, DOI 10.109/ICRK147710.2019.8967355, Publisher IEEE.

[44] Roshini Maithi, Kaushik Das Sharma, Gautham Sarkar "Optimal State feedback controller and observer design for Twin Rotor MIMO system", 2016 second international conference on control, instrumentation energy and communications, January 201, Publisher IEEE, DOI 10.1109/CIEC.2016.7513774, Kolkatta, India

[45] S.Mondal and C.Mahanta, " Adaptive sliding mode controller for a twin rotor Multiple input Multiple output system," IET Control Theory and Application, vol.6, pp.2157-2167, 2012.

[46] Samir Zeghlache, Abdderrahman Bougera and Muhammed Ladjal Sliding Mode Controller Using Nonlinear Sliding Surface Applied to 2-DOF Helicopter, Proceedings of 2nd international conference on Electrical and Information Technologies,ICEIT 2016.

[47] 15. Farah Faris, Abdelkrim Moussaoui, Boukhetala Djamel and Thadin Mohammed, Design and real-time implementation of a decentralised sliding mode for Twin rotor multi input multi output system, Journal of Systems and control Engineering. Vol. 231(1), pp. 3-13, 2017.

[48] 16. Yener Taskin, 1270. Improving pitch and yaw motion control of Twin Rotor MIMO system, Journal of Vibro Engineering , 16(4) July 2014.

[49] Ghosh A. Das S.K. " Open loop decoupling of MIMO plant," IEEE Transactions on Automatic Control, 54(8), pp.1977-1981, 2009.

[50] P.Wen, J.W.Lu " Decoupling control of Twin rotor MIMO system using robust dead beat control control Technique," IET Control Theory, vol.2, no.11, pp.999-1007, 2008.

[51] Jatin Kumar Pradhan, Arun Ghosh, "Design and implementation of decoupled compensation for a twin rotor multiple-input and multiple-output system," IET Control Theory Application, Vol.7, Issue 2, pp.282-289, 2013.

[52] Karteek Gummi and Mehdi Ferdowsi, "Double input DC-DC Power Electronic converters for Electric drive. Vechicles -Topology. Exploration and Synthesis using a Single pole Triple Pole switch," IEEE Transaction on Industrial Electronics. Vol.57, no.2, pp.617-623, 2010.

[53] Hongfei Wu, Kai Sun,Karteek Gummi and Yang Xiang, " Topology Derivation of Nonisolated Three port DC-DC converters from DIC and DOC," IEEE Transactions on Power Electronics, Vol.28, NO.7, pp.3297-3304.

[54] Yan Li, Xinbo Ruan, Dong sheng Yang, Fuxin Liu, and Chi K. Tse.,Fe, " Synthesis of Multiple- Input DC-DC converters," IEEE Transactions on Power Electronics, Vol.25, No.9, pp.2372-2385, 2010.

145

[55] ZiweiO uyang, Zhe Zang,Michle A.E. Anderson, and Ole E Thomson, Dong sheng Yang, Fuxin Liu, and Chi K. Tse.,Fe, " Synthesis of Multiple- Input DC-DC converters", IEEE Transactions on Power Electronics, Vol.27, o.6, pp.2697-2702, 2010.

[56] Deshang Sha, Kai Deng, nand Xiao Zong Liao, "Duty cycle Exchanging control for Input-Series Output-Series connected Two PS-SB DC-DC Converters," IEEE Transaction on Power Electronics, Vol.27, no.3, pp.1490-1501, 2012.

[57] Rong-Jong Wai, Chung- You Lin and BO-Han Chen, "High Efficiency DC-DC converters with Two input power sources," IEEE Transaction on Power Electronics, Vol.27, no.4, pp.1862-1875, 2012.

[58] N. Chimaobi Onwuchekwa and A. Kwasinki, "A modified time sharing switching Technique for Multiple-Input time sharing DC-DC converters," IEEE Transactions on Power Electronics, Vol.27, no.11, pp.4492-4502, 2012.

[59] D. Yang, M.Yang and X.Ruan, "One cycle control for a Double-Input DC/DC Converter ," IEEE Transactions on Power Electronics Vol.27, no.11, pp.4646-4655, 2012.

[60] ShijunQian, Hussan Al. Atrash Osama Abdel Rahman and Issa Batarseh, "Modeling and control of Three port DC/DC converter interface for satellite Applications," IEEE Transactions on Power Electronics Vol.25, no.3, pp.637-649, 2010.

[61] Reza Ahmadi and Mehdhi Ferdowsi, " Double- Input converters based on H-bridge cells. Derivation, Small signal modeling and power sharing Analysis," IEEE Transactions on Circuits and Systems Vol.59, no.4, pp.875-888.

[62] Vivek Kumar, Ashish Patra " Application of Ziegler-Nichols method for tuning of PID controller," 2nd International conference on recent innovations in Science , Technology, Management and Environment November 2016.

[63] Chritopher Edward and Sarah K.Spergeon, "Sliding Mode Control: Theory and Applications,' London, U.K.," Taylor Francis Ltd, 1998.

[64] F.Deepak, B.Bandyopadhyay, L.Fridman, "Non-linear sliding surface: towards high performance robust control," IET Control Theory Application, pp. 1-8, 2011.

[65] 20 Shyam kamal, Asif Chalanga, J.A Moreno, L.Fridman and B. Bandopadhyay, "Higher Order Super-Twisting Algorithm," 13th Workshop on variable structure system, vss 14, France 2014.

[66] Xuelian Zhou, Qiang He, "Modelling and simulation of Buck -Boost Converter with Voltage feedback Control," 2015 7th international conference on mechanical and electronics engineering, Vol. 31, November 2015 ,Publisher IEEE

[67] 20 Oledimeji Ibrahim, Nor shaiha Yahaya, "Comparative studies of PID tuning method on DC-DC boost converter," 2016 6th international conference on intelligent and advanced system,, DOI: 10.1109/ICIAS.2016.722404, Publisher IEEE.

[68] V.I. Utkin. "Variable Structure Systems with sliding modes, IEEE Transaction on Automatic control vol.2, no.2, 1977.

[69] V.I. Utkin, J. Guldner, and J.X. Shi., "Sliding mode controls in Electro mechanical systems, Taylor and Francis, 2008.

[70] A. Levant; and L. Alelishvili. "Integral higher order sliding modes, IEEE Transactions On Automatic control Vol.52, no.7, pp.1278-1282, 2007.

[71] Bhatt and Berstein "Geometric homogenity with applications to finite time stability, Math. Control.Signals.Systems," Vol.17, pp.101-127, 2005.

[72] Asif Chalanga, Shyam kamal, and B. Bandyopadhyay, "Continuous Integral sliding Mode Control: A chattering free approach, IEEE international symposium on industrial Electronics, 2013.

Chapter 8

Appendix

8.1 TRMS Parameter Values

Table 8.1: TRMS Parameter Values

Symbol	Parameters	Values
I_1	Moment of inertia of vertical rotor	$6.8 * 10^{-2} kg - m^2$
I_2	Moment of inertia of horizontal rotor	$2 * 10^{-2} kg - m^2$
a_1	static characteristic parameter	0.0135
b_1	static characteristic parameter	0.0924
a_2	static characteristic parameter	0.02
b_2	static characteristic parameter	0.09
M_g	Gravity momentum	0.32 N-m
$B_1\psi$	Friction momentum parameter	$6*10^{-3} N - m/rad$
$B_2\psi$	Friction momentum parameter	$1*10^{-1} N - m/rad$
$B_1\phi$	Friction momentum parameter	$1*10^{-2} N - m/rad$
$k_g y$	Gyroscopic momentum parameter	0.05 s/rad
k_1	Motor 1 gain	1.1
k_2	Motor 2 gain	0.8
T_{11}	Motor 1 denominator parameter	1.1 sec
T_{10}	Motor 1 denominator parameter	1
T_{21}	Motor 2 denominator parameter	1
T_{20}	Motor 2 denominator parameter	1
T_p	Cross reaction momentum parameter	2
T_o	Cross reaction momentum parameter	3.5
k_c	Cross reaction momentum gain	-0.2

8.2 DIBB Parameter Values

Table 8.2: DIBB Parameter Values

Description	Parameter	Values
Load Resistance	R	100 0hm
Inductance	L	3.75 mH
Internal resistance of inductor	R_L	0.01 0hm
Capacitance	C	450 micro F
Internal resistance of capacitor	C	0.01
Switching Frequency	F	25KHz
Input voltage1	V_1	12V
Input voltage 2	V_2	10V

List of Publications

Journal Publications

1. Lisy E.R., M.Nandakumar, Anasraj R., "Super-twisting Control for Improved Performance of Dual input Buck Boost converter," International Journal of Science and Research Vol. 6, Issue 5, pp.1067-1072, 2017.

2. Lisy E.R., M.Nandakumar, Anasraj R., "Design of Robust chattering free Integral Sliding Mode Controller for Dual Input Buck Boost converter," International journal of Applied Engineering Research, Vol.13, no.1, pp.358-365, 2018.

3. Lisy E.R., M.Nandakumar, Anasraj R., "Design and Real time Implementation of non-linear sliding surface with the application of super-twisting algorithm in non-linear sliding mode control for Twin Rotor MIMO system ," Journal of Vibro Engineering, Vol.21, Issue 8, pp.2159-2179, 2019.

Conference Publications

1. Lisy E.R., M.Nandakumar, Anasraj R., "Sliding mode controller for Dual input Buck Boost Converter," Proceedings of IEEE International conference on Power Instrumentation control and computing (PICC-2015),Govt. Engineering College Thrissur, Kerala., DEC.2015. Publisher IEEE.

2. Lisy E.R., M.Nandakumar, Anasraj R., "Design of Optimal Sliding Surface for 2-dof Twin Rotor MIMO System," Proceedings of 10 th Asian control conference (ASCC 2015),Kotakinabalu,Malaysia, pp.104-1051 May 31-June 3 2015. Publisher IEEE.

3. Lisy E.R., M.Nandakumar, Anasraj R., " Performance comparison of direct and Sliding mode controller for Dual Input Buck Boost Converter." Proceedings of International Conference on Emerging Trends in Electrical Engineering (ICETREE-2014), TKM Engineering College, Kollam,Kerala, pp.66-70, Sept.2014. Publisher elseviers, Chapter 31.

ABOUT THE AUTHOR

LISY E. R. was born at Peramangalam in Thrissur district in 1973. She had her graduation in Electrical and Elctronics Engineering in 1995 from Govt. Engineering College, Thrissur, Kerala. Her post-graduation in Control System was completed in 2008 from PSG College of Engineering Thamil Nadu. She had good academic record and is being actively involved in the various academic activities. She is working as Assistant Professor in Electrical and Electronics Engineering at Govt. Engineering College, Thrissur, Kerala. Her major area of interest includes sliding mode control, state space analysis, Power Converters.

Permanent Address:
Chiramel house,
Usha Garden, Amala Nagar P.O,
Thrissur, Kerala, India
Pin: 680555